Identifying a role for WASH in the endocytic pathway of *Dictyostelium discoideum*

by

Michael John Carnell

A thesis submitted to
The University of Birmingham
For the degree of
DOCTOR OF PHILOSOPHY

School of Biosciences
The University of Birmingham
September 2010

Abstract

Members of the WASP protein family are direct activators of the arp2/3 complex, thereby regulating the nucleation of branched actin assemblies within the cell. Each sub-class possesses a unique N-terminal domain architecture allowing a division of labour between its members, each coupling different signal transduction pathways to the nucleation of specific actin structures

WASH (WASP and SCAR homologue) is a newly identified member of the WASP protein family. Due to its disruption in *Drosophila* proving lethal (Linardopopoulou et al., 2007) little is know as to the functional role of WASH at the cellular level. Other than it is important in the development of multicellular organisms. Here we successfully disrupt WASH in the single celled amoebae *Dictyostelium discoideum* and discover a role for WASH in the endocytic pathway.

WASH was shown to be essential for the trafficking of indigestible material through the endocytic pathway, with its disruption causing a complete bock in cellular defecation. This was shown to be due to a defect in lysosomal maturation into neutral post-lysosomes. Using fluorescently tagged fusion proteins we show that WASH recruitment coincides with removal of the Vacuolar H+ ATPase from lysosomal membranes, and suggests a possible role for WASH and actin in regulating the luminal pH of intracellular compartments.

Table of Contents

List of figures

Supplementary movies

Movie 1: Parental cells performing folate chemotaxis

Cells were imaged with phase contrast microscopy chemotaxing under a layer of agar up a folate gradient. Frames taken every 30 seconds and played back at 7 frames/second

Movie 2: *wshA*^{null} cells performing folate chemotaxis

Cells were imaged with phase contrast microscopy chemotaxing under a layer of agar up a folate gradient. Frames taken every 30 seconds and played back at 10 frames/second

Movie 3: Pulse chase of FITC-dextran through wild type Ax2 cells

Cells were incubated with FITC-dextran for 20 minutes followed by imaging by fluorescent microscopy. Frames were taken every 30 seconds and played back at 10 frames/second.

Movie 4: Pulse chase of FITC-dextran through wild type Ax2 cells with latrunculin treatment and washout. Frames were taken every 30 seconds and played back at 10 frames/second

Cells were incubated with FITC-dextran for 20 minutes followed by imaging by fluorescent microscopy. Latrunculin A was added to a final concentration of 2uM at time point 32 and removed at time point ?. Frames were taken every 30 seconds and played back at 10 frames/second.

Movie 5: vatB removal results in luminal neutralisation

Wild type cells expressing *vatB*-mRFP were fed Oregon Greed dextran containing agarose beads and imaged by widefield fluorescent microscopy. Images taken every 30 seconds and played at 10 frames/second

Movie 6: Confocal microscopy of GFP-WASH and *vatB*-mRFP during lysosome neutralisation

wshA^{null} cells expressing GFP-WASH and *vatB*-mRFP were fed non-labelled agarose beads, compressed under a layer of agarose and imaged by confocal microscopy. Frames taken every minute and played at 7 frames/second.

Movie 7: Confocal microscopy of GFP-WASH and mRFP-vatM during lysosome neutralisation

wshA^{null} cells expressing GFP-WASH and *vatm*-mRFP were fed non-labelled agarose beads, compressed under a layer of agarose and imaged by confocal microscopy. Frames taken every minute and played back at 7 frames/second.

Movie 8: Widefield microscopy of GFP-WASH and vatB-mRFP during lysosome neutralisation

wshA^{null} cells expressing GFP-WASH and *vatB*-mRFP were fed non-labelled agarose beads, compressed under a layer of agarose and imaged by widefield microscopy. Frames were taken every 5 second and played back at 7 frames/second.

Abbreviations

DIC – Differential Interference Contrast

F-actin – Filamentous actin

G-actin – Globular actin

WASH – WASP and SCAR Homologue

REMI – Restriction Enzyme-Mediated Insertion

RNAi – RNA interference

SCAR – Suppressor of Cyclin AMP Receptors

V-ATPase – Vacuolar H+ ATPase

WASP – Wiskott-Aldrich syndrome protein

WAVE – WASP-family verprolin homology protein

NPF – Nucleation promoting factor

Chapter 1

Introduction

1.1 The Actin Cytoskeleton

The actin cytoskeleton collectively refers to all actin-based filaments found within eukaryotic cells. This filamentous network is an essential component of almost all eukaryotes, and recently an analogous structure has been discovered in prokaryotes (van den Ent *et al*., 2001) further emphasising the importance of these structures. In combination with accessory proteins actin filaments can form either branched arrays or parallel bundles. These structures can also be dynamic or transient with some structures disassembling moments after their formation, or some persisting for the lifetime of the cell. Cells utilise the actin cytoskeleton in a range of cellular processes as a means of providing structural rigidity, protrusive, or contractive forces. A traditional example is that of cellular motility, an event critical during development, immune response and wound healing. Filament elongation provides force for cellular protrusions (Miyata *et al*., 1999), whilst a branched cortical actin scaffold supplies rigidity to maintain cell shape. Along with myosin, actin filaments also create contractile forces for the retraction of the rear (Iwadate & Yumura, 2008).

Other biological processes documented to utilise the actin cytoskeleton include endocytosis (Kaplan, 1977), exocytosis (Muallem *et al*., 1995), cytoplasmic streaming (Wehland *et al*., 1978), vesicle propulsion (Taunton *et al*., 2000), cell-cell and cell-matrix adhesions (Vasioukhin *et al*., 2000), and cytokinesis (Carter, 1967) (Figure 1.1).

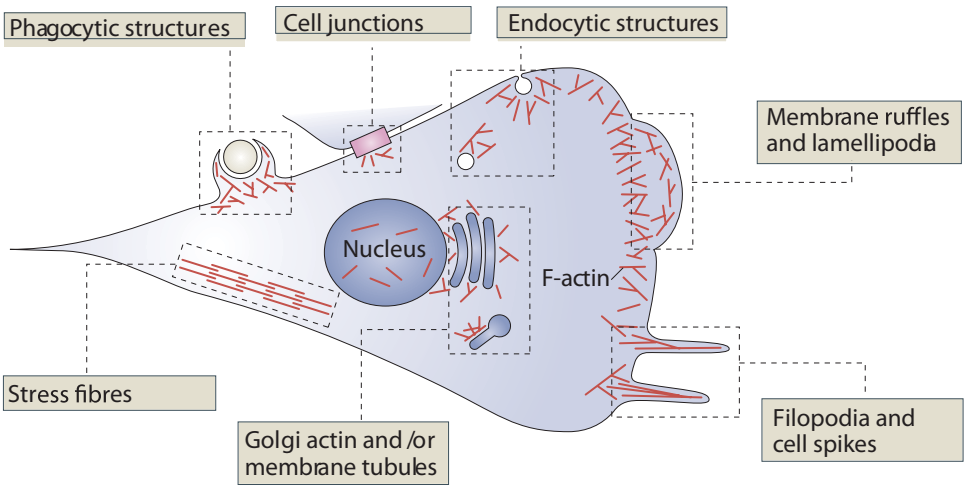

Figure 1.1: The actin cytoskeleton in eukaryotic cells

Depiction of filamentous actin structures within eukaryotic cells. Branched actin structures are involved in phagocytosis, pinocytosis, membrane ruffles, lamellipodia and serves unknown roles on golgi and membrane tubules. Bundled actin structures are involved in forming stress fibres, spiky filopodia protrusions , and unknown roles in the nucleus. Image adapted from Campellone & Welch (2010)

1.2 Actin polymerisation

Actin is a highly conserved 42KDa protein that is typically the most abundantly expressed protein within eukaryotic cells. In a concentration dependent manner, monomeric actin (G-actin) can spontaneously self-assemble into helical filaments (F-actin). G-actin also contains an ATP binding cleft, and ATPase activity once incorporated into a filament. This supplies filaments with two forms of polarity, 1) structurally due to the head-to-tail orientation of monomers with the cleft exposed at one end but not the other, and 2) ATP-bound actin at newly formed polymerising tips (for a detailed review of filament formation see Pollard & Borisy, 2003). The polarity of the filament results in each end having varying kinetics, a fast and a slow growing end. The fast growing end, and the site of filament elongation in vivo, is known as the 'barbed' end. The slow growing end, and typically the site of filament depolymerisation in vivo is termed the 'pointed' end.

In vitro experiments with purified actin have revealed that the rate limiting step in polymerisation is the initial formation of a stable actin trimer (nucleation). This is thermodynamically unfavourable because actin dimers are unstable and rapidly dissociate before the addition of the next monomer. However, once formed trimers are more stable allowing G-actin to be incorporated to elongate the filament (Pollard & Mooseker, 1981). In vivo spontaneous de novo formation of actin filaments is thought not to occur. Cells have evolved several mechanisms for overcoming the thermodynamically unfavourable step of actin nucleation in a regulated manner.

Recently a new group of actin nucleators have been identified. Spire was discovered in *Drosophila* and shown to be required for axis specification in oocytes and embryos during development (Quinlan *et al*., 2005). Cordon-Bleu was discovered as a brain enriched protein controlling neuronal morphology where its depletion by RNAi decreased neurite branch points (Ahuja *et al*., 2007). Finally, Leiomodin is a protein specific to skeletal and cardiac muscle and is thought to nucleate tropomyosin-decorated filaments in muscles (Chereau *et al*., 2008).These proteins have all been shown to nucleate unbranched actin filaments in *in vitro* actin polymerisation assays (Quinlan *et al*., 2005; Ahuja *et al*., 2007; Chereau *et al*., 2008). They all contain three or more actin binding domains in tandem that may either form a long pitch polymer stabilising monomers in a head to tail arrangement (Quinlan *et al*., 2005), or arrange actin monomers in a short pitch trimer configuration forming a stable barbed end (Ahuja *et al*., 2007).

Formins are a second class of actin nucleators that generate unbranched actin filaments. Although formins have attracted a great deal of research the mechanism by which they nucleate actin filaments is still not clear. All formins contain conserved formin homology domains, FH1 and FH2. These alone are sufficient for actin nucleation (Sagot *et al*., 2002), and this is dependent upon their ability to dimerise (Moseley *et al*., 2004). These structures however have no affinity for monomeric actin, but have high affinity for the barbed ends of filaments (Kovar *et al*., 2003). Formins are unique amongst actin nucleators in that they remain bound to the barbed end of the filament they nucleate and enhance the polymerisation rate whilst protecting the end from capping proteins (Zigmond *et al*., 2003; Kovar *et al*., 2006). It has been proposed that formins nucleate actin by binding to transiently formed actin dimers and stabilising these making trimers more thermodynamically favourable (Pring *et al*.,

2003). Formins have been reported to have roles at adhesion junctions (Kobielak *et al*., 2004), filopodia (Peng *et al*., 2003) and formation of the contractile ring (Chang *et al*., 1997).

Finally, the first identified and best characterised of the actin nucleators is the Arp2/3 complex. It is unique in its ability to generate branched actin structures and nucleates actin through structural mimicry of the barbed end of a filament.

1.3 Arp2/3 complex

The Arp2/3 complex was first discovered in *Acanthamoeba* by affinity chromatography with the actin binding protein profilin (Machesky *et al*., 1994). It consists of 7 subunits; ARPC1-ARPC5, Arp2 and Arp3, each present in a single copy (Mullins *et al*, 1997). Arp2 and Arp3 subunits are structurally similar to actin and are thought to simulate a stable actin dimer, requiring the addition of only a single monomer to mimic the 'barbed' end of a filament (Machesky *et al*., 1994; Mullins *et al*., 1997). In vitro the addition of the Arp2/3 complex with purified actin shows a minor increase in the rate of nucleation, however in the presence of a suitable activator it drastically increases the rate of actin nuclei formation (Higgs & Pollard, 1999). Like actin, arp2 and arp3 possess ATP binding clefts (Kelleher *et al*., 1995) and ATPase activity (Dayel *et al*., 2001). The crystal structure of the arp2/3 complex has been solved both with and without bound nucleotides, and in both cases the spatial separation of the arp2 and arp3 subunits suggested that by the current model this was an inactive complex (Robinson *et al*., 2001; Nolen & Pollard, 2007). The binding of WASP, an Arp2/3 activator

(discussed in section 1.4.1), was shown to induce a conformational shift in the complex (Rodal *et al*., 2005) and this is thought to reposition the arp2 subunit into close proximity to arp3 stimulating its nucleation efficiency (Egile *et al*., 2005). To date a crystal structure of the active complex has not been solved. However, X-ray scattering experiments on purified arp2/3 complex bound with the activating domain from a WASP family protein supports this widely accepted model (Boczkowska *et al*., 2008) (Figure 1.2).

The arp2/3 complex is unique amongst other known actin nucleators in its innate ability to generate branched actin structures. These are thought to be necessary to provide rigidity for further polymerisation and generation of protrusive force that could not be achieved by parallel arrangements (Mogilner & Oster., 1996). It has been localised to sites of phagocytosis, macropinocytosis, membrane protrusions and ruffles, intracellular vesicles, dynamic puncta in filopodia, invadopodia and adhesion junctions (Insall *et al*., 2001; Johnston *et al*., 2008; Yamaguchi *et al*., 2005; Kovacs *et al*., 2002), showing that it is a common component of the cells force generating machinery. In electron micrographs the arp2/3 complex could be seen at branch-points binding simultaneously to two filaments, one at its side and the other capping its 'pointed' end (Mullins *et al*., 1998). This was later confirmed by immunogold labelling with antibodies towards the complex (Svitkina & Borisy, 1999). This led Mullins *et al*., (1998) to propose the now widely accepted dendritic model of actin polymerisation. In this model the arp2/3 complex binds to the side of an existing filament ('mother' filament) and nucleates a new 'daughter' filament at a 70° angle. Figure 1.3 shows the dendritic nucleation model together with other components of the actin remodelling machinery (see Figure legend for description).

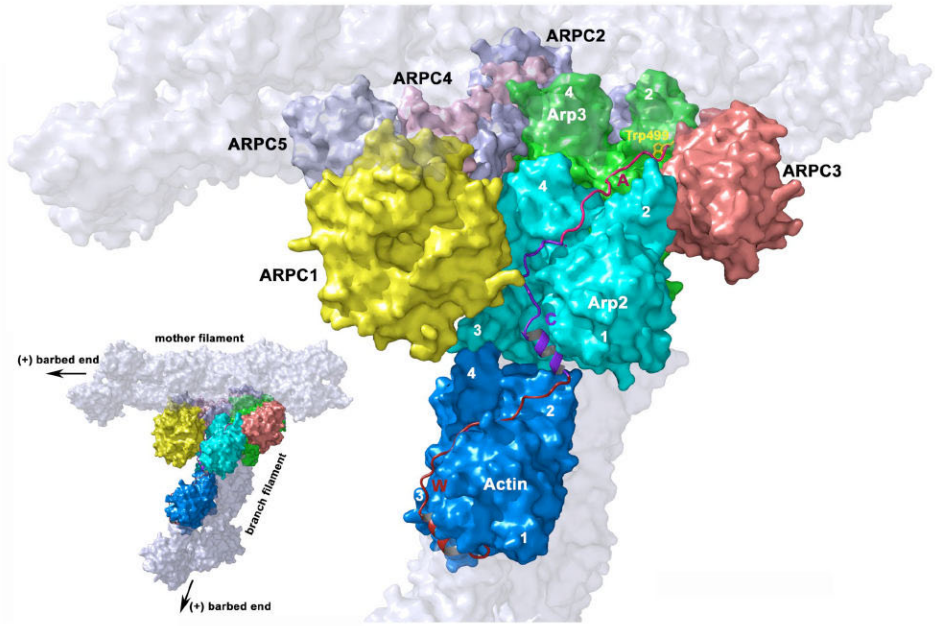

Figure 1.2: Structure of the Arp2/3 complex.

Proposed model of activated Arp2/3 complex with bound actin at the barbed end of arp2. Mother and daughter filaments are greyed out, and the position of the VCA domain peptide is shown in its most likely position. Image taken from Boczkowska *et al.*, (2008).

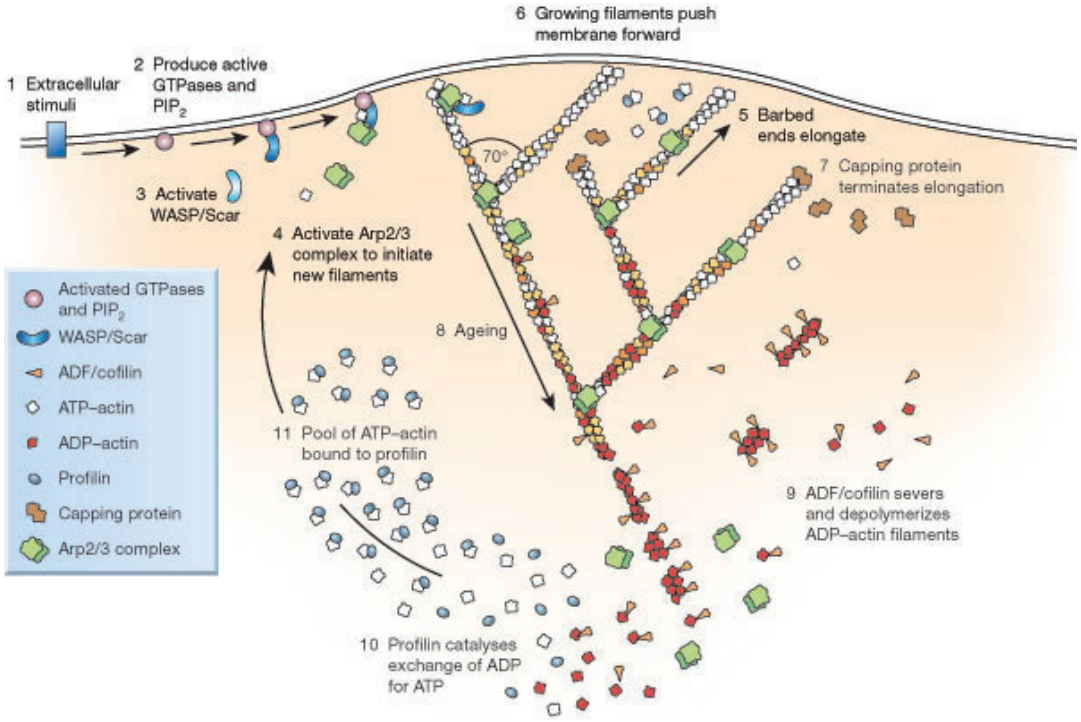

Figure 1.3: Arp2/3 mediated dendritic nucleation model.

Illustration of the dendritic nucleation model proposed by Mullins *et al*., (1998) and the interaction of key components of the actin regulatory machinery. WASP family members are activated by GTPases in response to stimuli and localised to the cytosolic surface of membranes. Here they activate the Arp2/3 complex on the side of filaments. Profilin bound ATP is then incorporated at the barbed ends of uncapped filaments activating actins' ATPase activity. Cofilin binds and severs old ADP-bound actin filaments adding to the pool of G-actin. Profilin binds to ADP-actin catalysing the exchange with ATP creating monomers for reinsertion into the barbed end of actin filaments. Image taken from Pollard (2003).

Observations that the rate of arp2/3 nucleation was dependent on the number of free barbed ends, and not on the length of actin filaments has also led to the less popular barbed end branching model (Pantaloni *et al*., 2000). In this model the arp2/3 complex binds to the barbed end of filaments nucleating two new filaments creating a Y branch. The dendritic model is much better supported by structural data.

There are a number of factors that are thought to contribute towards the activity of the arp2/3 complex. Binding of ATP in the nucleotide binding clefts of arp2 and arp3 are essential for nucleation (Goley *et al*., 2004). Although ATP hydrolysis is not required for nucleation it has been shown to be required for debranching, a process important for endocytosis in budding yeast (Clainche *et al*., 2003; Martin *et al*., 2006). Additionally, the binding to the side of filaments is also thought to induce conformational changes that stabilises the branch point and increases its nucleation activity (Rouiller *et al*., 2008).

The first activator of the Arp2/3 complex to be identified was ActA from the bacterium Listeria monocytogenes (Kocks *et al*., 1992). Although this organism does not possess actin or the arp2/3 complex, it is an intracellular pathogen that utilises the hosts own actin machinery to drive internalisation and propulsion. ActA is tethered to the surface of the bacterium with a polarised distribution (Kocks *et al*., 1993). This protein then binds to the arp2/3 complex enhancing its nucleation ability 50 fold (Welch *et al*., 1998), and is therefore commonly referred to as a nucleation promoting factor (NPF) This generates a branched actin network on one side of the bacterium creating a comet tail of polymerising actin propelling the bacterium through the cytoplasm (Welch *et al*., 1998; Cameron *et al*., 2001). ActA is

thought to activate the Arp2/3 complex by mimicking a group of proteins present within the host cell belonging to the WASP family. These proteins are currently the best characterised activators of the Arp2/3 complex.

1.4 WASP family proteins

The WASP family are a group of proteins responsible for coupling signalling pathways to the activation of the arp2/3 complex. They all share a conserved C-terminal domain architecture, containing a polyproline rich region, one or more actin binding WH2 (V) domains, a connector (C) motif and terminate in a region rich in acidic residues (A). In vitro experiments have shown that this VCA domain alone is necessary and sufficient to activate the arp2/3 complex (Machesky *et al*., 1999). The C and A regions contribute to binding of the arp2/3 complex (Marchand *et al*., 2001). This interaction is mediated by a conserved tryptophan residue within the acidic region that interacts with ARPC1 (Pan *et al*., 2004), and its mutation was shown in vitro to reduce the efficiency of Arp2/3-dependent nucleation (Marchand *et al*., 2001). The WH2 domain is a generic G-actin binding structure found in many actin regulating proteins (Paunola *et al*., 2002), and its location near the arp2/3 binding region is thought to guide the first actin monomer into position upon arp2/3 activation (Marchand *et al*., 2001).

The domain architecture is more divergent amongst the N terminal region of WASP family proteins, causing them to be sub-grouped. For more than a decade it was thought that there were only two subgroups of the WASP-family, WASP and SCAR/WAVE proteins. Recently three new subgroups have been identified, WASH (Linardopoulou *et al*., 2007), WHAMM

(Campellone *et al*., 2008), and JMY (Zuchero *et al*., 2009). WHAMM and JMY however are only present in vertebrates, whereas WASH has been identified in organisms in every branch of the eukaryotic tree, and found to be even more ubiquitous than WASP or SCAR (Veltman & Insall. 2010). Figure 1.4 shows the domain architecture of the 5 known sub-classes of WASP family proteins.

It is the domains within N-terminal region of WASP family proteins that are thought to couple signalling and localisation signals to Arp2/3 activation. Therefore the different subgroups allow multiple Arp2/3 dependent actin structures to be regulated independently of each other, in response to different signalling cascades.

1.4.1 WASP

WASP was the first identified member of the WASP-family proteins. It was discovered in search of the causative mutation responsible for the X-linked hereditary disease Wiskott-Aldrich Sydrome (WAS) (Derry *et al*., 1994), a disease characterised by thrombocytopenia, defects in T and B cell function and eczema (Ammann & Hong, 1989). In mammalian cells WASP was found to be expressed only in haematopoietic cell lines (Derry *et al*., 1994). It was later discovered that mammals possess another WASP protein that is more ubiquitously expressed and termed N-WASP (neuronal WASP) due to its enrichment within the brain (Mike *et al*., 1996).

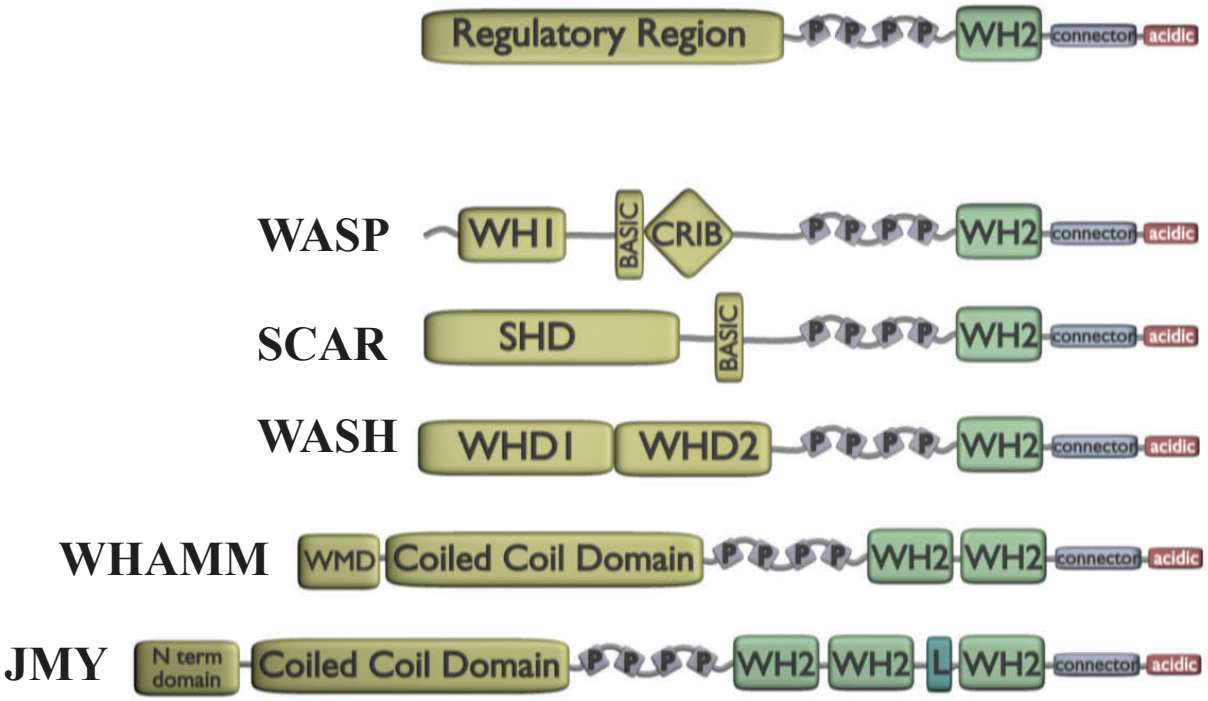

Figure 1.4: Domain architecture of WASP family proteins.

WASP: WH1 (WASP homology 1), CRIB (Cdc42 and Rac interactive domain), WH2 (WASP homology domain 2). SCAR: SHD (SCAR homology domain). WASH: WHD1 (WASH homology domain 1), WHD2 (WASP homology domain 2). WHAMM: WMD (WHAMM membrane interaction domain). JMY: L (actin monomer binding Linker)

WASP proteins contain a WH1 (WASP Homology 1) domain followed by a basic region, CRIB (Cdc42 and Rac interactin domain) domain, polyproline rich region and terminate in an Arp2/3 activating VCA domain. Purified WASP proteins, with the exception of the *Drosophila* and yeast homologuoes, are inactive in vitro due to an auto-inhibitory interaction between the VCA domain and the N-terminus of the protein (Kim *et al*., 2000; Liu *et al*., 2009; Rodal *et al*., 3003). Binding of signalling molecules to regions within the N-terminus is thought to disrupt this inhibitory conformation freeing the VCA domain to activate the Arp2/3 complex (Rohatgi *et al*., 2001).

N-WASP was first discovered in a screen for proteins that interacts with the small GTPase, cdc42 (cell division cycle 42). When active cdc42 was microinjected into Swiss 3T3 cells it was found to induce the formation of filopodia (Nobes *et al*., 1995). N-WASP was thus suggested to mediate filopodia formation by activating the arp2/3 complex in response to binding with active cdc42 (Symons *et al*., 1996, Miki *et al*., 1998). Its role in filopodia formation remains unclear due to conflicting studies showing that disruption of N-WASP can reduce the number of filopodia (Martinez-quiles *et al*., 2001), whilst others report no defect (Lommel *et al*., 2001; Benesch *et al*., 2005).

In knockout studies disruption of WASP in mice was shown to produce similar defects to human WAS patients, with defective chemotaxis of B-cells toward chemokines (Snapper *et al*., 1998; Westerberg *et al*., 2005). Disruption of N-WASP in mice and the single WASP homologue in *Dictyostelium* proved lethal (Snapper *et al*., 2001; Myers *et al*., 2005).

However, a conditional N-WASP mouse has been made and it was shown that cells with disrupted N-WASP have defects in EGF-receptor internalisation and actin assembly at sites of clathrin-coated pits (Benesch *et al*., 2005). This role is consistent with roles of the yeast WASP homologue (Las17/Bee1) that is essential for clathrin-mediated endocytosis (Naqvi *et al*., 1998). In contrast knockout studies of the single WASP homologue in *Drosophila* were viable, with only mild developmental abnormalities due to defects in cell-fate decisions. (Ben-Yaacov *et al*., 2001). These defects could be recovered by expression of full length WASH but not a C terminally truncated form missing its VCA domain implying that it is the actin organising function of WASP that is important in controlling cell-fate (Tal *et al*., 2002).

N-WASP has been found to localise to the leading edge of a variety of cell types (Bensenor *et al*., 2007; Kawamura *et al*., 2004; Le Clainche *et al*., 2007; Lorenz *et al*., 2004), and depletion of N-WASP in MDBK cells by siRNA was shown to disrupt cell migration (Bensenor *et al*., 2007). However, this effect has not been seen with disruption of N-WASP in other cell types (Snapper *et al*., 2001., Innocenti *et al*., 2005; Rogers *et al*., 2003).

N-WASP has also been shown to be essential for the formation of invadopodia (Mizutani *et al*., 2002). These are projections from metastatic cancer cells that are involved in matrix degredation and believed to be a contributing factor to the invasiveness of cells (Chen, 1989).

Propulsion of internal structures within cells has also been attributed to WASP-dependent actin structures. Similar to *Listeria*, the intracellular pathogen *Shigella* utilises the hosts actin

polymerisation machinery to generate an asymmetric actin comet tail for cytoplasmic propulsion, however this pathogen requires the host's N-WASP to activate the Arp2/3 complex (Suzuki *et al*., 1998). A similar mechanism has been observed for vesicle propulsion in *Xenopous* extracts where WASP dependent polymerisation results in rocketing of endosomes and lysosomes (Taunton *et al*., 2000).

1.4.2 SCAR/WAVE

SCAR (suppressor of cAR) was first discovered in *Dictyostelium* in a screen for mutants that supressed the developmental defects caused by deletion of the cAMP receptor (Bear *et al*., 1998). Homologues in mammalian cells were then simultaneously identified by two labs, one lab retaining the name from *Dictyostelium* (Machesky & Insall *et al*., 1998) and the other proposing the new name WAVE (WASP-family verprolin homology protein) (Miki *et al*., 1998). Two further isoforms were later discovered revealing a total of 3 isoforms in mammalian cells (Suetsugu *et al*., 1999).

Unlike WASPs, SCARs when purified were found to be active and also do not contain any known GTPase binding domains (Machesky *et al*., 1999), showing a different regulatory mechanism. It was shown that in vivo SCAR exists in a 350kDa complex with 4 other proteins; Nap125 (Nck-associate protein), PIR121 (p53-inducible mRNA), Abi2 (Abl interactor 2) and HSPC300) (Eden *et al*., 2002), and the disruption of any of these members

results is SCAR degradation (Kunda *et al*., 2003; Ibara *et al*., 2006). This suggested that these proteins may hold SCAR inactive and that the regulatory input for SCAR activation may reside on one of these proteins (Eden et la., 2002). Previous data showing that PIR121 and Rac interact (Kobayashi *et al*., 1998), and that activated Rac induces lamellipodia formation (Nobes *et al*., 1995) generated a model whereby SCAR orchestrates Arp2/3 dependent actin formation in lamellipodia in response to Rac activation (Miki *et al*., 1998; Eden *et al*., 2002).

Genetic disruption of the single gene encoding SCAR in *Dictyostelium* generated small cells with defects in movement. Although this showed a role for SCAR in generating cellular protrusions, the presence of small protrusions demonstrated that it was not the only mechanism (Bear *et al*., 1998; Blagg *et al*., 2003). Deletion of SCAR in *Drosophila* however was lethal with development arresting during oogenesis. Mutations in alleles of SCAR also revealed a reduction in the quantity of cortical actin in these cells (Zallen *et al*., 2002). Of the three SCAR isoforms in mammalian cells SCAR1 and SCAR2 have been disrupted in mice. SCAR1 null mice have sensorimotor defects, reduced learning and memory and reduced viability (Dahl *et al*., 3003; Soderling *et al*., 2003). Removal of SCAR2 is lethal with embryos showing defects in angiogenesis, heart and brain development (Yamazaki *et al*., 2003; Yan *et al*., 2003)

1.4.3 WASH

WASH is the most widely distributed member of the WASP family among eukaryotes (Veltman & Insall, 2010). It was identified as a new sub-class of the WASP protein family

whilst investigating duplicated genes in the sub-telomeric regions of primate chromosomes (Linardopolou *et al*., 2007).

The N terminal region of WASH members is conserved across all eukaryotes and contains two domains of unknown function, WHD1 (WASH homology domain 1) and WHD2 (WASH homology domain 2) (Linardopolou *et al*., 2007), although recently the WHD2 domain was shown to interact with tubulin (Gomez & Billadeau., 2009).

In vivo WASH exists in a large multi-protein complex containing Strumpellin, VPEF, SWIP, CCDC53 and capZ (Jia *et al*., 2010; Derivery & Gautreau, 2010; Veltman *et al*., 2010). Little is known about these complex members other than VPEF has previously been described as a protein required for entry of the vaccinia virus in to HeLa cells (Huang *et al*., 2008), and Strumpellin when mutated was found to be the cause of a hereditary form of spastic paraplegia (Valdmanis *et al*., 2007). How this data fits in with current literature on WASH is unclear. Although little is known as to the regulation of WASH, due to its presence in a large complex parallels have been drawn between WASH and regulation of SCAR (Jia *et al*., 2010). In addition, work in *Drosophila* suggests WASH may be activated downstream of Rho (Liu *et al*., 2007).

Genetic disruption of WASH in *Drosophila* was lethal, with pupae failing to progress to adulthood (Linardopolou *et al*., 2007). A further study in which WASH expression levels were only reduced rather than completely disrupted discovered a role for WASH in ooplasmic streaming during *Drosophila* development, although the function of WASH in this role is unclear (Liu *et al*., 2009). Recently numerous reports have been published identifying roles

for WASH in the endocytic pathway of mammalian cells. WASH disruption by RNAi revealed defects in transferrin receptor recycling (Derivery *et al*., 2009), retromer-mediated CI-MPR trafficking back to the golgi (Gomez & Billadeau 2009) and altered endosome morphology with increased tubulation (Duleh *et al* 2010). WASH has also been documented to be involved in the invasive entry of Salmonella, with WASH localising to sites of internalisation, while RNAi depletion reduces uptake (Hanisch *et al*., 2010).

In mammalian cells WASH was shown to localise predominantly to sorting and recycling endosomes and to a lesser extent with late endosomes and lysosomes. On these compartments It was seen to reside in spatially restricted puncta rather than being uniformly dispersed (Gomez & Billadeau *et al*., 2009; Derivery *et al*., 2009). Taken together these observations were suggested to show a role for WASH in vesicle scission (Gomez & Billadeau, 2009; Derivery *et al*., 2009). Authors argued that in cells where WASH had been depleted by RNAi, the increased tubulation observed suggested a role for WASH in resolving elongating tubules into carrier vesicles.

1.4.4 WHAMM and JMY

WHAMM and JMY are two of the newest identified members of the WASP-protein family, however they are restricted to vertebrates (Campellone *et al*., 2008; Zuchero *et al*., 2009). Both WHAMM and JMY have distinct N-terminal domains followed by a region predicted to form a coiled coil domain. In addition WHAMM contains an addition WH2 domain upstream of its VCA domain, whereas JMY contains 3 WH2 domains in total as well as an actin

binding linker. Interestingly this allows JMY to nucleate unbranched actin structures in the absence of the Arp2/3 complex (Zuchero *et al*., 2009).

Campellone *et al*, (2008) showed WHAMM localisation to the cis-golgi and to tubulovesicular structures. Altering expression levels of WHAMM was found to disrupt the morphology of the golgi and disrupt traffic from the ER to the golgi.

Zuchero *et al*., (2009) showed that JMY has a nuclear localisation in non-motile cells, but during motility its localisation shifts to the plasma membrane. Increasing and decreasing expression levels of JMY enhanced and decreased migration respectively.

1.5 Vesicular compartmentalisation

The cytoplasm of eukaryotic cells is densely packed with a diverse array of internal organelles. These are analogous to organs in higher multicellular organisms, acting as distinct subunits performing specialised functions. These membrane bound compartments allow cellular processes to be physically separated, for example restricting degradative proteases required for catabolism within lysosomes where they cannot degrade cytoplasmic enzymes that are essential for metabolism.

The endocytic and biosynthetic-secretory pathways are involved in trafficking of membrane and material throughout the cell. The endocytic pathway is involved in the internalisation of plasma-membrane and extracellular material. Membrane and receptors destined for return to the plasma membrane are sorted and trafficked separately from material destined for degradation in lysosomes. The biosynthetic pathway is responsible for the trafficking and post-translation modifications of newly synthesised transmembrane proteins or proteins destined for lysosomes, secretion or involved in post-translation modification within these compartments. Both pathways require transport of material between compartments whilst maintaining the unique identity and assortment of luminal enzymes of the compartments.

Vesicle identity is maintained by an assortment of small GTPases (Arfs and Rabs), SNAREs and lipid modifications. These ensure specificity between vesicle-vesicle fusion events. Although it is the cytosolic surface of vesicles that contains the markers that allow the cell to distinguish vesicle identity, each compartment is also characterised by a distinct combination of luminal proteins and pH.

1.5.1 pH and function

The luminal pH of intracellular vesicles has been shown to be important for a range of cellular processes. Acidification of early endosomes causes release of ligands from internalised receptors, such as low density lipoprotein, insulin, and iron allowing the unoccupied receptors to be trafficked back to the plasma membrane (Dunn *et al*., 1989, Marshall *et al*., 1983;). By

the same mechanism the low pH in lysosomes causes hydrolytic enzymes to dissociate from the mannose-6-phosphate receptor allowing its return to the golgi, where it can again bind proteins destined for lysosomal compartments (Westcott *et al*., 1986). As material progresses through the endocytic and biosynthetic pathways each compartment is accompanied by a change in pH, typically a pH drop (Mellman *et al*., 1986, Yamashiro *et al*., 1984, Paroutis *et al*., 2004) (Figure 1.5). This is presumably to allow retrograde recycling of unoccupied receptors at each stage.

Luminal pH has also been reported to play a role in budding. The formation of beta-COP coated carrier vesicles that transport material from early to late endosomes has been shown to be dependent on luminal pH (Gu & Gruenberg, 2000). These processes are fundamental for maintaining distinct vesicular compartments and controlled targeting of luminal contents.

In addition to its importance in receptor trafficking and budding, regulation of pH is critical for biochemical activity within the lumen. The catalytic activity of enzymes is highly dependent upon pH. Therefore the activity of enzymes as they pass through the endocytic or secretory pathways will change, allowing two organelles with different luminal pH to undergo different biochemical reactions even when they contain the same complement of luminal proteins.

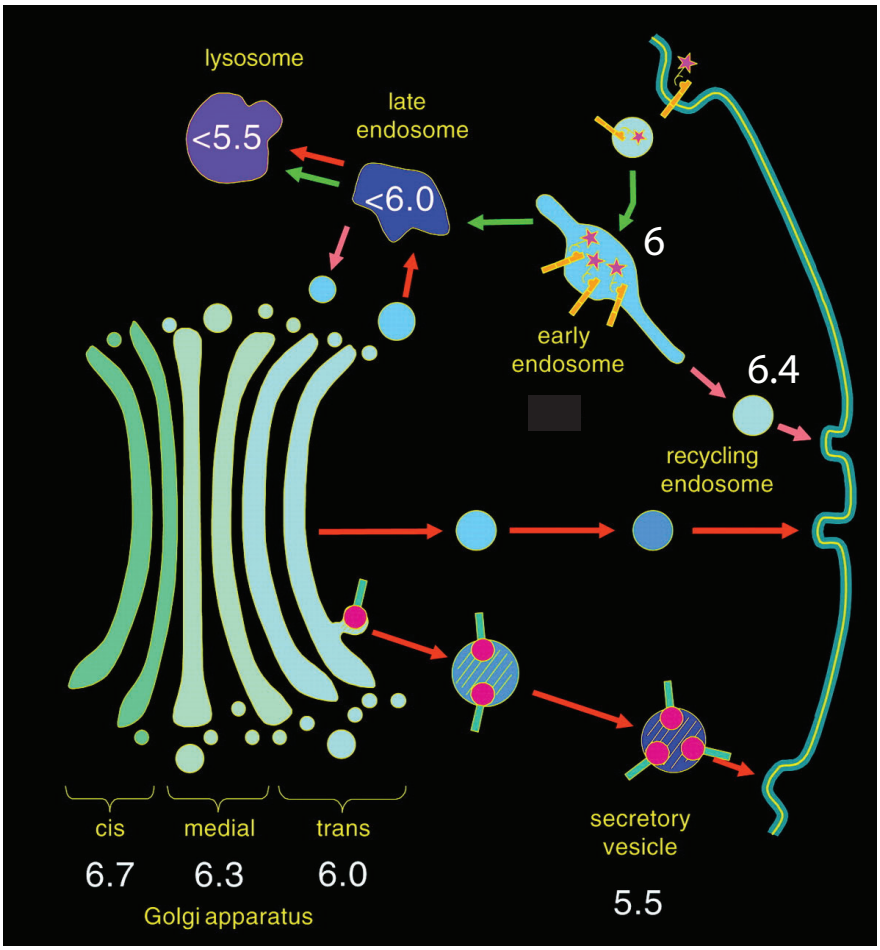

Figure 1.5: Luminal pH of intracellular vesicles.

Illustration of luminal pH of vesicular compartments of both the endocytic and biosynthetic secretory pathways. Image adapted from Demaurex (2002)

1.5.2 pH regulation

The luminal pH of each compartment is maintained within in a narrow range. Due to a neutral cytoplasm, producing acidic vesicles requires active transport of protons into the lumen. This is done by the evolutionary conserved V-ATPase (Vacuolar H+ ATPase) which is found on all compartments of the endocytic and biosynthetic pathways, except the ER and recycling endosome (Kim *et al*., 1998, Gagescu *et al*., 2000). Experiments with specific inhibitors towards the V-ATPase revealed that without continual proton pumping the acidic compartments neutralise therefore inferring that the membranes are proton 'leaky' (Demaurex *et al*., 1998). This has resulted in the 'pump and leak' model (reviewed in Demaurex, 2002) whereby vesicles reach a steady state pH when the rate of protons pumped into the lumen matches that of protons leaked. Although the V-ATPase is the primary mechanism for acidification it is not well understood what regulates the luminal pH with in a specific range. Mathematical models predict that endosomes containing only V-ATPase would have luminal pH values of 3 – 4 for endosomes of radius 0.1 -1 μm respectively (Rybak *et al*., 1997). As this is lower than the range observed in endocytic compartments it is largely thought that endosomal pH is adjusted by other mechanisms other than V-ATPase localisation.

V-ATPase is electrogenic creating a high concentration of positively charged H+ ions inside the lumen. This creates an electrical potential across the membrane that limits V-ATPase activity and acidification. The presence of Na+, K+ ATPase is suggested to limit acidification of endosomes by increasing the concentration of positive ions in the lumen increasing the membrane potential (Fuchs *et al*., 1989). By the same reasoning it is also thought that the

ability of a vesicle to acidify is limited by the flow of counter-ions such as Cl-. An influx of Cl- through chloride channels would dissipate the membrane potential allowing a lower pH to be reached (van Dyke, 1983). This is a widely accepted model for regulation of luminal pH, however studies have also shown that membrane potential is not a factor in the acidification of the Golgi, casting doubt on the significance of these factors (Demaurex *et al*., 1998; Schapiro & Grinstein, 2000).

Another mechanism that could regulate luminal pH is by regulating the rate of leaking protons. It was shown that the rate of proton leaking was highest in the ER and this rate decreased along the secretory pathway. This suggested that the rate of leaking can be and is modulated (Wu *et al*., 2000), possibly through voltage-gated proton channels or H+ antiporters (reviewed in Decoursey., 2003)

There is however growing evidence that pH may be regulated by directly effecting V-ATPase localisation or activity. It was observed that recycling endosomes containing transferrin receptor were less acidic than early endosomes and this correlated with lack of V-ATPase on that compartment. The receptor was observed to have initially gone through an acidic compartment and thus the neutralisation of the recycling endosome may be due to changing the density of the V-ATPase within the membrane (Gagescu *et al*., 2002). Additionally, the V-ATPase is also suggested to dissociate into two components to disrupt activity (discussed in section 1.6.1). It has recently been reported that the ratio of these two components on membranes differs along the endocytic pathway, with a higher abundance of intact V-ATPase on later compartments (Lafourcade *et al*., 2008)

1.6 V-ATPase

V-ATPase (Vacuolar H+ ATPase) is a highly conserved proton pump that is structurally and functionally similar to F-type ATPase (ATPsynthase). It is responsible for coupling ATP hydrolysis with the transport of protons across membranes. In addition to driving the acidification of intracellular vesicles, the proton gradient is used to drive transport of molecules across membranes such as K+, Na+, Ca+ and neurotransmitters by H+ anti-porters (Wieczorek *et al*., 1991; Onken & Putzenlechner, 1995; Moriyama *et al*., 1992). Although it is primarily associated with internal vesicles it has also been observed in some cases within the plasma membrane. In osteoclasts it is targeted to the membrane at sites of bone reabsorption, acidifying the extracellular space required for reabsorbtion (Blair *et al*., 1989). The intercalated cells of the distal tubule maintain the blood at a constant pH by either excreting acid into the urine when blood pH is too low (Karet *et al*., 1999), or reabsorbing acid from the urine when the blood pH is too high (Wagner *et al*., 2004). The clear cells in the vas deferens use membrane bound V-ATPase to acidify the extracellular space maintaining an acidic environment suitable for sperm maturation and storage, and cell types such as macrophages and neutrophils which occasionally encounter acidic environments may utilise plasma membrane V-ATPase to maintain a neutral cytosol (Brisseau *et al*., 1996). The localization of V-ATPase on the plasma membrane has also been seen on human breast cancer cell line MB-231 cells and thought to account for its invasiveness.

The structure of the V-ATPase is closely related to that of both A and F type ATPases (Cross & Muller *et al*., 2004). It is composed of two complexes (Figure 1.6). The peripheral complex (V_1) consists of 8 different proteins, A-H, many of which are present in multiple copies. The

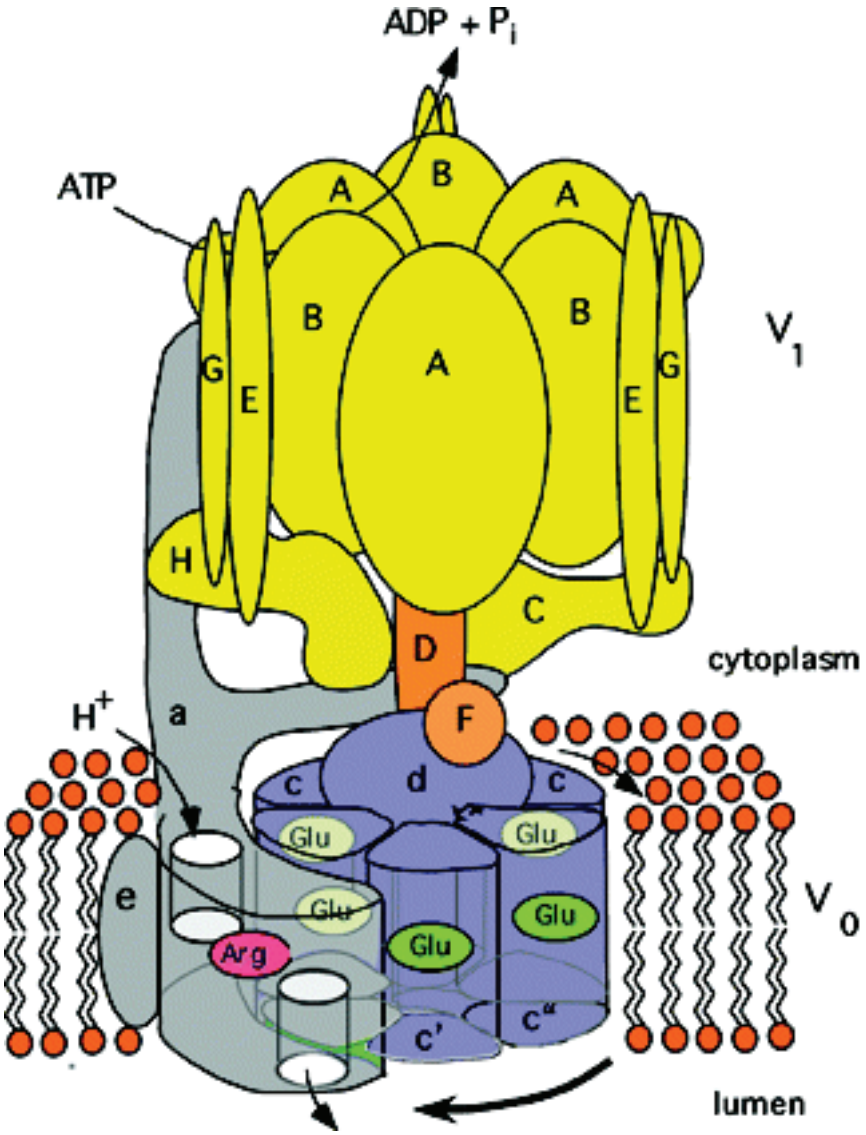

Figure 1.6. Structure of the Vacuolar H+ ATPase

Image shows the intact structure of the V ATPase. Yellow and orange subunits A-H make up the cytosolic V1 domain. Gray and purple subunits a-e belong to the transmembrane domain. Upon ATP hydrolysis the V1 domain drives rotation of the central rotor (orange and purple. Protons enter the channel at the cytosolic face of the a subunit gaining acess to the glutamic acid residues upon rotation these transport protons the luminal channel in subunit a, completing the transport process. Image taken from Toei *et al.*, (2010)

transmembrane complex (V_0) is a pore forming channel dependent upon the rotatory action of the V_1 complex to drive the rotation of a proteolipid ring for proton translocation. It is composed of 6 different proteins (a, c, c', c'', d, and e) with the c subunit present in multiple copies.

The V-ATPase is a rotatory pump coupling ATP hydrolysis dependent rotation to transport of protons across membranes (Imamura *et al*., 2003). A nucleotide binding site on the interface between Subunits A and B is the site of ATP hydrolysis. As this occurs it causes a conformational shift that drives the rotation of the stalks and the proteolipid ring (for a detailed review of V-ATPase mechanics see Nakanishi-Matsui *et al*., 2010). Within the a subunit of V_0 there is believed to possess a pore that gives access to the concealed glutamic acid residues of the proteolipid ring. These residues can undergo reversible protonation during rotation facilitating the transport of the protons to the luminal space (Hirata *et al*., 1997)

1.6.1 V-ATPase regulation

Much of what is known about cellular regulation of the V-ATPase has come about from studies in yeast. Yeast have a unique trait in that unlike other organisms disrupting the V-ATPase is not lethal providing they are grown in acidic conditions, making then an ideal system for disruptional based studies (Nelson & Nelson, 1990). There appears to be two mechanisms by which V ATPase can be directly regulated and these are 1) adjusting coupling efficiency of ATP hydrolysis to proton translocation, and 2) reversible dissociation of V_1 and V_0 complexes.

In yeast it was noticed that the V-ATPase of the vacuole contained a much higher coupling efficiency than that of V-ATPase molecules within the Golgi (Kawasaki-Nishi *et al*., 2001). Interestingly mutations introduced into subunit d of V_0 and subunit A of V_1 have both been shown to increase the coupling efficiency of V-ATPase molecules (Owegi *et al*., 2006; Shao *et al*., 2003)

Reversible dissociation is to date the best characterised mechanism for V-ATPase regulation. This process was first discovered in yeast upon glucose starvation (Kane, 1995) and also in the gut of insect larvae (Sumner *et al*., 1995). Upon dissociation the V_1 complex becomes incapable of hydrolysing ATP, and V_0 is impermeable to protons (Parra *et al*., 2000). Several studies have also shown that similar mechanisms may be taking place in mammalian cells, with glucose stimulating V-ATPase assembly in kidney cells (Sautin *et al*., 2005), and differences in the ratio of V_1/V_0 on compartments of the endocytic pathway suggests dissociation (Lafourcade *et al*., 2008). In yeast this process is thought to be an energy saving response to prevent ATP hydrolysis in response to low sugar levels (kane, 1995). A great deal is known about how this process is regulated in yeast, however a recent study has shown that when grown in neutral conditions the V-ATPase is resistant to dissociation (Diakov & Kane, 2010). This raises questions as to how ubiquitous this regulatory mechanism is, and if it is a yeast specific response only feasible due to their ability to withstand V-ATPase disruption.

1.6.2 V-ATPase and actin

The V-ATPase was first documented to interact with actin by Lee *et al*., in 1999 whilst studying V-ATPase localisation in osteoclasts. They showed that V-ATPase from mouse marrow or bovine kidney bound rabbit actin with a 0.05μM affinity. They also went on to confirm this interaction using electron microscopy of negatively stained samples showing V-ATPase bound to F-actin filaments. In a disrupted complex the B subunit was shown to bind actin (Holliday *et al*., 2000), and this was later shown to be a direct interaction with a sequence bearing homology to profilin (chen *et al*., 2004). Alteration of the sequence to that of a homologue for *Pyrococcus horikoshii* that does not have an actin cytoskeleton was found to disrupt actin binding (Chen *et al*., 2004; Zuo *et al*., 2008). Disruption of the actin binding site in osteoclasts revealed it was an important interaction targeting of V-ATPase to ruffled membranes (Zuo *et al*., 2006). Interestingly it has also been observed in epididymis clear cells, involved in acidifying the extracellular space to maintain an environment for sperm maturation, that accumulation of V-ATPase at their plasma-membrane requires the depolymerisation of cortical F-actin suggesting that actin also has an inhibitory role in preventing plasma-membrane localisation (Beaulieu *et al*., 2005; Shum *et al*., 2010).

Additionally the C subunit has also been shown to bind actin. The C subunit separates from both V_1 and V_0 after dissociation. The intact complex (V_1/V_0) was found to have a 2-3 fold higher affinity than just V_1 alone (Vitavsk *et al*., 2003). Purified C subunits were later shown to bind both F-actin and G-actin with a dissociation constant of ~50nM (Vitavsk *et al*., 2005)

1.7 *Dictyostelium discoideum*

Dictyostelium discoideum is natively a soil dwelling amoeba found feeding upon bacteria. It belongs to a class of 'social amoeba', named due to a survival technique by which upon starvation they group to form a multicellular fruiting body. It has been popular as a model organism for the study of cell motility due to its active lifestyle. During its growth phase it is independent, existing as a single cell migrating in search of food sources. When these are depleted a developmental program is engaged. Figure 1.7 shows the lifecycle of *Dictyostelium*. Upon starvation surrounding cells migrate together forming aggregates that are capable of undergoing differentiation. After aggregation motile slugs are formed that migrate toward heat, light and humidity. As they migrate cells differentiate into pre-stalk or pre-spore cells. After the slug has settled the culmination stage begins, where pre-stalk cells vacuolise lifting up the spores forming a fruiting body.

1.7.1 As a model organism

Dictyostelium discoideum is established as a model organism for the study of cell migration, and more recently gaining momentum in the areas of pathogenicity, autophagy, and vesicular trafficking. As an experimental system it benefits from being easily handled, genetically tractable, having a fully sequenced genome and that its growth phase is distinctly separated and independent from its developmental phase.

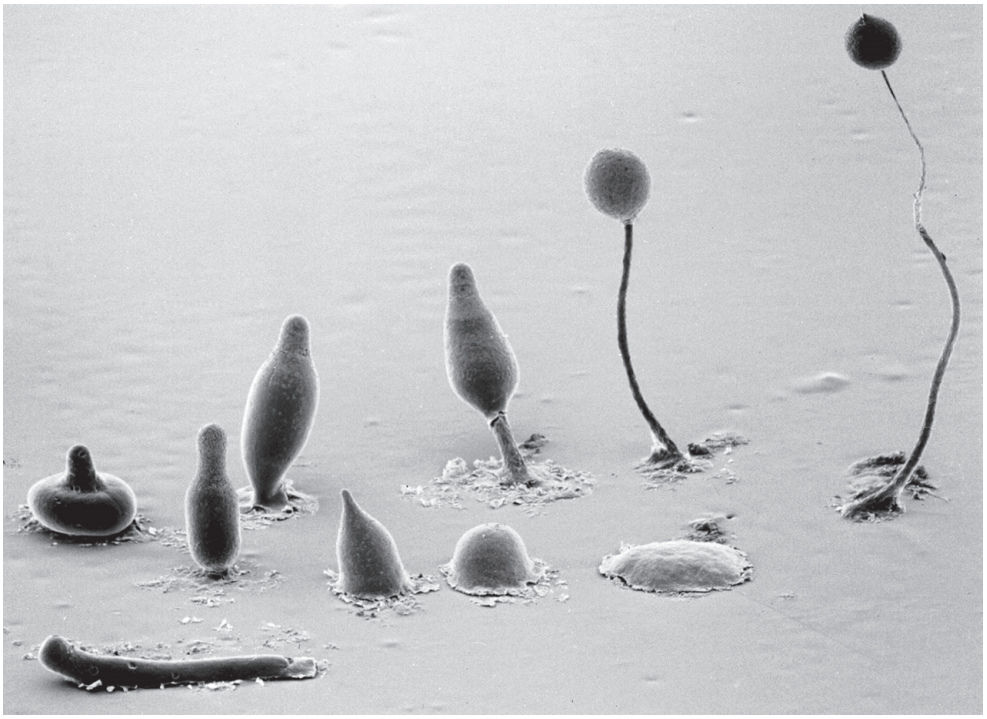

Figure 1.7: Development cycle of Dictyostelium discoideum

Image of the developmental cycle of Dictyostelium discoideum. Starting from bottom right and moving clockwise. Cells aggregate to form a loose aggregate, tight aggregate, tipped aggregate, an elongated structure called the finger, this topples to form a migratory slug, and then progresses through stages of culmination from the Mexican hat to a fully formed fruiting body. (Image is a scanning electron microphraph by Blanton & Grimson)

Dictyostelium naturally feed on bacteria by phagocytosis. Several strains have been generated that can be grown in liquid medium within the laboratory (Sussman & Sussman, 1967), These have acquired several mutations (Williams *et al*., 1974), that confer an ability to take up nutrient rich medium by a process called macropinocytosis. This allows cells to be cultivated in defined medium in the absence of bacteria or particles, a trait historically beneficial for aiding biochemical experiments but more recently proving useful for live cell imaging.

Genetically *Dictyostelium* are naturally found as haploids. This in combination with a method for transformation (Nellen *et al*., 1985) makes gene disruption a simple and rapid process. Additionally the genome has been sequenced and is freely available (Eichinger *et al*., 2005). Given the genetic strengths of *Dictyostelium* several methods have been developed to further utilise this organism.

Although there are a number of selection markers for use in *Dictyostelium* such as Blasticidin, Hygromycin and G418, some are more effective than others at selecting gene disruptants, namely Blasticidin. The Cre-loxP recombination system used to create conditional gene disruptants in mice has been adapted for use in this system (Faix *et al*., 2004). This enables generation of multiple gene disruptants using the same selection marker. This works by using selection cassettes flanked by loxP recombination sites and contain downstream translational stop codons. After successful gene disruption transient expression of Cre recombinase causes a recombination event excising the selection cassette but leaving the stop codons in place. This selection cassette can then be re-used for further gene disruptions in that cell line.

Another tool for generating multiple disruptants is the use of a diploid system (King & Insall 2003). If the desired disruptants already exist in different cell lines, providing each are resistant to a different selection when starved together they will fuse to form diploids at a frequency of 1 in 10^5 that can then be isolated by addition of both selections. This allows for specific mutants to be crossed. Providing each mutation resides on separate chromosomes these diploids can then be segregated back to haploids using microtubule disrupting drugs. Finally, libraries of *Dictyostelium* mutant strains can also be generated by the random insertion of a vector into the genome using restriction-enzyme-mediated integration (REMI) (Kuspa *et al*., 1994).

Generation of mutants in *Dictyostelium* does not require cells to undergo development. This allows mutants to be generated whose homologous in multicellular organisms when disrupted would be lethal due to defective development.

1.7.2 Endocytic pathway in *Dictyostelium*

Dictyostelium is increasingly being utilised as a model system for the study of the endocytic pathway. It bears many similarities to that of its mammalian counterpart including mechanisms for uptake of membrane and material, early trafficking stages of acidic vesicles involving tabulation and vesiculation, formation of multi-vesicular bodies and lysosome biogenesis(Neuhaus *et al*., 2002; Marchetti *et al*., 2004). Additionally they also perform

lysosome secretion (Dimond *et al*., 1981), a process carried out by a number of specialised cell types such macrophages, T cells, and osteoclasts.

Similarities between these systems are also emphasised by a shared susceptibility to pathogenic microorganisms, such as *Legionella*, that escape the antimicrobial environment of lysosomes by hijacking the hosts endocytic trafficking machinery (Solomon & Isberg., 2000).

As single celled amoebae the emphasis of the endocytic pathway in *Dictyostelium* is the internalisation and trafficking of foreign material for nutrient uptake, and the expulsion of indigestible material. In *Dictyostelium* fluid and solid particles are engulfed by macropinocytosis and phagocytosis respectively. These two actin-dependent processes although morphologically similar (Hacker *et al*., 1997) have been shown to be regulated by different mechanisms (reviewed in Cardelli, 2001). Figure 1.8 shows key events that take place after internalisation by macropinocytosis. As the pathway is not linear, timings are a rough guide to the observed transit of fluid phase markers through the pathway.

Newly internalised macropinosomes retain a residual actin-coat for ~1 minute (Maniak *et al*., 1995). After this has disassembled, various endocytic vesicles fuse with the compartment delivering V-ATPase that acidifies the luminal space (Padh *et al*., 1991; Clarke *et al*., 2010). Membrane is then retrieved from this compartment in small carrier vesicles that return membrane back to the cell surface (Neuhaus & Soldati, 2000). These carrier vesicles were shown to selectively remove p25 from macropinosomes and return it to the plasma membrane similar to recycling endosomes in mammalian cells (Ravanel *et al*., 2001),. These small carrier vesicles have a high surface to volume ratio, causing removal of membrane from the macropinosome whilst leaving the majority of the luminal contents. The decreasing size of the

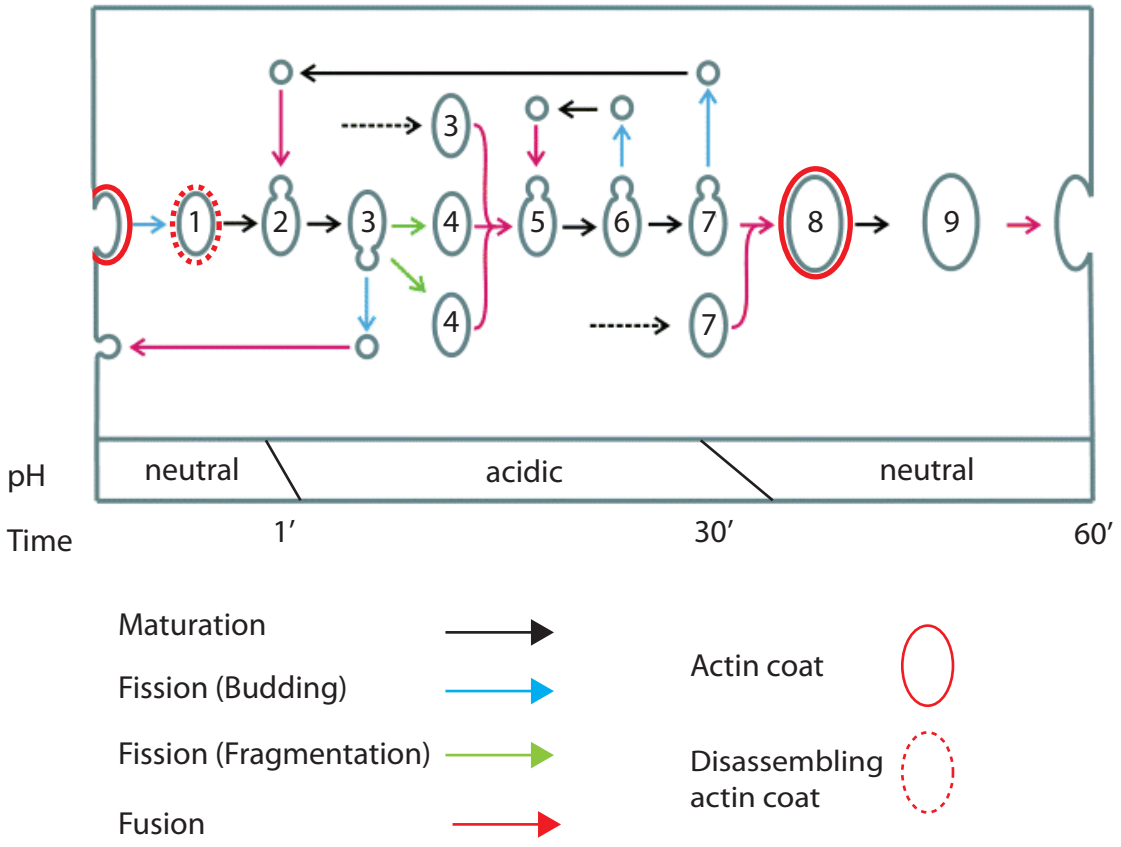

Figure 1.8: The endocytic pathway in *Dictyostelium discoideum*

Represetation of fission/fussion events throughout the endocytic pathway in *Dictyostelium.* following macropinocytosis (1) Internalised macropinosome maintains a neutral pH and residual actin-coat for ~1 minute. (2) After the actin-coat is removed the vesicle begins to fuse with other endocytic compartments that deliver V ATPase to the membrane acidifying its lumen. (3) Carrier vesicles bud from this compartment selectively recycling transmembrane proteins and membrane back to the plasma-membrane. This compartment can also fragment intosmaller compartments. These compartments can also undergo homotypic fusion. (5) compartment looses ability to fuse with earlier compartments and receives a complement of hydrolytic enzymes. (6) A seperate stage of lysosomal maturation containing a different combination of hydrolytic enzymes. (7) Lysosomes that can undergo homotypic fusion and also neutralisation by removal of V ATPase by budding. (8) Post-lysosomal compartment that is identified by neutral pH and presence of a persistent coat of filamentous actin. (9) Vesicle competent to fuse with the plasma membrane for exocytosis. Image adapted from Maniak 2003).

macropinosome drives the expulsion of water concentrating membrane impermeant material inside the lumen (Neuhaus *et al*., 2002). These vesicles are then capable of undergoing homotypic fusion, resulting in what has previously been termed a mixing compartment (Clarke *et al*., 2002). This presumably serves to concentrate the contents of numerous macropinosomes into a smaller number of dense vesicles. These vesicles then lose the ability to undergo fusion with earlier compartments (Clarke *et al*., 2002), and progress through a series of lysosomal stages each containing a specific profile of hydrolytic enzymes (Souza *et al*., 1997).

Further progression through the endocytic pathway is accompanied by an increase in luminal pH forming a post-lysosomal compartment (Padh *et al*., 1993; Aubry *et al*., 1993). This is achieved through removal of the V-ATPase that is then recycled back to acidify newly formed macropinosomes (Nolta *et al*., 1994; Clarke *et al*., 2010). These compartments then persist in the cell for ~30 minutes before fusing with the plasma-membrane expelling its contents into the extracellular space.

Post-lysosomes in *Dictyostelium* have been shown to be surrounded by a coat of filamentous actin and the Arp2/3 complex (Rauchenberger *et al*., 1997; Insall *et al*., 2001). Disruption of these actin coats by treatment with the actin depolymerising drug Latrunculin caused vesicles to aggregate into clusters and prevent further trafficking of endocytic markers (Drengk *et al*., 2003). A unique approach was undertaken to specifically disrupt these actin-coats by creating a fusion between the actin depolymerising protein cofilin, and a previously identified marker of post-lysosomes vacuolin A (Drengk *et al*., 2003). The construct successfully targeted cofilin to post-lysosomes increasing the rate of actin depolymerisation resulting in clustering

of post-lysosomes but normal trafficking of endocytic markers. The authors argued that these actin coats act as a physical barrier preventing docking and fusion events with other endocytic markers. By a similar strategy the actin binding protein VASP was targeted to these compartments increasing the size and density of the actin coats (Schmauch *et al*., 2009). This was shown to sequester actin binding proteins to such an extent that phenotypes were observed resembling their individual knockouts.

1.8 Aims of this work

The aim in this study is to further characterise the cellular function of the newly identified member of the WASP protein family, WASH. I will achieve this by utilising *Dictyostelium discoideum* as a model organism as its genetics allow easy disruption of the single gene encoding WASH, and the functional separation of its growth and development cycle may yield more success than previous studies using *Drosophila*.

Chapter 2

Materials and Methods

All reagents/solutions were purchased from Sigma unless otherwise stated.

2.1 Cell culture

2.1.1 Axenic

Cells were grown axenically in HL-5 medium + Glucose (Formedium) at 22°C, either adhered to 10cm petri dishes or in suspension within shaken flasks rotating at 120rpm. For fluorescent imaging cells were transferred to glass-bottomed dishes and incubated in LoFlo medium (Formedium) for at least 2 hours prior to imaging, but not exceeding a 24 hour period.

HL-5 medium (5 Litres): Peptone 14g; Yeast extract 7g; Sodium phosphate (Na2HPO4) 0.5g; Potassium phosphate (KH2PO4) 0.5g; Glucose 13.5g.

LoFlo medium (1 Litre): Glucose 11g; KH_2PO_4 0.68g; Casein Peptone 5g; NH_4Cl 26.8mg; $MgCl_2$ 37.1mg; CaCl2 1.1mg; $FeCl_3$ 8.11mg; Na2-EDTA 4.84mg; $ZnSO_4$ 2.3mg; $H3BO_3$ 1.11mg; $MnCl_2.4H_20$ 0.51mg; $CoCl_2$ 0.17mg; $CuSO_5.5H_20$ 0.15mg; $(NH_4)6MO7024.4H_2O$ 0.1mg.

2.1.2 Bacterial

For bacterially grown cells *Dictyostelium* were cultivated on lawns of *Klebsiella aerogenes* on SM Agar plates and incubated in humidity chambers at 22°C.

SM Agar medium (1L): SMM agar (42g) [Formedium]; 20mM MES pH6.5

*40ml SMM Agar per 10cm petri dish.

2.2 Electroporation

Protocol adapted from Howard *et al*. (1988). DNA preparations were obtained from either mini/maxipreps (qiagen) or purified PCR fragments and placed in sterile ice-cold eppendorf tubes (extrachromosomal plasmids: 10µl at 0.1µg/µl; Genomic integration: 10µl at 2.5µg/µl). Cells were harvested during log phase, spun down and resuspended at a density of $4x10^7$ cells/ml in ice cold E-Buffer. 0.4ml of cell suspension was mixed with DNA and placed in an ice cold 2mm cuvette (Biorad). The cuvette was electroporated using a 3µF capacitor in series with a 5Ω resistor at a voltage of 1kV giving a time constant of roughly 0.6 milliseconds. The cuvette was immediately placed on ice for 10 minutes after electroporation followed by mixing with 2ul of healing solution in a 10cm petri dish for 15 minutes at room temperature. 10mL of HL-5 medium was added and left for 24 hours before addition of an appropriate antibiotic selection.

E-Buffer:	10mM Potassium phosphate pH6.1; 50 mM Sucrose. (Filter sterilised and stored frozen).
Healing Solution:	100mM CaCl2; 100mM MgCl2. (Filter sterilised and stored frozen).
Antibiotic Selections:	Blasticidin 10µg/ml. G418 10µg/ml. Hygromycin 50µg/ml.

2.3 Cloning of GFP and mRFP fusion constructs

WASH was isolated by PCR from Ax3 genomic DNA using primers $^{5'}$AGATCTAAAATGACAACTCAAATCTAT $^{3'}$ and $^{5'}$TCTAGATTATTCCCATTCAGAAGAATCGG TATCAG$^{3'}$. WASHΔVCA, WASHΔA and WASHΔW471A were isolated by PCR from cDNA using Forward primer $^{5'}$GGATCCATGACAACTCAAATCTATCAGGTTCC$^{3'}$ and reverse primers $^{5'}$TCTAGATTAACTTGGTGGATTAAATGGTGGTGGAGC$^{3'}$ (ΔVCA),$^{5'}$ATCTAGATTATTTCTTTGATT TTGATTGTTTTTTAGTTGATTTTG$^{3'}$ (ΔA) and $^{5'}$ATCTAGATTATTCTGCTTCAGAAGAATCGGTA TCAG$^{3'}$ (W471A). *vatB* was isolated by PCR from cDNA whilst removing its stop codon using primers $^{5'}$GGATCCAAAATGGTTGGATTTGAAGATCATATCGC$^{3'}$ and $^{5'}$TCTAGAGTTAGTTG AATCTACAGTACCC$^{3'}$ and vatM from cDNA using primers $^{5'}$GGATCCATGAGCTTTTTAAGACC ATCCATTTGGAG$^{3'}$ and $^{5'}$TCTAGATTATTCATCATCTTCAGAACCAGAAAGAATACG$^{3'}$. For N terminal GFP constructs genes were inserted into pDM352. *vatB* and *vatM* were inserted into mRFP module vectors pDM413 and pDM411 respectively. Followed by digestion with NgoMIV and then inserted into a GFP-WASH construct with a pDM352 backbone.

2.3 Cell line generation

2.3.1 *wshA* Disruptants

DNA constructs pMJC07 and pMJC57 were created by PCR from genomic DNA. Deletions to sequence and insertion of restriction enzymes sites was accomplished by a method utilizing four primers (Figure 2.1).

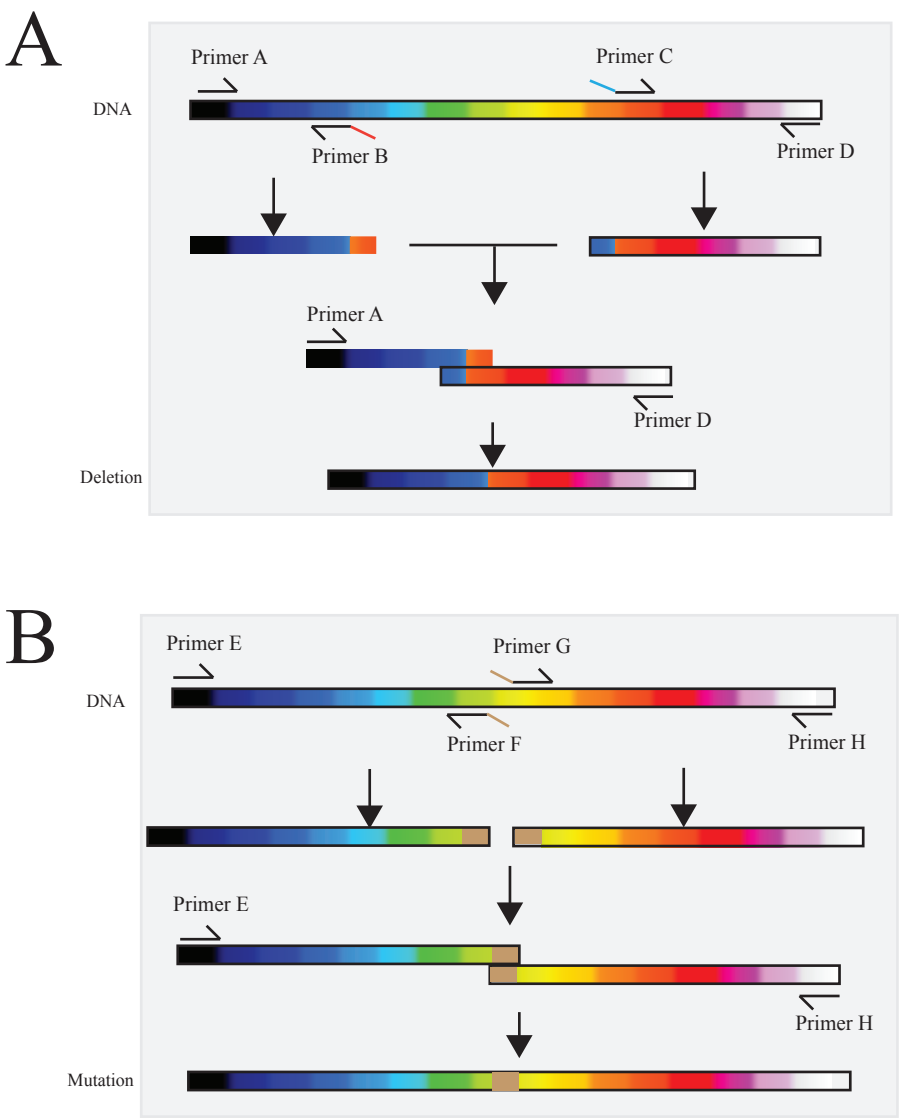

Figure 2.1: 4-primer PCR

Illustration of method to create deletions (A) and/or site directed mutations (B) into DNA by using 4 primers. First two separate PCR reactions are carried out amplifying unaltered DNA. Internal primers (B & C) or (F & G) are designed with 5' sequences that reverse compliment each other. Products from the first two PCR reactions are purified and mixed for use as a template in a final PCR reaction containing the most outward primers. The engineered sites on internal primers result in products annealing and elongating introducing desired changes.

pMJC07 was created by three separate PCR reactions (Figure 2.2). Primers 1 & 2 and Primers 3 & 4 using genomic DNA, and primers 1 & 4 using a mixture of products from the previous two PCR reactions as a template:

Primer 1: 5' TTCAACAATTTCTGCAAGAGTATCACATG 3'

Primer 2: 5' AGATCTGTCGACGTGTAGTCATCTTCACCACCATCACCAC 3'

Primer 3: 5' GTCGACAGATCTAGAGATTGGGTGACGCTCCAGTCACCG 3'

Primer 4: 5' TTATTCCCATTCAGAAGAATCGGTATCAG 3'

[BglII, SalI]

This removed 29bp of coding sequence, and inserted BglII and SalI restriction sites for cloning purposes.

pMJC57 was created by 3 separate PCR reactions (Figure 2.3). Primers 5 & 6 and primers 7 & 8 using genomic DNA as a template, and primers 5 & 8 using a mixture of products from the previous 2 PCR reactions as a template:

Primer 5: 5' AACAGTACCATCAAAAACTACAACACCAGTTGC 3'

Primer 6: 5' GTCGACGATGATAGATCTAACTGGAACCTGATAGATTTGAGTTGTAAT 3'

Primer 7: 5' AGATCTATCATCGTCGACAACCACCACCAGTTTCTGATGGAGGTGGCGG 3'

Primer 8: 5' AACTAATTGTGGGGTTGCATTGATTACTGG 3'

[BglII, SalI, Start Codon point mutation]

This removed 1344bp of *wshA* sequence, introduced a point mutation to augment the start codon and inserted BglII and SalI restriction sites for cloning purposes.

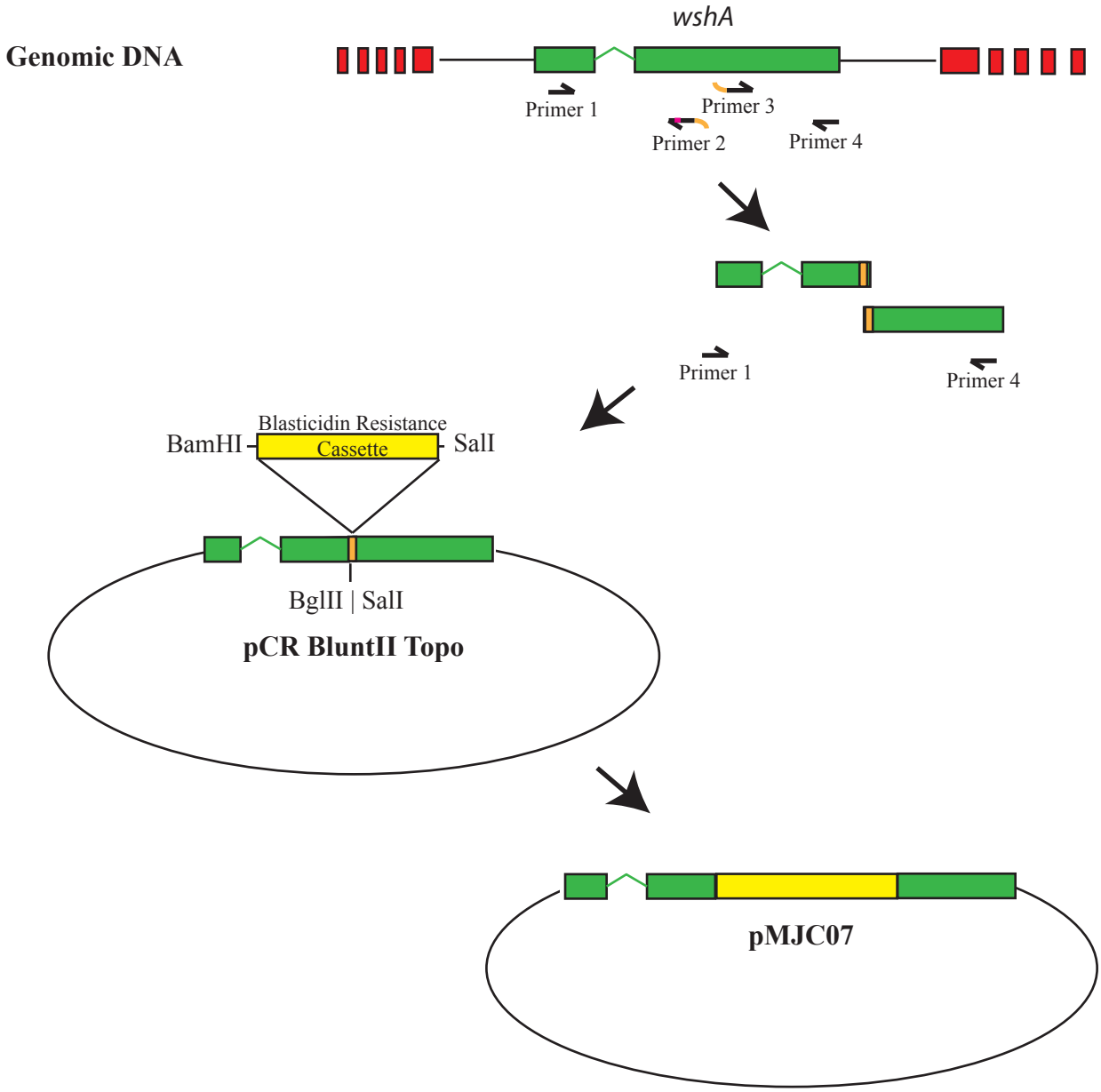

Figure 2.2: Creation of *wshA* disruption construct of pMJC07

Schematic representation of pMJC07 construction. Primers 1, 2, 3, 4 were used to clone *wshA* by 4 primer PCR. Primers 2 and 3 inserted BglII and SalI restriction sites for cloning purposes whilst removing 29bp of coding sequence. PCR product was cloned into pCR BluntII Topo and the BSR cassette from pLPBLP was inserted into engineered BglII and SalI sites.

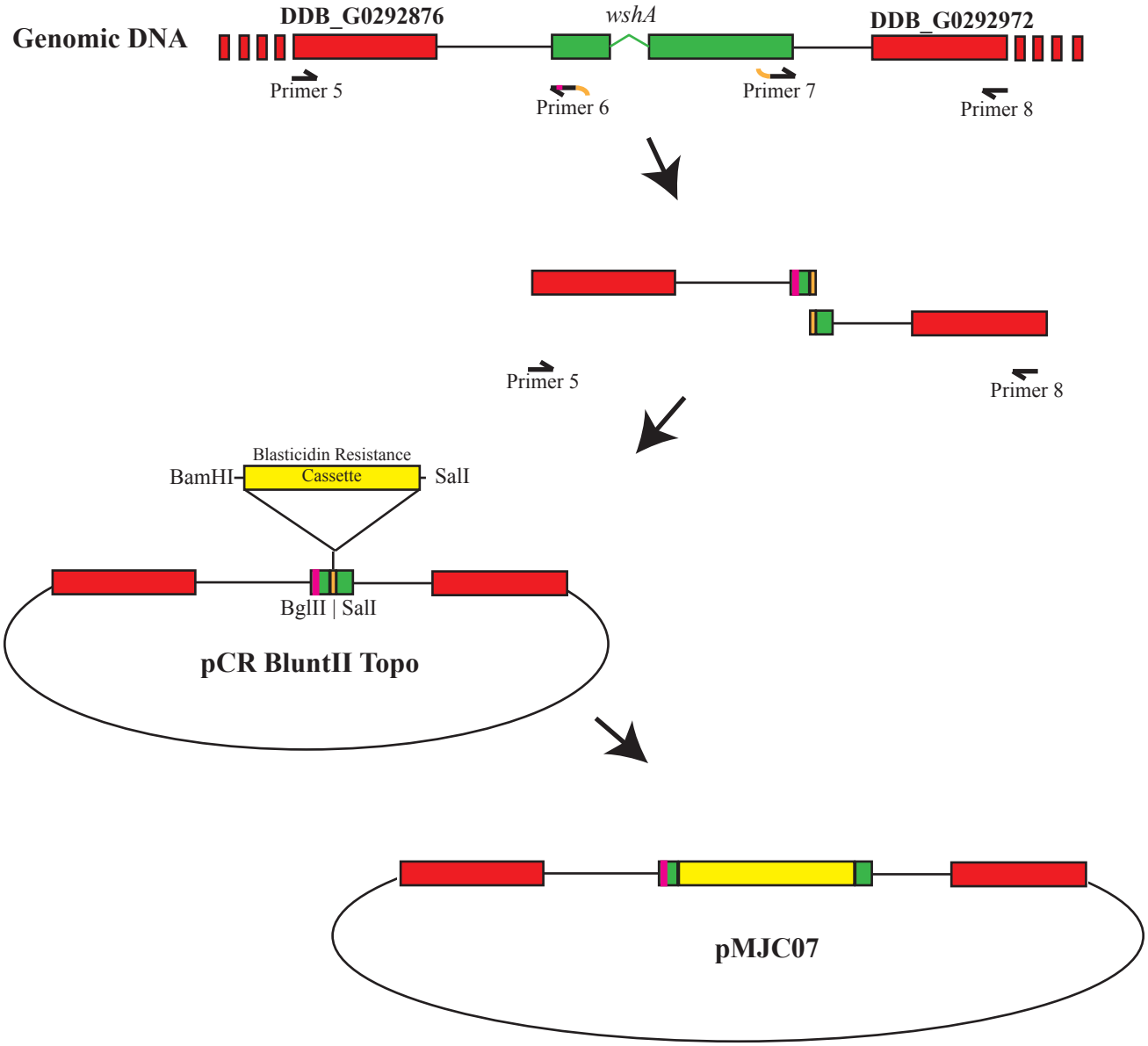

Figure 2.3: Creation of *wshA* disruption construct pMJC57

Schematic representation of pMJC57 construction. Genes flanking wshA were used as recombination arms. Primers 5, 6, 7, 8 were used to clone recombination arms by 4 primer PCR and cloned into pCR BluntII Topo vector. Primers 6 and 7 engineered in BglII and SalI restriction sites for BSR cassette insertion whilst removing 1344bp of *wshA*. BSR cassette from pLPBLP was inserted into engineered sites.

The final PCR fragments for pMJC07 and pMJC57 were cloned into pCR BluntII Topo (Invitrogen). A floxed BSR cassette was digested from pLPBLP using BamHI and SalI enzymes, and inserted into both pMJC07 and pMJC57 at engineered BglII and SalI sites. pMJC57 was sequenced to ensure no unintentional mutations were introduced during cloning. Linearized constructs were electroporated into Ax2 cells, and 24 hours after transfection cells were cloned into 5 x 96 well plates with the addition of Blasticidin. Colonies resulting from electroporation with pMJC57 were screened by western blot. Colonies resulting from electroporation with pMJC07 were screened using the following primers:

Forward: $^{5'}$ AGATCTAAAATGACAACTCAAATCTAT $^{3'}$

Reverse: $^{5'}$ TTATTCCCATTCAGAAGAATCGGTATCAG $^{3'}$

2.3.2 Non-actin binding vatB Knockins

pMJC87 and pMJC88 were created to alter the endogenous coding sequence of *vatB*. pMJC87 was created as follows. PCR1 (primer 9 & 10: genomic DNA), PCR2 (primer 11 & 12: genomic DNA), PCR3 (primer 9 & 12: products from PCR1 & 2). Product from PCR3 was cloned into pCR BluntII Topo (Invitrogen) and the BSR cassette from pLBPLP excised by BamHI and SalI restriction digest was inserted into engineered BglII and SalI sites. PCR4 (primers 9 & 12: product of PCR 3 with BSR cassette insertion), PCR 5 (primers 14 & 16: genomic DNA) PCR6 (primers 9 & 16, products from PCR 4 & PCR 5). Product from PCR 6 was cloned into pCR BluntII Topo (Invitrogen). pMJC88 was construct in the same manner,

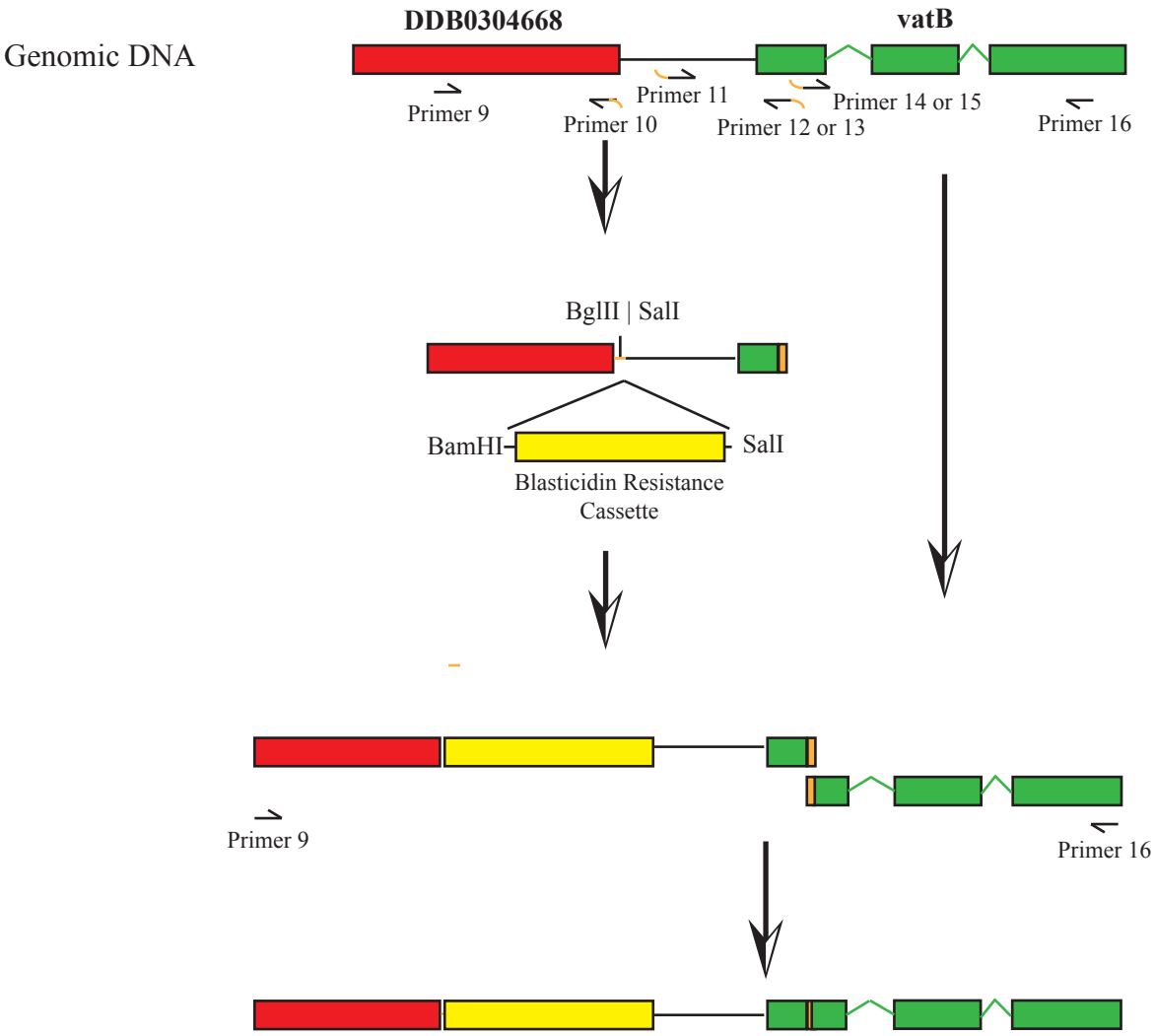

Figure 2.4: Creation of *vatB* alteration constructs pMJC87 and pMJC88

Schematic representation of construction of pMJC87 and pMJC88. Primers were used to amplify DDB0304668 as upstream recombination arm, and promoter and *vatB* as downstream recombination arm. BSR cassette was introduced at engineered BglII and SalI restriction sites. Using 4 primer PCR alterations were introduced into the upstream recombination arm. Primers 12 and 14 were used for pMJC87 and primers 13 and 15 were used for pMJC88. Linearised plasmids were electroporated into wid type cells and screened for recombination by PCR and verified by sequencing.

however primer 12 was replaced by primer 13, and primer 14 replaced with primer 15 (Figure 2.4).

Primer 9: 5' AATCACACAAAATAGATCACCAAATCAATTGG 3'

Primer 10: 5' CCAGATCTAAAGTCGACCCTCAAACAATTTGTTGTTGTTGTTG 3'

Primer 11: 5' GGGTCGACTTTAGATCTGGTTTTCAAAATTTTGTATATATTG 3'

Primer 12: 5' TCCTTTACCTCCTTCAACAGATCCGAGTGGACCATTTACTGC 3'

Primer 13: 5' AGCACCACCAGCAACAATAACGAGTGGACC 3'

Primer 14: 5' GGATCTGTTGAAGGAGGTAAAGGATCTGAAATTGTAACTTTAAC 3'

Primer 15: 5' GTTGCTGGTGGTGCTGGTCCAAAATTCTCTGAA 3'

Primer 16: 5' TAATAGTTTTTTCAGTGATACGTTTGAGG 3'

Screen Fwd: 5' AATCACACAAAATAGATCACCAAATCAATTGG 3'

Screen Rev: 5' TCTAGATTAGTTAGTTGAATCTACAGTACCC 3

[BglII, SalI, Altered sequence]

DNA was amplified from pMJC87 and pMJC88 and electroporation into Ax2 cells. After 24 hours transfected cells were cloned into 5 x 96 well plates with the addition of Blasticidin. Colonies resulting from electroporation with pMJC07 were screened using the following primers:

Forward: $^{5'}$ AATCACACAAAATAGATCACCAAATCAATTGG $^{3'}$

Reverse: $^{5'}$ TCTAGAGTTAGTTGAATCTACAGTACCC $^{3'}$

2.4 *Dictyostelium* Cell line preservation

Generated cell lines were frozen and stored at -80°C; aliquots for long term storage were placed in liquid nitrogen. Cells were harvested from shaken cultures and suspended in a 50:50 mix of sterile HL5/foetal calf serum at a density 10^8 cells/ml. Aliquots where placed into freezing vials containing an equal volume of HL5/foetal calf serum containing 20% (v/v) DMSO. Freezing vials were mixed gently and slowly cooled to -80°C in a cell freezer box.

2.5 Western Blotting

2.5.1 Sample preparation

Harvested cells were washed and resuspended in KK2 buffer at a density of $1x10^7$cells/ml. 100µl of cell suspension was added to 900µl of boiling 1.1X Laemmli sample buffer. After 5 minutes samples were removed from heat source and placed on ice.

Laemmli Sample buffer (4x):	125mM Tris-CL (pH8); 2% SDS; 20% Glycerol; 5% β-mercaptoethanol; 0.004% Bromophenol Blue.

2.5.2 Generating Blots

Samples were run on NuPAGE® 10% Bis-Tris gels (Invitrogen, Cat No: NP0301BOX) in 1x NuPAGE® MOPS SDS running buffer (Invitrogen) at 150V for 50 minutes in an Invitrogen Xcell SureLock™ Novex Mini-Cell tank. Proteins were then transferred from the gel to methanol soaked PVDF Hybond-P membrane (Amersham) in transfer buffer for 2 hours at 240mA using BioRad Mini-PROTEAN® Tetra Cell transfer apparatus. Membranes were then soaked in Ponceau S solution for 10 minutes followed by successive rounds of washes in TBST to confirm even protein loading. Blots were then blocked for at least one hour in TBST + 5% powder milk (w/v).

TBST (pH 7):	20mM Trizma base; 140mM NaCl; 1% Tween
Transfer Buffer:	200mM Trizma base; 190mM Glycine; 1% SDS; 20% Methanol

2.5.3 Antibody generation

Antibodies were created through BioGenes custom antibody service (www.biogenes.de/). Two peptide sequences from WASH were selected and independently used to raise antibodies in rabbits. One sequence resides in the WHD1 domain at the N terminus (FNTQENPYKKYSNT) and the other within the WHD2 domain of the C terminus (KADVGGDNGDGEGN). Antibodies were supplied with lyophilised peptide and this was used for affinity purification. Aliquots from the fourth and final bleed were used in affinity purification using a MicroLink® Peptide Coupling Kit (Pierce) according to manufacturer's instructions. Antibodies were recovered from the peptide column by three separate acid wash elutions followed by neutralisation with 5µl 1M Tris (pH9). Eluents were assayed for protein content using PrecisionRed (cytoskeleton) and the ones with the highest titre were used for probing western blots.

2.5.4 Probing blots

Blots were probed with affinity purified peptide antibodies at a 1:5000 dilution in TBST for 1 hour at room temperature. Following several rinses in TBST blots were probed with a secondary goat anti-Rabbit HRP antibody at a 1:10000 dilution in TBST for 1 hour at room temperature. After several rinses with TBST blots were incubated with MILLIPORE® Immobilon Western chemiluminescent HRP substrate for 5 minutes then imaged on a CHEMIgenius imaging system.

2.6 Immunofluorescence

2.6.1 Picric Acid/Formaldehyde Fixation

Cells were seeded onto coverslips (N^o:1.5) and given 30 minutes or longer to adhere. The cells were then fixed with picric acid as described in Humbel & Biegelmann (1992). In summary, cells were fixed with 2% (w/v) formaldehyde, 15% (v/v) concentrated picric acid, 10mM piperazine-N,N'-bis2-ethanesulfuric acid (PIPES) pH6.5 for 15 minutes. Coverslips were washed in PBS prior to post-fixation for two minutes with 70% ethanol followed by sequential washes in PBS glycine.

Fixative: 0.8g paraformaldehyde was added to 10ml dH_2O; 3-4 drops of 1M NaOH was then added, and the solution was heated at 42°C with occasional mixing until dissolved. The volume was adjusted to 14ml with dH_2O, and aliquots of 1.75ml were frozen. 0.75ml saturated picric acid and 2.5ml 20mM PIPES was added to an aliquot of paraformaldehyde. The pH is adjusted to 6.5 using NaOH.

PBS/Glycine: 100ml PBS and 0.75g glycine (made fresh each time).

2.6.2 Staining

Following fixation coverslips were incubated with 33nm TexasRed phalloidin (Invitrogen) in PBS to visualise cellular F-actin structures. Cells were rinsed by successive washes with PBS prior to mounting upon glass slides using Prolong Gold (Invitrogen).

2.7 Folate chemotaxis assay

Observation of *Dictyostelium* cells migrating towards folate under a thin layer of agar was performed as previously described by Laevsky & Knecht (2001). Three troughs roughly 2mm wide were cut into SM agar. The central trough was filled with 0.1mM folic acid, which diffuses out forming a gradient between its neighbouring troughs. Cells harvested from log phase of growth were added to the troughs either side of the folic acid at a density of $1x10^6$cells/ml. Using a Nikon TE2000 inverted microscope phase-contrast time-lapse movies were taken of cells as they moved under the agar towards the folate stimulus. Cells were imaged within 8 hours of adding the folic acid.

2.7.1 Cell speed quantification

The mean speed of chemotaxing cells under agar was determined using the manual cell tracker plugin for ImageJ (ImageJ: http://rsb.info.nih.gov/ij/). Time-lapse images were taken every 30 seconds for a period of 20 minutes. The centroid of the cell was estimated by eye on each frame and the xy coordinates used for calculating cell speed.

2.8 Endocytosis/Exocytosis assays

Rates of fluid phase uptake and exocytosis were assessed in *Dictyostelium* cells by fluorometrically measuring intracellular levels of FITC conjugated Dextran as described by Rivero & Maniak (2006).

2.8.1 Endocytosis

Dictyostelium cells were harvested from shaken culture during log phase of growth. Flasks containing 10 ml of culture at $1x10^6$ cells/ml were placed on a rotary shaker at 120rpm. 200µl of culture was pelleted and measured for protein content using PrecisionRed (cytoskeleton). 20mg of FITC-Dextran was added to flasks and 500µl samples were removed at each time point. Samples were pelleted and washed twice with ice cold KK2 buffer and finally pelleted and stored on ice until all time points had been collected. Samples were measured for FITC content by resuspending cell pellets in lysis buffer and measuring emission at 515nm with 470nm excitation on a PTI fluorimeter. Results were normalised to protein content

KK2 Buffer:	16mM KH_2PO_4; 4mM K_2HPO_4.
Lysis Buffer:	50mM Na2HPO4; pH9.3 (adjusted with NaOH); 0.2% Triton X-100 (v/v).

2.8.2 Exocytosis

10ml Shaken cultures at $1x10^6$ cells/ml were incubated with HL5 medium containing 20mg FITC-dextran. Cultures were then pelleted and washed twice with HL5 medium and finally resuspened in 10ml of HL5 medium with FITC-dextran. Samples were collected and measured for FITC fluorescence as above. Values were normalised to the fluorescent value at time point 0.

2.9 Growth rate assay

Cultures were grown in shaken culture on a rotary shaker at 120rpm. Samples were periodically taken and analysed using a CASY® Technology Cell counter (Roche Innovatis) and the data exported using CASYexcell 2.2. To measure the effects of dextran on axenic growth cells were cultivated in HL-5 medium containing 20% (w/v) dextran (65 – 90 KDa). Growth was assessed over a period of 5 days in which cultures exceeding $2x10^6$ cells/ml were diluted down to $1x10^5$ cells/ml with fresh medium.

2.10 Post-Lysosome visualisation

Visualisation of *Dictyostelium* post-lysosomes was performed utilising FITC and TRITC conjugated dextran as previously described by Rivero & Maniak (2006). Cells were seeded onto glass-bottomed dishes and incubated in LoFlo medium containing 4mg/ml FITC-Dextran and 40mg/ml TRITC-Dextran. After 60 minutes dishes were imaged on a Nikon A1 confocal microscope (FITC: excitation 488, emission 500-550. TRITC: excitation 561.4, emission 570-620). Microscope settings were adjusted using wild type Ax2 cells so that a range of intracellular pH values could be visualised. These settings were not changed between subsequent cell types or dishes. Settings used were not sensitive enough to detect any WASH GFP fusions due to their low level of expression. This allowed these cell lines to still be used in this assay without the GFP signal interfering and yielding false positives.

2.11 Pulse chase experiments

Wild type Ax2 cells were briefly incubated in LoFlo medium containing 4mg/ml FITC for either 10 or 20 minutes. After the pulse period the dish was rinsed with two rounds of fresh LoFlo medium, and imaged on an Olympus widefield fluorescence microscope at low magnification (40x objective). LatrunculinA was added to the dish at a final concentration of 2µM at various times during imaging. For washout experiments the dish was removed and

rinsed twice with fresh LoFlo medium and immediately returned to the microscope. Post-lysosomes were quantified with ImageJ using its built in Analyze Particles routine.

2.12 Agarose Beads

Microscopic agarose beads were made by placing 100µl of molten 1.5% agarose into 20ml of water saturated Butan-1-ol at 45°C. The mixture was placed in a sonicating water bath with ice and agitated by sonication and repetitive pipetting until the solution changed from transparent to opaque. The resulting beads underwent several rounds of washes in distilled water and finally passed through a 5µm filter. For fluorescent beads Oregon Green® conjugated dextran (Invitrogen) was added to molten agarose at 50°C before mixing with Butan-1-ol.

2.13 Microscopy

DIC and Phase Contrast microscopy were performed on an inverted Nikon ECLIPSE TE2000-E with a Retiga EXi (QImaging) camera. Timelapse data was captured using µManager 1.3 (www.micro-manager.org).

Fixed samples were imaged on a Olympus IX81 with a Coolsnap HQ^2 (photometrics) camera captured using Velocity 5.1 (PerkinElmer). The microscope was fitted with a piezo z stage for acquiring z steps for deconvolution. The acquisition setup was assessed for spherical aberrations by measuring point spread functions (PSFs) using PS-Speck^{tm} microscope point source beads (Invitrogen). After determining there were no spherical aberrations samples were deconvolved with Volocity 5.1 using a calculated PSF.

Widefield live cell fluorescent imaging was performed on a custom built Nikon ECLIPSE TE2000-U TIRF microscope. The CASCADEII (Photometrics) camera was fitted with a beam splitter for simultaneous imaging of GFP and mRFP. Time lapse movies were acquired using Metamorph (Molecular Devices).

Confocal microscopy was performed on a Nikon ECLIPSE Ti using NIS-Eliments AR3.1 for acquisition.

Chapter 3

Identifying a role for WASH in the endocytic pathway of *Dictyostelium discoideum*

WASH was identified by Linardopoulou *et al*. (2007) and belongs to a novel subgroup of the WASP protein family widely conserved amongst eukaryotic organisms. In vitro work on purified proteins showed that WASH enhanced the nucleating activity of the Arp2/3 complex, a defining feature of WASP family proteins. However, their attempts to disrupt WASH in *Drosophila* yielded unviable larvae hindering further characterisation of its molecular role. The identification of a novel subgroup of the WASP protein family with no idea as to its cellular function raises a great deal of interest in the field of actin dynamics.

3.1 Identification of gene encoding WASH in *Dictyostelium*

Linardopoulou *et al* (2007) identified the human gene MGC520000 as a new subgroup of the WASP protein family and as a result renamed the coded protein WASH (**W**ASP **A**nd **S**CAR **H**omologue). A BLAST search using the *Drosophila* WASH homologue was performed against the *Dictyostelium* genome with a single homologue being identified coding by the gene DDB_G0292878. In keeping with the naming convention of *Dictyostelium* genes, DDB_G0292878 will now be referred to as *wshA*. Figure 1.1 shows a sequence alignment of *Dictyostelium* WASH against homologues from other organisms, including *Homo sapiens* and the disrupted *Drosophila* homologue.

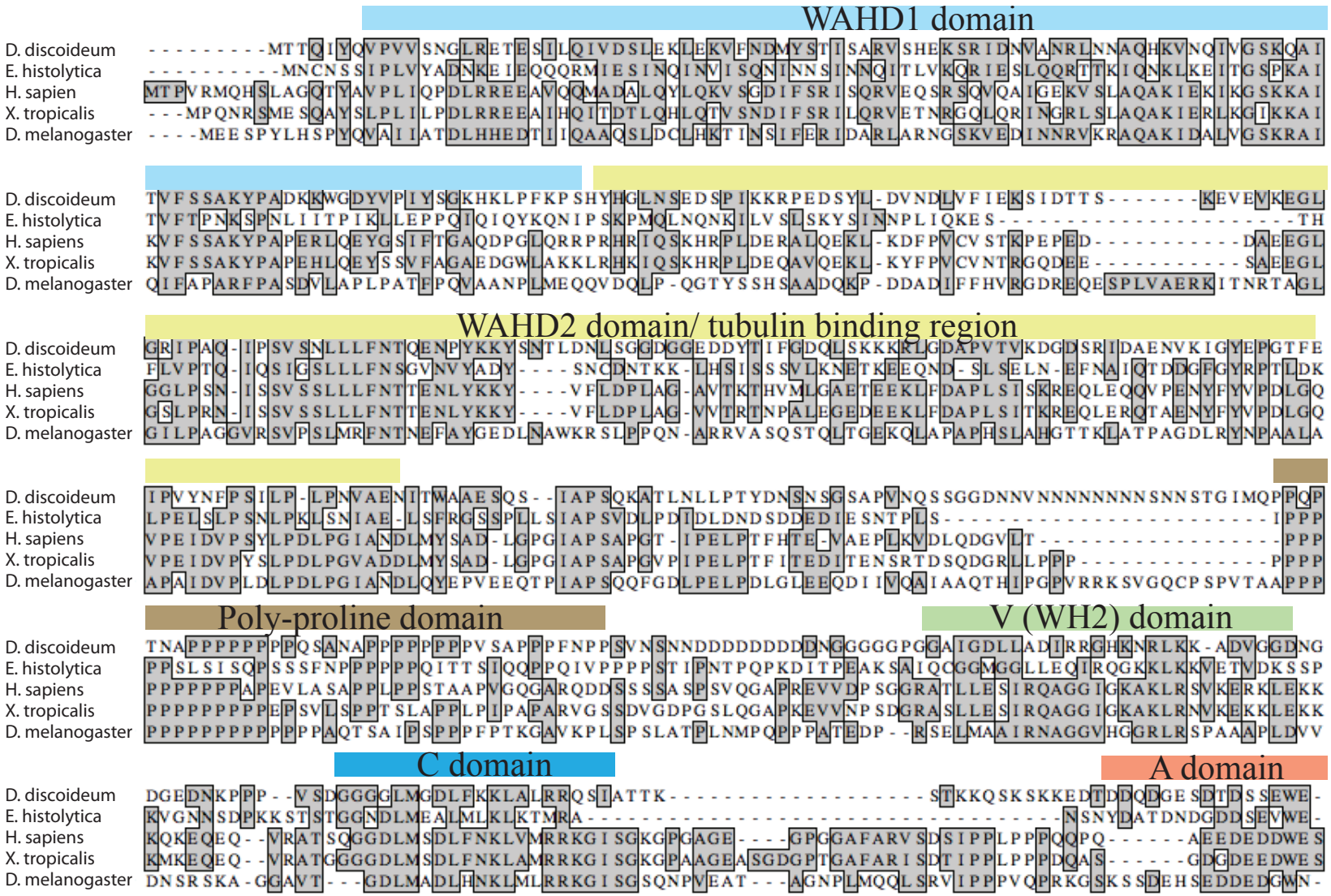
WAHD1 domain
WAHD2 domain/ tubulin binding region
Poly-proline domain
V (WH2) domain
C domain
A domain
D. discoideum
E. histolytica
H. sapien
X. tropicalis
D. melanogaster
H. sapiens

Figure 3.1: Alignment of WASH homologues.

Multiple sequence alignment of WASH homologues from *Dictyostelium discoideum* (Accession number: XP_629407), *Entamoebae histolitica* (Accession number: XP_656631), *Homo sapiens* (Accession number: NP_878908), *Xenopous tropicalis* (Accession number: NP_001016854) and *Drosophila melanogaster* (Accession number: NP_610739) using clustalW. Percentage Identity [**I**] and similarity [**S**] to the Dictyostelium homologue are as follows, *H. sapiens* **I**: 24.3% **S**: 39.6%, *E. histolitica* **I**: 18.8% **S**:31.3%, *X. tropicalis* **I**: 24.8% **S**: 38.1% *D. melanogaster* **I**: 22.3% **S**: 38.1%

3.2 Generation of WASH null mutants

To gain insight into the cellular function of WASH we set out to disrupt the single WASH homologue in *Dictyostelium* discoideum. Figure 3.2:A depicts the initial approach used to disrupt *wshA*. A DNA construct (pMJC07) was designed to insert a Blasticidin resistance (BSR) cassette half way into the genomic sequence of *wshA* by homologous recombination. In addition 29bp of coding sequence was removed to safeguard against genomic or mRNA rearrangements resulting in a full length *wshA* transcript. Wildtype Ax2 cells were transfected with pMJC07, from which 48 transformants were screened. Two successful recombinants (MC1 and MC2) were identified. Successful recombinants could be distinguished from random integrants by PCR of *wshA* from genomic DNA, yielding a product ~3kb compared to the parental 1.5kb band (Figure 3.2:B). This increase is due to the successful insertion of the BSR cassette (~1.4kb) into the middle of the genomic *wshA* gene.

To detect the presence of endogenous WASH, antibodies were raised against two different peptide sequences, one towards the N terminus and the other within the VCA domain of the C terminus (Figure 3.3:B). Both antibodies were affinity purified and used to probe Western blots of lysates from parental (Ax2) and MC1 cells (figure 3.3:A). Blots revealed the loss of a 60kDa band from MC1 lysate with both N and C terminal antibodies. WASH is predicted to have a molecular weight of 51kDa, however, some factors such as post-translational modifications and residual secondary structure can cause proteins to run at higher molecular weights than predicted. As both antibodies are targeted to different epitopes the loss of the 60KDa band in each blot likely represents the loss of full length WASH.

An additional band was observed in blots of MC1 lysates when probed with the N terminal antibody (Figure 3.2:B). This additional band ran at ~26KDa, roughly 43% the size of full

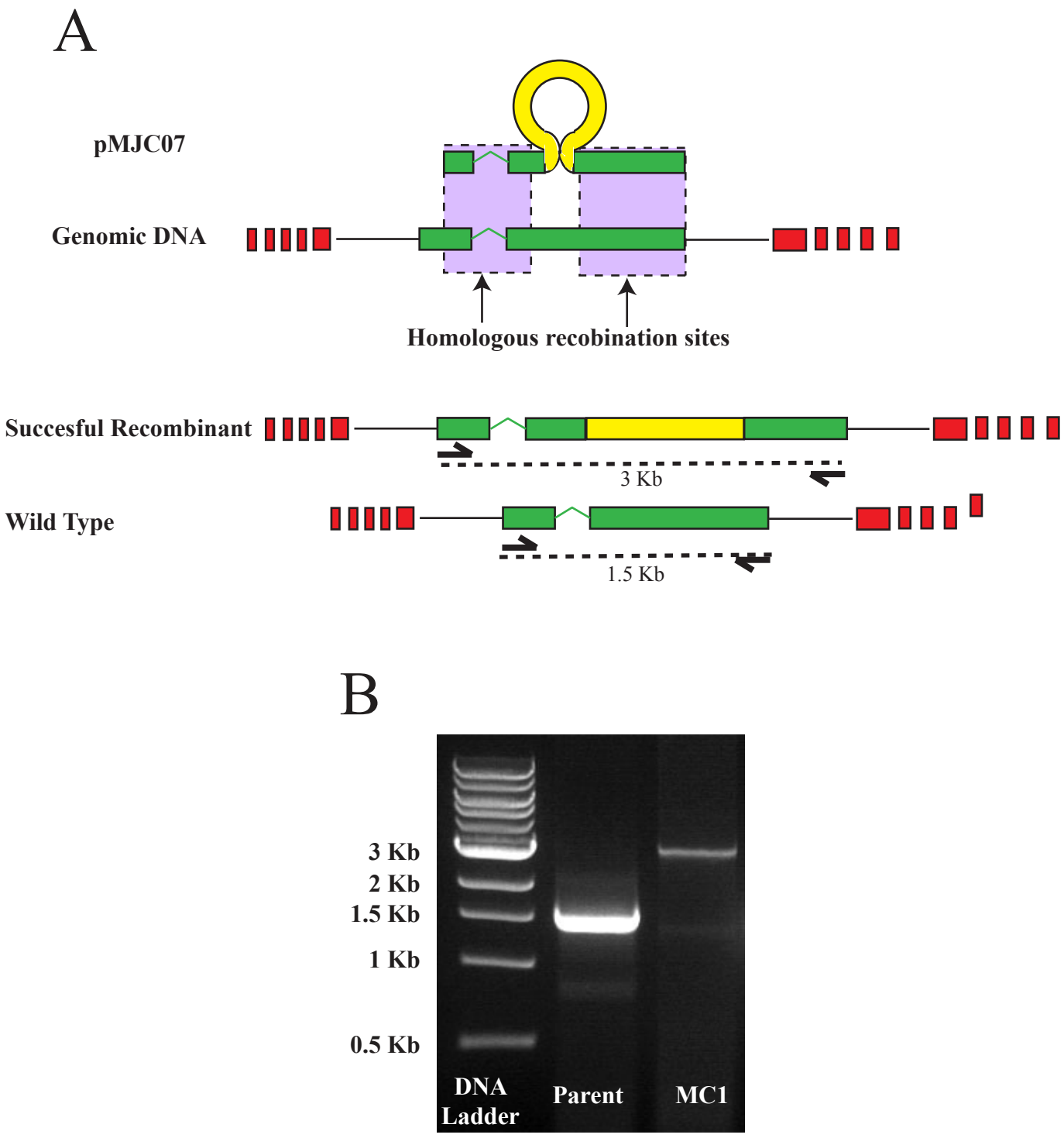

Figure 3.2: Generation of *wshA* disruptant using pMJC07.

(A) Schematic representation of method for targeted disruption and of wshA using DNA construct pMJC07, and identification. pMJC07 has two regions of homology within wshA. If both result in homologous recombination a Blasticidin resistance cassette will be introduced into the genomic sequence enabling selection by Blasticidin and identification by an increased size of PCR product of the wshA gene. (B) DNA gel of wshA PCR products form parental and MC1 genomic DNA. An increase of ~1.3Kb in MC1 is consistent with successful insertion of the BSR cassette, therefore disrupting WASH.

A

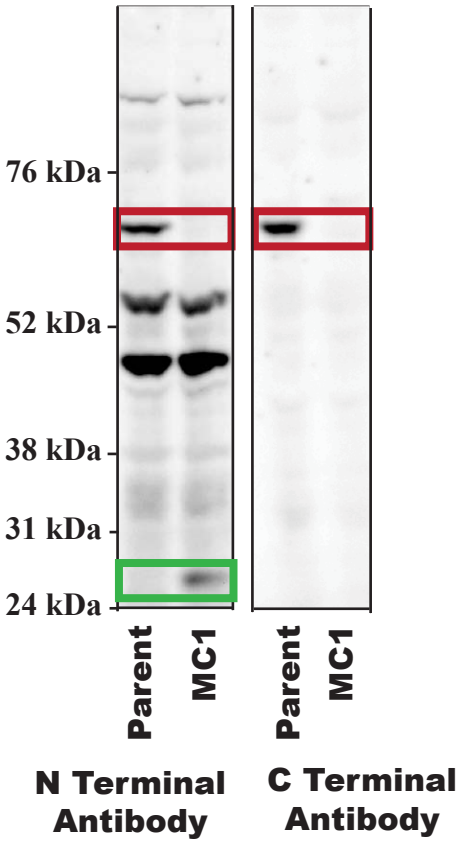

B

MTTQIYQVPVVSNGLRETESILQIVDSLEKLEKVFNDMYSTISARVSHEKSRIDNVANRLNNA
QHKVNQIVGSKQAITVFSSAKYPADKKWGDYVPIYSGKHKLPFKPSHYHGLNSEDSPIKKRPE
DSYLDVNDLVFIEKSIDTTSKEVEVKEGLGRIPAQIPSVSNLLLFNTQENPYKKYSNTLDNLS

BSR cassette

GGDGGEDDYTIFGDQLSKKKRLGDAPVTVKDGDSRIDAENVKIGYEPGTFEIPVYNFPSILP
LPNVAENITWAAESQSIAPSQKATLNLLPTYDNSNSGSAPVNQSSGGDNNVNNNNNNNSNN
STGIMQPPQPTNAPPPPPPPQSANAPPPPPPPVSAPPPFNPPSVNSNNDDDDDDDDDNGG
GGGPGGAIGDLLADIRRGHKNRLKKADVGGDNGDGEDNKPPPVSDGGGGLMGDLFKKLALRR
QSIATTKSTKKQSKSKKEDTDDQDGESDTDSSEWE

Figure 3.3: Verifying disruption of WASH and antibody validation

(A) Western Blots of parental and MC1 lysates showing loss of a 60KDa band (red box) when probed with N or C terminal antibodies revealing loss of full length WASH in MC1 cells. Green box shows additional band in MC1 lysate ~43% the size of full length WASH. (B) WASH protein sequence depicting site of disruption by BSR cassette insertion, and binding sites of the N (blue) and C (orange) terminal antibodies. This shows that 40% of wshA coding sequence is upstream of BSR insertion site, and contains the epitope for the N terminal antibody suggesting the upstream fragment is still being translated.

length WASH. The coding sequence upstream of the BSR insertion site accounts for 41% of the full length sequence suggesting this region is still being translated.

Concerns that the truncated protein expressed in MC1 cells may hinder interpretation of experimental results due to residual functionality required that a new cell line be created. Cell line MC4 was generated using the gene disruptant construct pMJC57 which utilises genes upstream (DDB_G0292876) and downstream (DDB_0292972) of *wshA* as recombination arms (Figure 3.4:A). This allowed removal of 86% of *wshA* sequence, and the engineering of a point mutation augmenting the start codon from ATG to ATT. Wild type Ax2 cells were transfected with pMJC57, from which 48 transformants were screened by western blot, identifying one successful recombinant (MC4). MC4 showed loss of a 60KDa band when probed with both N and C terminal antibodies showing the loss of full length WASH (Figure 3.4:B). No truncated protein was observed.

All future work and references to *wshA*^{null} indicates use of cell line MC4. It should be noted that all experiments in chapter 3 and section 4.1 and 4.3 were also performed using cell lines MC1 and MC2 yielding identical results. All references to parental cell lines indicate the use of wild type Ax2 cells. Cells where the constructs targeted to disrupt *wshA* had randomly integrated into the genome were briefly observed to display similar characteristic as wildtype Ax2 cells.

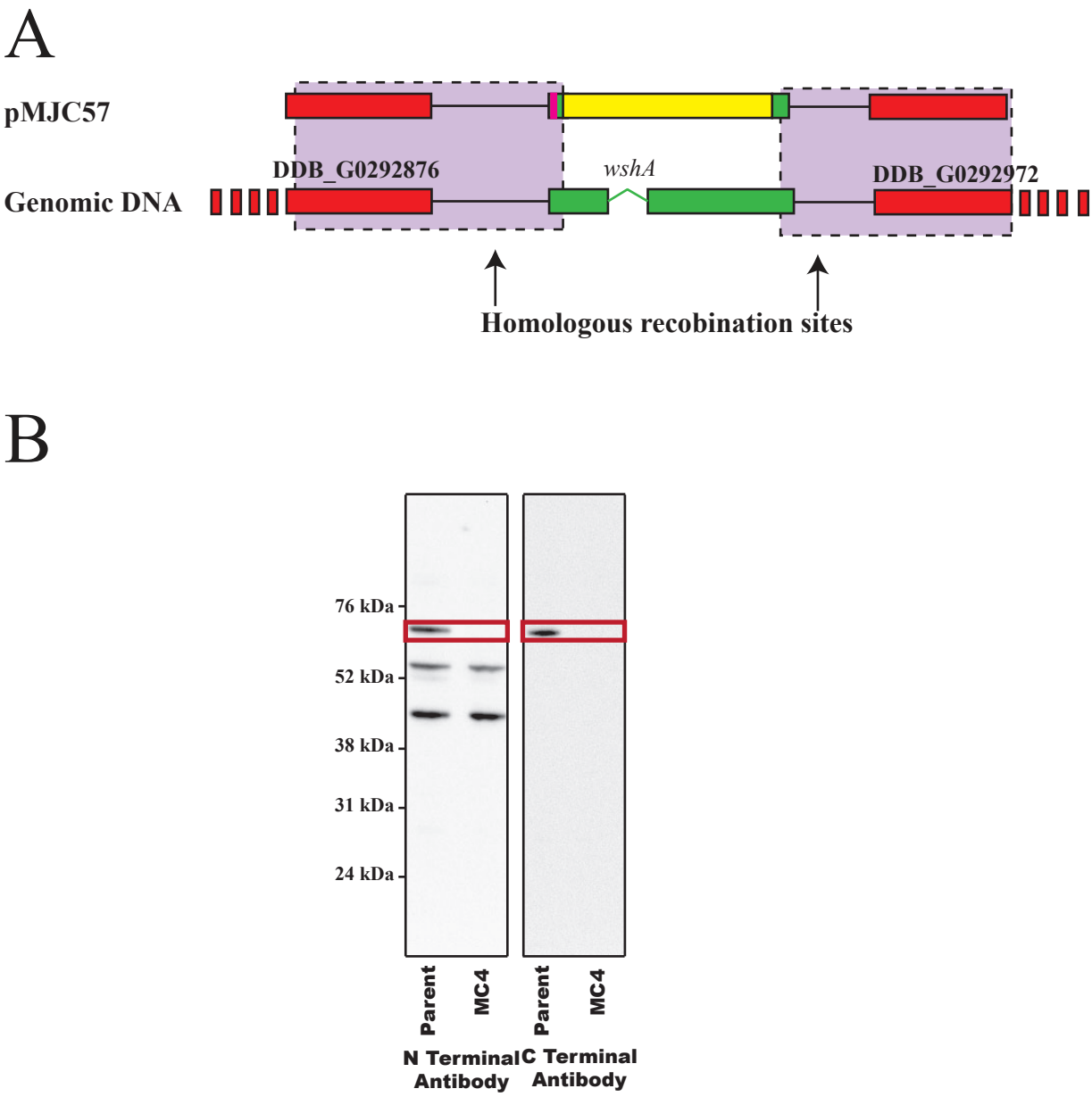

Figure 3.4: Generation of *wshA* disruptant using pMJC57

(A) Schematic representation of method for targeted disruption of wshA using DNA construct pMJC57. Using genes flanking wshA as sites of homologous recombination 86% of wshA was removed, the start codon augmented and a Blasticidin resistence cassette inserted for selection. (B) Western blots of parental and MC4 lysate with N and C terminal antibodies showing the absence of a 60KDa band (red box) consistent with loss of full length WASH.

3.3 Disruption of WASH does not hinder cell growth

As disruption of WASH in *Drosophila* resulted in unviable larvae, the growth of *wshA*^{null} cells was assessed as a general indication of cell wellbeing. Laboratory cell strains are typically maintained in axenic culture, and when grown in suspension growth rate and cell size distribution are easily monitored. Shaken cultures were periodically measured using a CASY counter ensuring cultures stayed above 1 x 10^5 and below 5 x10^6 cells/ml. Changes in population density were used to calculate average generation times for parental and *wshA*^{null} cells. Measured results indicated a small change in growth rate after disruption of WASH, however this could not be substantiated with statistics and was not significantly different (p value = 0.13; t-test) (Figure 3.5A).

Figure 3.5:B shows a representative cell size distribution from parental and *wshA*^{null} culture samples, as well as representative images of cells grown in shaken culture placed on glass-bottomed dishes and imaged by DIC microscopy. No gross changes were observed in population distribution or cell morphology of spread cells. Given there were no significant changes in generation time or cell size, disruption of WASH appears to have little effect on cell growth or division.

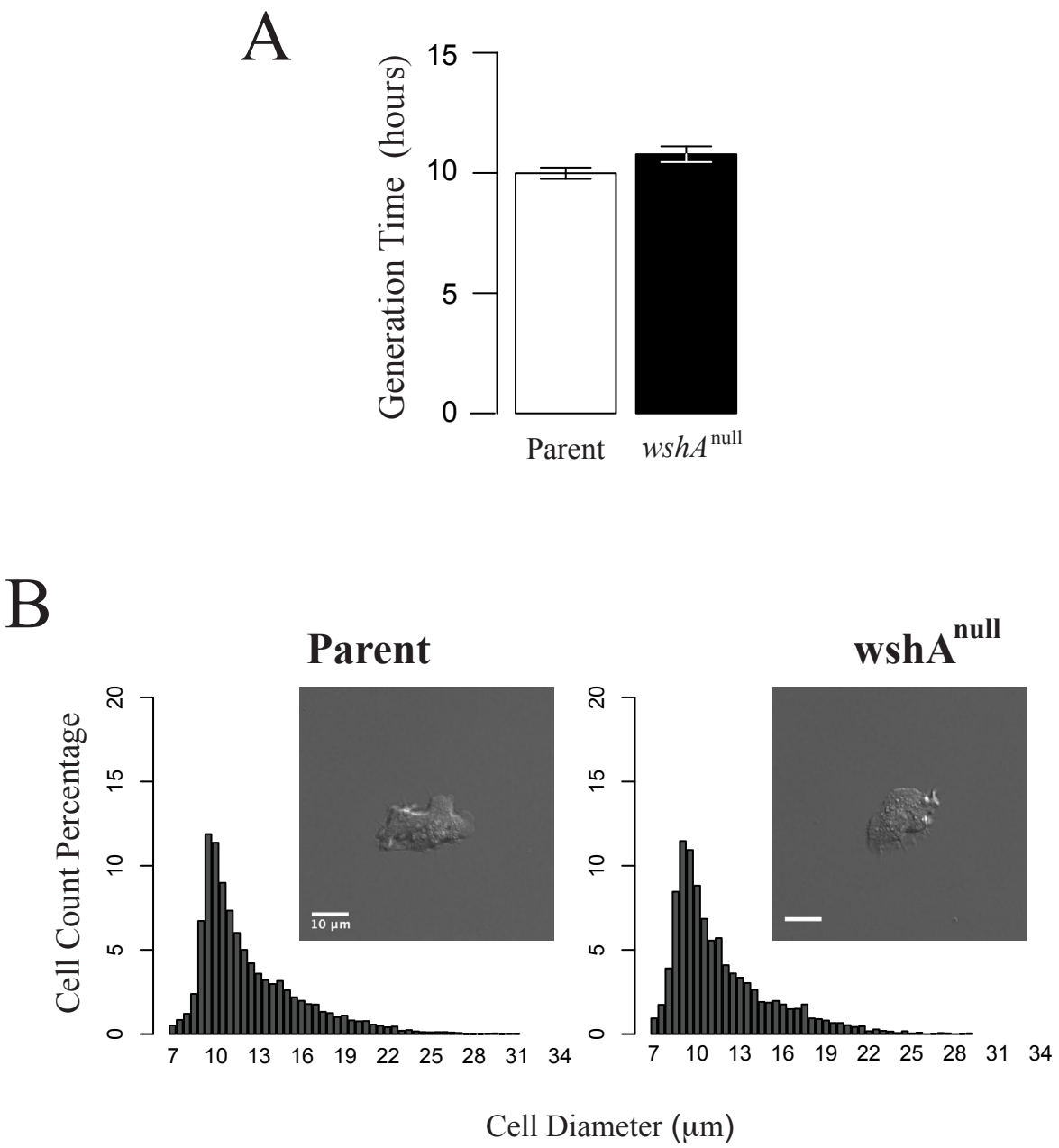

Figure 3.5: Growth of Parental and *wshA*^{null} cells in axenic shaken culture

Showing no difference in growth between parental and *wshA*^{null} cells grown in suspension shaken cultures. (A) Mean generation time calculated from growth curves of 3 independent experiments. Error bars represent standard error. No significant difference was seen ($p = 0.13$) (B) Graphs showing a representative population size distribution from a typical sample. Inset is an image of a representative cell from that sample placed on a glass-bottomed dish and imaged with DIC microscopy. Scale bar is 10µm.

3.4 *wshA*^{null} cells have defective growth on bacterial lawns

Disruption of WASH in *Dictyostelium* proved not to be lethal yielding opportunities to assess its cellular function.

During screening of *wshA* disruptants cells were seeded onto bacterial lawns as a way of ensuring that cell strains are clonal. During this process it was noticed that *wshA*^{null} cells showed a noticeable defect when grown upon bacterial lawns. *Dictyostelium* utilise a range of cellular processes when growing on bacteria lawns including phagocytosis, cytokinesis, and chemotaxis, all of which have previously been documented to utilise the actin cytoskeleton (See Introduction). Any of these if perturbed would be predicted to yield visual signs when cultivated on bacterial lawns.

Dictyostelium were clonally seeded onto lawns of *Klebsiella* and incubated in humidity chambers at room temperature for 72 hours. Each cell seeded onto this lawn undergoes successive rounds of bacterial consumption, growth and division. As bacteria become scarce the cells migrate outward to locate and consume more bacteria. Over time this results in an expanding circular plaque as the bacteria are consumed. Figure 3.6 shows that at comparable time points *wshA*^{null} cells have noticeably smaller plaques than parental cells. Given *wshA*^{null} cells grew normally in axenic culture this indicated that disruption of WASH could be hindering either chemotaxis or phagocytosis.

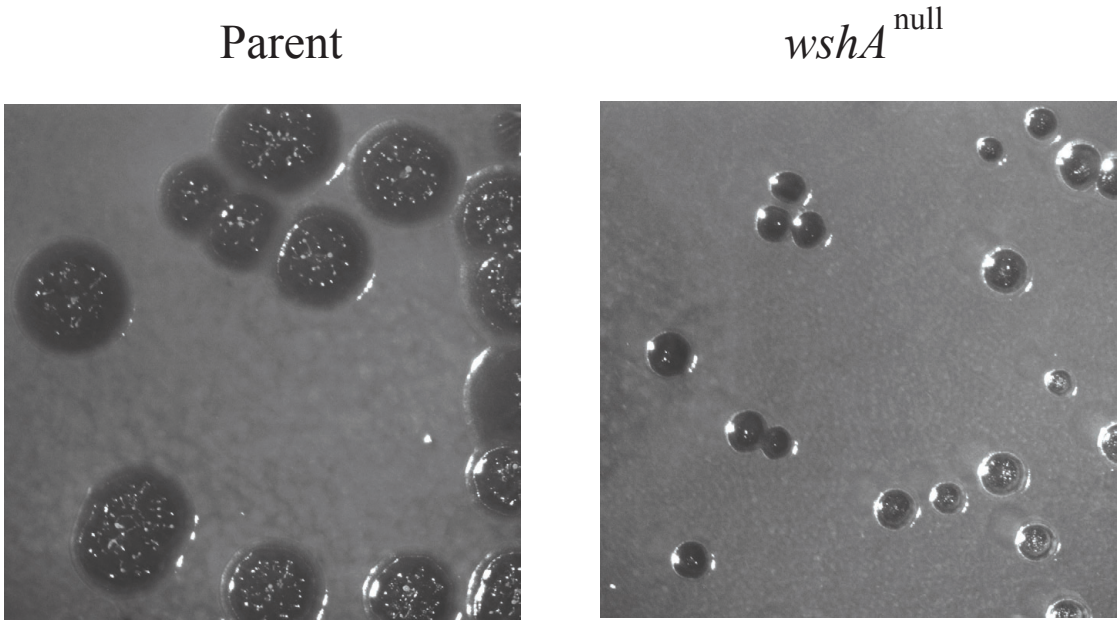

Figure 3.6: Growth of parental and *wshA*^{null} cells on bacterial lawns

Parent and *wshA*^{null} cells were clonally seeded onto *Klebsiella* bacterial lawns. Images were taken after 72 hours of incubation. This shows that *wshA*^{null} cells producenoticably smaller plaques than wildtype cells at comparable time points.

3.5 *wshA*^{null} cells have increased cellular motility

It had previously been shown that disruption of SCAR in *Dictyostelium* also resulted in defects when grown upon a bacterial lawn (Pollitt & Insall 2008). SCAR is involved in generating actin in cellular protrusions, disruption of which results in reduced cellular motility (Blagg *et al*., 2003). Cell motility requires the concerted efforts of several actin dependent processes, such as cellular protrusion (Miyata *et al*., 1999) and myosin aided contraction (Iwadate & Yumura, 2008). Therefore the effect of WASH disruption on motility was measured.

The migration of cells towards bacteria can be simulated in an optically favourable setting by observing axenic cells migrating under a layer of agarose towards folate. Using phase contrast time-lapse microscopy, chemotaxing cells were observed and cell speed was quantified (Figure 3.7). In this assay WASH was not required for cells to detect and migrate up the folate gradient (See supplementary movie 1 and 2). Interestingly however the disruption of WASH resulted in significantly faster migrating cells ($p = 0.001$; t-test). This is not a phenotype expected from disruption of actin machinery involved in cellular protrusions or retraction, and it is not clear how an increase in cell speed would yield a decrease in plaque size upon bacterial lawns. However, the phenotype of increased cell speed following gene disruption has been observed before with the disruption of *RasS* and *gefB* (Chubb *et al*., 2000). This previously demonstrated that wild type cells do not migrate at the fastest possible speed and that perturbing other processes can enhance migrational speed. This suggests that the increased speed may well be a secondary effect from the disruption of some other WASH related process.

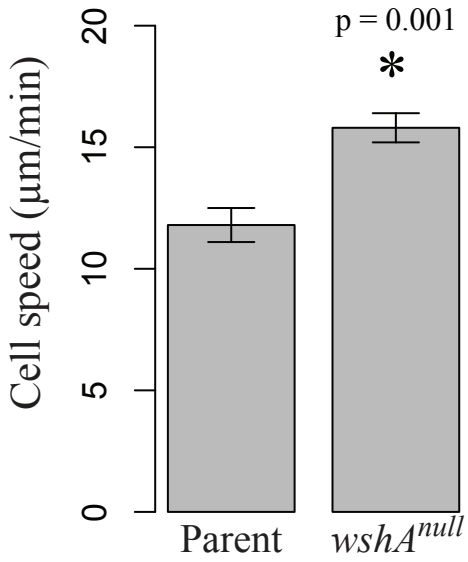

Figure 3.7: Cell speed of Parental and *wshA*$^{\mathbf{null}}$ cells during folate chemotaxis.

Graph depicting quantified average cell speed of cells migrating under a layer of agarose up a gradient of folate. wshA^{null} cells were shown to migrate significantly faster than that of parental cells (p value = 0.001). Values represent the average cell speed calculated from 5 independent experiments, in which the centroid of 9 cells were tracked in each instance. Error bars represent standard error.

During the course of measuring cellular motility several cytokinesis events were observed for both parental and *wshA*^{null} cells. Cytokinesis is also a process known to involve the actin cytoskeleton. Figure 3.7 shows still images from representative movies of cells dividing on glass-bottomed dishes under a layer of agar, however no gross defect was seen when comparing *wshA*^{null} cells to parental, visually confirming findings from axenic growth experiments.

3.6 *wshA*^{null} cells have normal endocytosis

In order to further determine the cause of the bacterial growth defect we looked at macropinocytosis and phagocytosis, both of which are actin-dependent processes required for the uptake of fluid and solid objects respectively. A defect in phagocytosis but not in endocytosis could explain the discrepancy between normal axenic growth rates yet a clear defect when cultured upon bacterial lawns.

Phagocytosis was indirectly assessed by briefly incubating cells adhered to glass-bottomed dishes with *S. cerevisiae*. The yeast are relatively large creating a more challenging obstacle to uptake in comparison to bacteria, and also making them easily identifiable after phagocytosis using DIC microscopy. Figure 3.9:A shows images of parental and *wshA*^{null} cells after 15 minutes incubation, showing *wshA*^{null} cells possessed a similar quantity of phagocytosed yeast particles. This indicated no major defect in phagocytosis.

Macropinocytosis was quantitatively assessed by measuring the cellular accumulation of fluorescently conjugated dextran over time. Following the addition of FITC-dextran to the

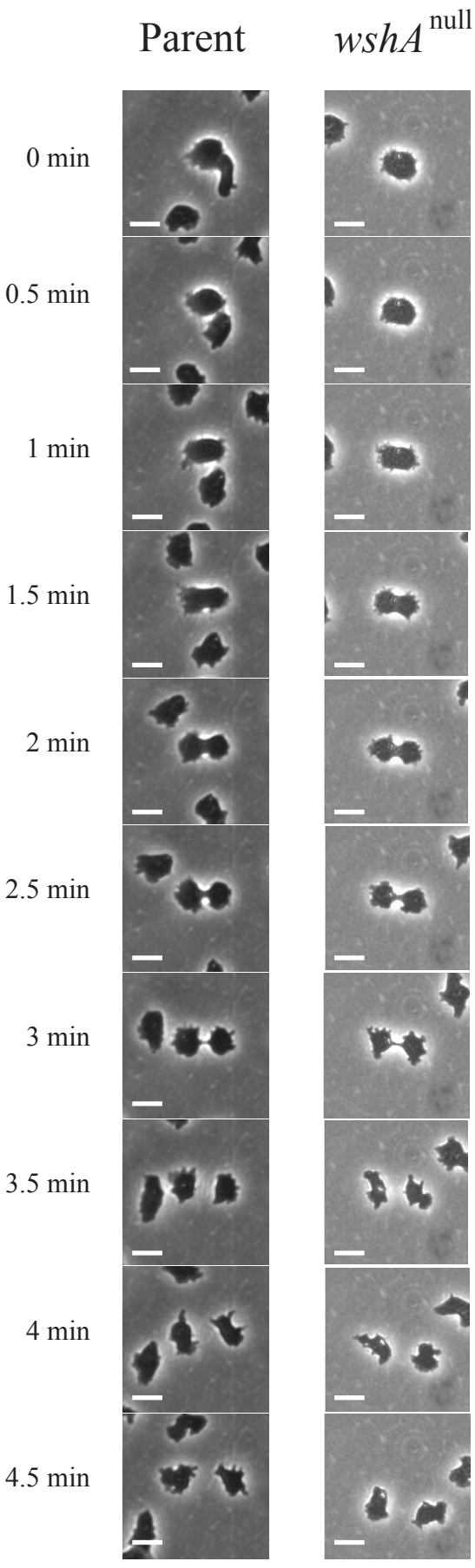
Parent
wshA null
0 min
0.5 min
1 min
1.5 min
2 min
2.5 min
3 min
3.5 min
4 min
4.5 min

Figure 3.8: Cytokinesis of Parental and *wshA*$^{\mathbf{null}}$ cells

Representative images of Parental and *wshA*^{null} cells undergoing cytokinesis on glass-bottomed dishes under a layer of agarose. Shows no gross defect in *wshA*^{null} cells ability to undergo cytokinesis. Scale bar shows 10μm.

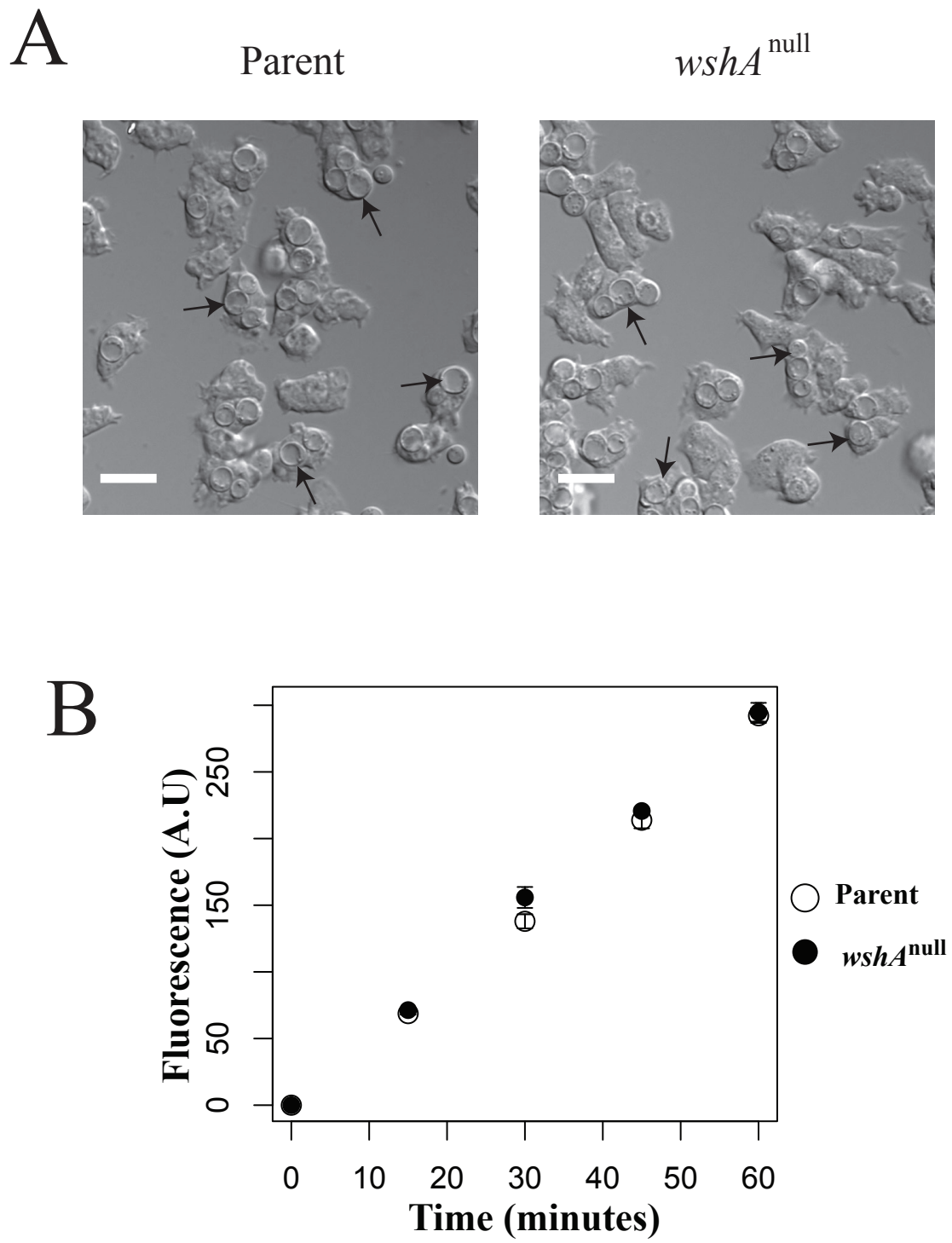

Figure 3.9: Endocytic uptake in parental and *wshA*^{null} cells.

(A) DIC Images of parental and wshA^{null} cells after a brief incubation (15 min) with

S. cerevisiae, showing that wshA^{null}, like parental cells, can efficiently phagocytose solid objects. Arrows highlight some internalised yeast. Scale bars show 10μm. (B) Graph showing identical rates of fluid phase uptake in parental and wshA^{null}cells. Cells were grown in shaking culture and following addition of FITC-dextran monitored for intracellular fluorescence levels (ex:470, em: 515). Readings were normalised based on culture protein content prior to addition of FITC-dextran. Error bars represent standard error from triplicate experiments.

medium of shaken cultures, samples were periodically taken and used to measure the cellular FITC levels using a fluorimeter (Excitation: 470nm; Emission 515nm). Figure 3.9:B shows accumulation of FITC-dextran in parental and *wshA*^{null} cells over time. Disruption of WASH showed no measurable difference in fluid-phase uptake.

3.7 *wshA*^{null} cells have a defect in exocytosis

Although no difference was seen in the rate of fluid phase uptake between parental and *wshA*^{null} cells, during the course of this experiment an unanticipated observation was made. Measuring the cellular accumulation of FITC-dextran only gives an accurate readout of endocytic uptake during the first 60 minutes. After this the earliest engulfed dextran will have traversed the endocytic pathway and begun to have been expelled. As the rate of exocytosis approaches that of endocytosis the cellular level of internalised FITC-dextran reaches equilibrium. Figure 3.10:A shows the fluid-phase uptake assay with extended time points. Interestingly, unlike the parental cell line that clearly shows a plateau after 90 minutes *wshA*^{null} cells continue to accumulate dextran at the same rate of endocytosis even at the last collected time point of 5 hours. This strongly suggests a defect in exocytosis of ingested material.

To more directly confirm a defect in exocytosis shaken cultures were incubated for > 4 hours in HL-5 medium containing FITC-dextran to saturate the endocytic pathway. The growth medium was then replaced with HL-5 medium without FITC-dextran and the cellular level of

FITC was measured over time. Figure 3.10:B shows the level of cellular fluorescence (ex: 470, em: 515) over time with fluorescence values normalised to the initial fluorescence level. It shows that parental cells after 1 hour have less than 50% of their initial fluorescence level, and by two hours ~20%. At comparable time points *wshA*^{null} cells have >90% with only a marginal drop even after 5 hours.

To confirm that the loss of WASH was responsible for the observed defect in exocytosis, WASH was re-introduced into *wshA*^{null} cells. Two constructs were generated to express exogenous WASH. Both contained a GFP tag at their N terminus, one construct expressed full length WASH (GFP-WASH) and the other a truncation removing the arp2/3 activating VCA domain (GFP-WASHΔVCA). Figure 3.11 shows western blots from lysates of *wshA*^{null} cells expressing these constructs. Even protein loading was confirmed with Ponceau S solution during blotting and is also clearly visible by the nonspecific bands when probed with the N terminal antibody (Figure 3.11:A). Both N and C terminal antibodies were used to show that both constructs are successfully overexpressed in *wshA*^{null} cell, and the loss of the VCA domain in GFP-WASHΔVCA is confirmed by the presence of a band in the cell lysate only when probed with the N terminal antibody (Figure 3.11:B).

The exocytosis defect in *wshA*^{null} cells is fully rescued by the over-expression of GFP-WASH (Figure 3.12). This confirms that exocytosis of dextran is dependent upon WASH, and that WASH can functionally tolerate an N terminal GFP fusion. Expression of GFP-WASHΔVCA failed to rescue the defect showing that the function of WASH in the endocytic pathway is dependent upon its ability to activate the arp2/3 complex (Figure 3.12).

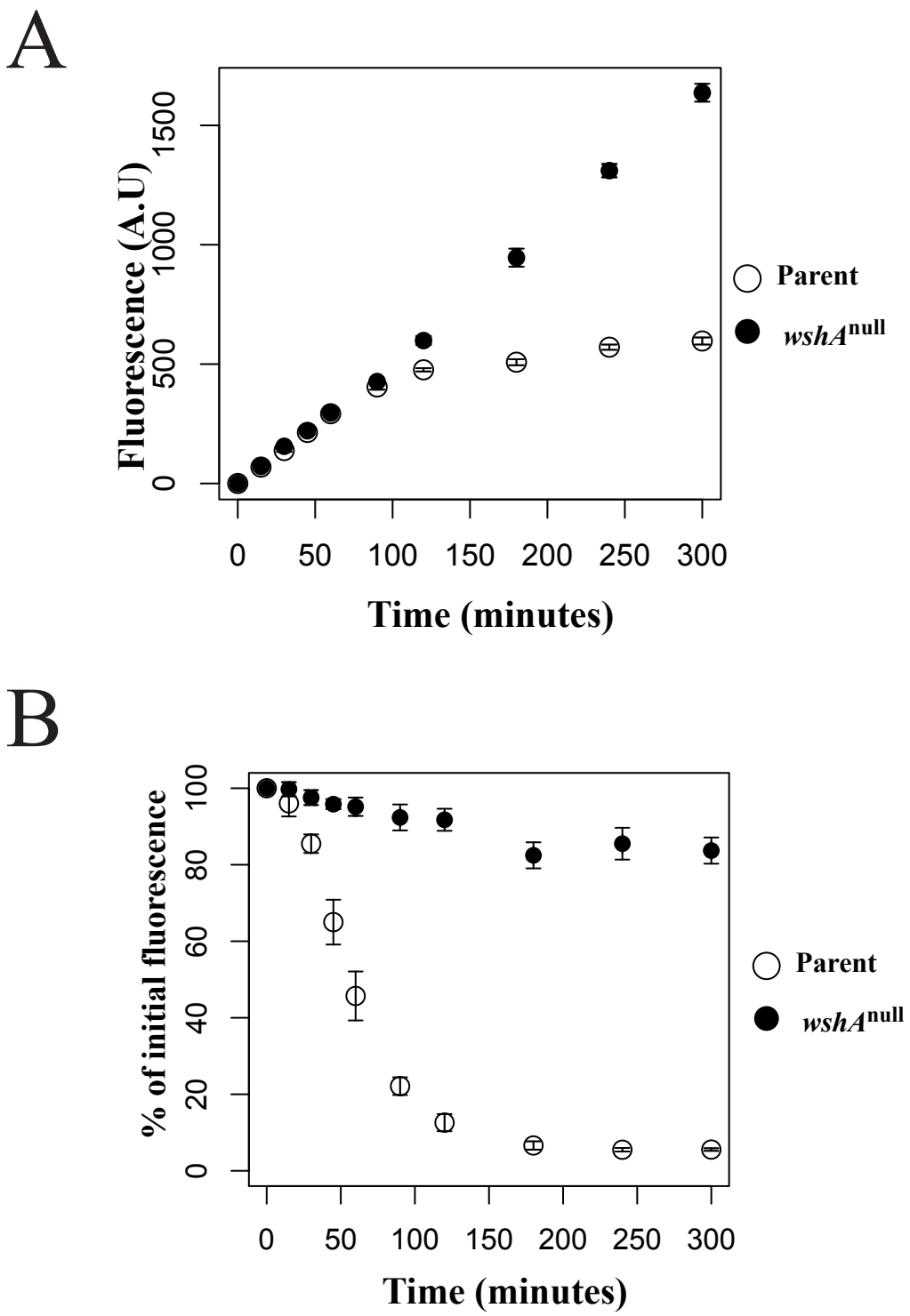

Figure 3.10: Exocytosis of FITC-dextran in parental and wshA^{null} cells.

(A) Extended time course of macropinocytosis assay (see. Figure 3.9). Graph shows

cellular accumulation of FITC-dextran over time. After 90 minutes parental cells begin to plateau, whereas wshA^{null} cells continue to accumulate at the same rate, suggesting a failure to exocytose dextran. (B) Graph showing rate of exocytosis. The endocytic pathway of cells was loaded with FITC-Dextran. After its removal from the medium the cells were measured for decreasing internal fluorescence (ex:470, em: 515) over time. wshA^{null} cells were drastically hindered in their ability to expel the dextran. Error bars represent standard error.

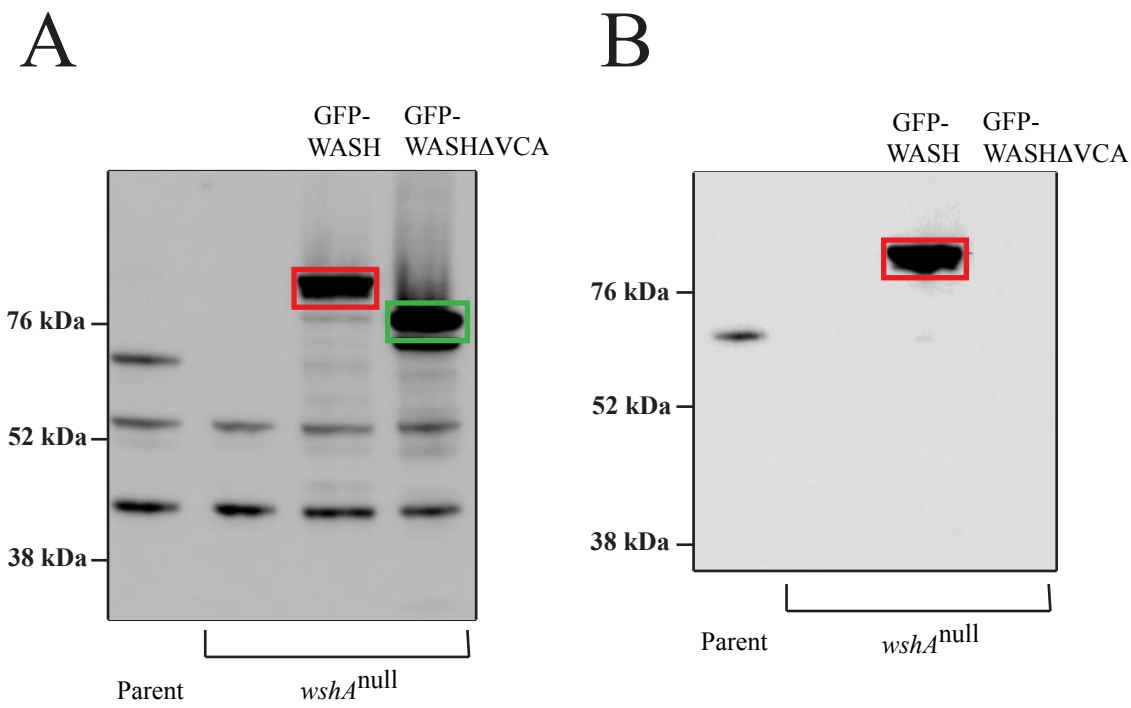

Figure 3.11: Expression levels of GFP-WASH and GFP-WASHΔVCA

Western blots of lysates from *wshA*^{null} cell lines expressing GFP-WASH or GFP-WASHΔVCA. (A) Blot probed with an antibody targeted towards the N terminus of WASH. Red box shows overexpression of GFP-WASH, running at a larger size due to addition of GFP. Green box shows overexpression of GFP-WASHΔVCA, with a smaller band due to removal of the VCA domain. (B) Blot probed with an antibody targeted towards the VCA domain of WASH. Red box shows overexpression of GFP-WASH, whilst the loss of a band in the GFP-WASHΔVCA lane shows that the expressed protein is lacking the VCA domain.

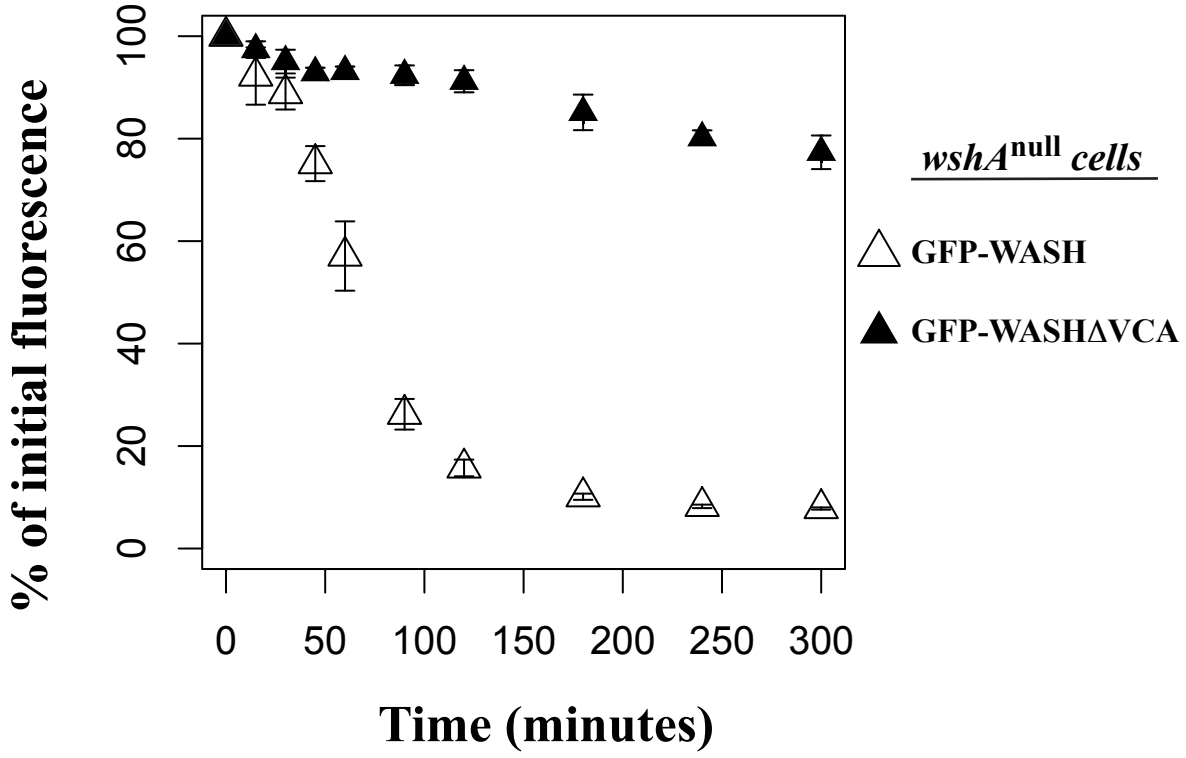

Figure 3.12: GFP-WASH rescues exocytosis defect in *wshA*^{null} cells.

wshA^{null} cells expressing GFP-WASH or GFP-WASHΔVCA were assessed to see if either construct could compensate for loss of endogenous WASH. The endocytoic pathway of cells was loaded with FITC-dextran, and following its removal from the medium cells were monitored for decreasing intracellular fluorescence (ex: 470, em: 515). Expression of GFP-WASH [Δ] rescued the defect in exocytosis where as the expression of GFP-WASHΔVCA [▲] did not. This shows that exocytosis of dextran is WASH dependent and requires its arp2/3 activation domain.

3.8 Effect of defective exocytosis on growth rate

A defect in exocytosis from the endocytic pathway provides a possible explanation regarding the discrepancy between the growth defect upon bacteria and normal axenic growth. Postulating that growth upon bacteria results in the consumption of a larger amount of indigestible material in comparison to axenic HL5 medium, and that in *wshA*^{null} cells this material accumulates hindering growth, cultures were grown in HL-5 medium containing indigestible 20% (w/v) dextran and observed for growth abnormalities (Figure 3.13:A). After 4 days growth in shaken culture containing 20% dextran both parental and *wshA*^{null} cells showed a statistically significant increase in generation time ($p = <0.05$; T-test). However, the differences in these increases were much larger in *wshA*^{null} cells resulting in a doubling in generation time in comparison with only a 10% increase in parental cells (p value = 0.001; T-test).

We also noted that the presence of dextran had clear effects on whole cell and intracellular vesicle size. Figure 3.14:A shows the percentage cell size distribution of representative samples from cells after 4 days growth with or without dextran. Dextran has a clear effect in *wshA*^{null} cells, broadening the cell size distribution resulting in larger cells (Figure 3.14:A). This was not seen in parental cells, where the presence of dextran was surprisingly observed to result in a narrowing of the distribution indicating an increase in uniformity. This may have implications on tissue culture implying that the addition of dextran to axenic medium may help reduce cell variability. When these cells were observed spreading on a solid surface with DIC microscopy, *wshA*^{null} cells showed dramatically enlarged intracellular compartments not observed in parental cells under similar conditions, or in parental or *wshA*^{null} cells without

dextran (Figure 3.14). This demonstrates that failure to expel indigestible material can have secondary effects on growth, potentially due to the disruption of processes such as cytokinesis by an overcrowding of the cytoplasm with distended vesicles

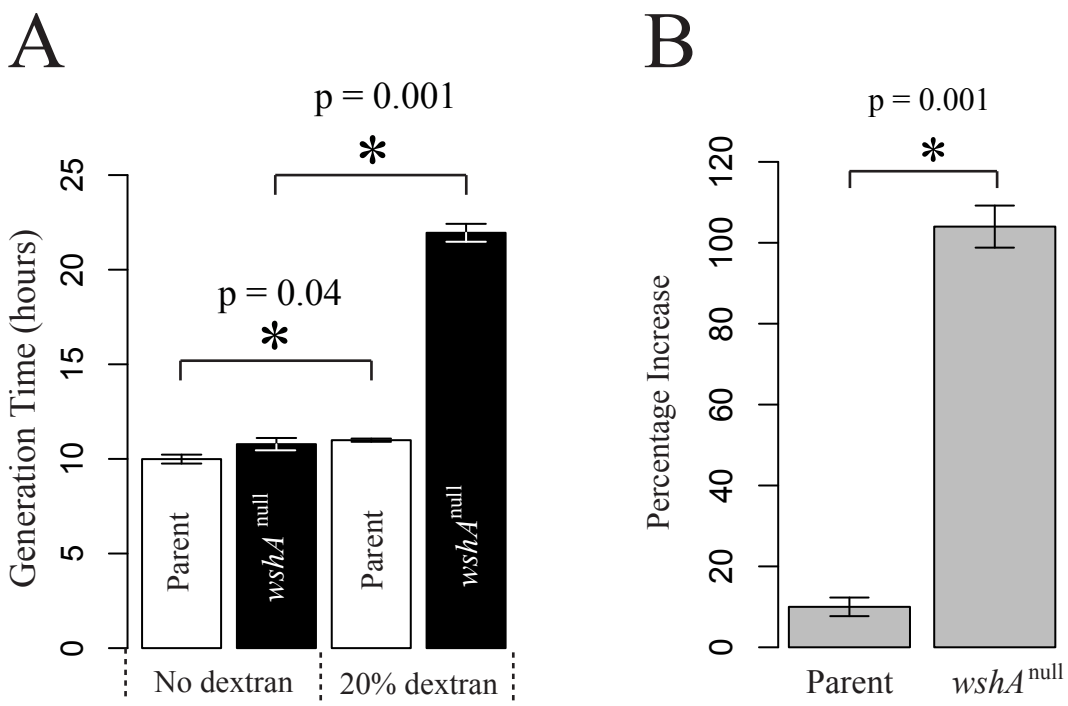

Figure 3.13: Effect of 20% dextran on generation time of parental and *wshA*^{null} cells.

Cells were grown in shaking culture containing 20% dextran (w/v). After 4 days growth curves were used to calculate average generation times. Error bars represent standard error. (A) Graph showing generation times of parental and *wshA*^{null} cells grown with and without dextran. A statistically significant increase was observed with both cell lines. (B) Graph showing that the increase in generation time was significantly larger in *wshA*^{null} cells compared to parental.

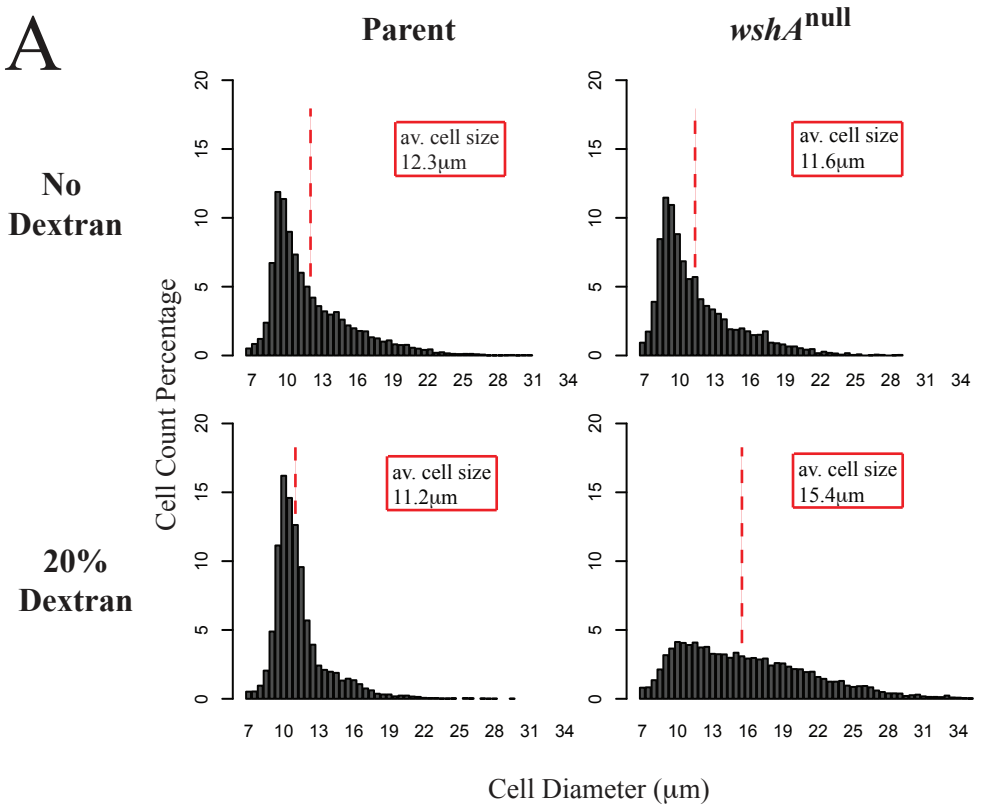
A
Parent
wshA null
No Dextran
20% Dextran
av. cell size 12.3µm
av. cell size 11.6µm
av. cell size 11.2µm
av. cell size 15.4µm
Cell Count Percentage
Cell Diameter (µm)

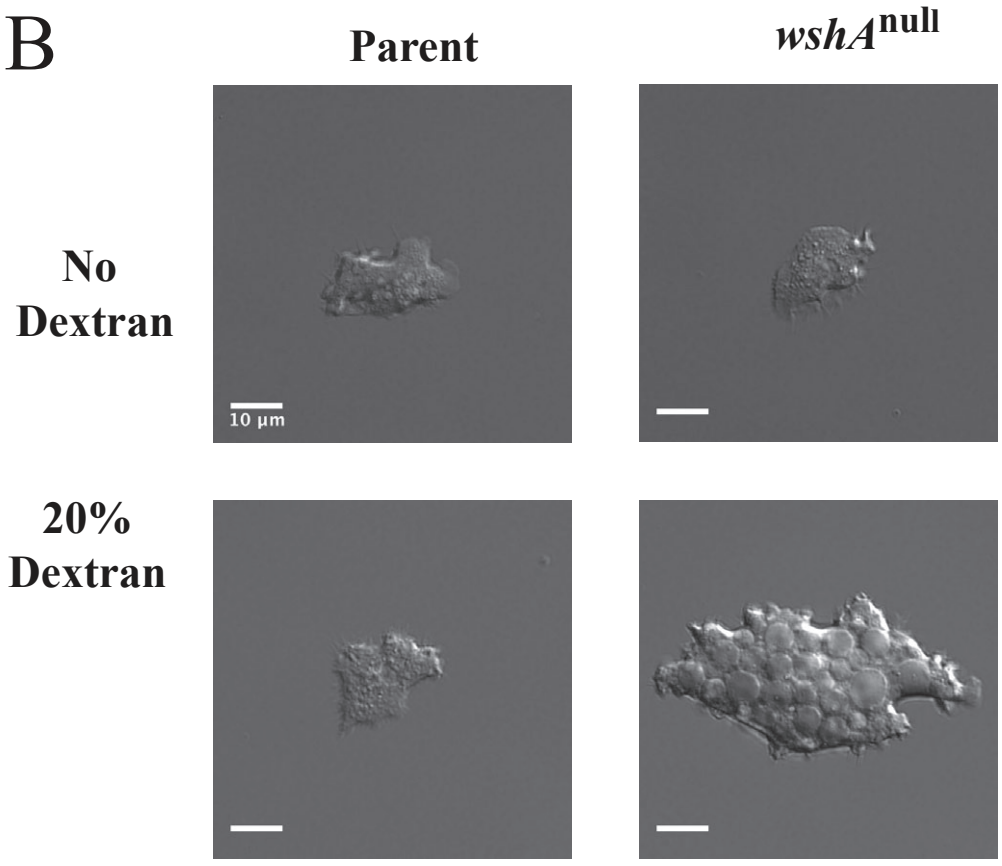
B
Parent
wshA null
No Dextran
20% Dextran
10 µm

Figure 3.14: Effect of 20% dextran on cell morphology of parental and *wshA*^{null} cells.

Cells were grown in shaken culture containing 20% Dextran (w/v) for 4 days. (A) Shows representative cell size distributions for parental and *wshA*^{null} cells grown with and without 20% Dextran. A visually noticeable difference was observed with *wshA*^{null} cells resulting in a larger spread of cell sizes. (B) Still images of cells taken from cultures on day 4 and allowed to spread on glass-bottomed dishes. *wshA*^{null} cells when grown in dextran were substantially bigger in size and contained enlarged vesicles. Scale bars show 10 μm.

3.9 Conclusions

The production of a viable WASH null cell line in *Dictyostelium* is a valuable tool for elucidating the cellular function of WASH. It removes doubts over residual expression levels continually troubling siRNA studies and questions of cell type specificity from multicellular organisms. However, care should be taken when generating knockout strains in *Dictyostelium*. It is common practice within the field to disrupt genes by inserting a selection cassette into the genomic coding sequence in the belief that the resulting transcript will be unstable and subsequently degraded. Expression of a truncated WASH protein in MC1 cells shows that this is not always the case. A default strategy should be the use of an upstream gene as a recombination arm allowing removal of the start codon and reducing the amount of upstream coding sequence of the targeted gene.

Disruption of WASH was shown not to have any direct negative effects on endocytosis, cellular growth, cytokinesis or cell motility, but was shown to be essential for exocytosis of indigestible material from the endocytic pathway. This is an observation that has not been seen with any other members of the WASP protein family suggesting WASH is functionally distinct from, and whose loss cannot be compensated for by other members of the WASP family. Surprisingly a block in exocytosis is not lethal. The endocytic pathway functions to take up nutrients and involves the equivalent of internalising the entire plasma membrane every 4 - 10 minutes (Aguado-Velasco & Bretscher, 1999). As no change was seen in growth rate or cell size in the absence of dextran, membrane retrieval and degradative pathways of

the endocytic pathway must remain intact. For clarity, from this point on the defect in *wshA*^{null} cells will be referred to a defect in defecation, to distinguish it from other membrane fusion events that must still occur.

Since this work was undertaken several papers have been published identifying roles for WASH in the endocytic pathway of mammalian cell lines. Knockdown experiments showed subtle defects in transferrin recycling (Derivery *et al*., 2009), retromer-mediated CI-MPR trafficking (Gomez & Billadeau, 2009) and enlargement and elongation of endosomes (Duleh & Welch, 2010). The observed defecation defect in *wshA*^{null} cells is not a direct measurement of the exocytosis process itself, but evidence of a defect somewhere along the endocytic pathway, suggesting an evolutionary functional conservation between *Dictyostelium* and mammalian WASH supporting its use as a model organism.

Depletion of WASH also had an unexpected increase in the rate of cellular motility. WASP protein family members act as positive regulators of actin assembly, and it is not clear how disruption of which can result in increased motility. However, it has previously been reported that the disruption of either *RasS* or *gefB* results in increased cellular speed (Chubb *et al*., 2000). In this study the authors argue that these proteins control the proportion of actin involved in macropinocytosis and motility, and there disruption results in more actin machinery available for motility processes. This showed that wild type cells do not already move at a maximum possible speed. Although disruption of WASH had no effect on fluid phase uptake, showing that the WASH specific defect is unrelated to *RasS* and *gefB* pathways, by a similar logic disruption of WASH may perturb other processes that clearly accelerates cellular motility.

Chapter 4

WASH-dependent actin formation is essential for post-lysosome formation.

The actin cytoskeleton has previously been shown to interact with internal organelles. However, to date its role has primarily been associated with vesicle translocation by actin-comet tail formation (Merrifield *et al*., 1999) actin cables for myosin aided movement (Aschenbrenner *et al*., 2003), or actin-coats as physical barriers to vesicle fusion (Drengk *et al*., 2003). The discovery of WASH as a nucleation promoting factor involved in the endocytic pathway of *Dictyostelium* could advance the understanding of the role of actin in vesicular trafficking.

4.1 WASH is required for formation of actin-coats surrounding endocytic vesicles

We previously showed that WASH was essential for trafficking of indigestible material through the endocytic pathway, and that this was dependent upon its VCA domain which is known to initiate actin nucleation through activation of the arp2/3 complex. To better understand the role of WASH-dependent actin in the endocytic pathway, F-actin structures in *wshA*^{null} and parental cells were compared for differences. Cells were fixed using formaldehyde and stained with fluorescently labelled phalloidin, which specifically binds and stabilises filamentous actin. Cells were then visualised using widefield fluorescence microscopy. Cells lacking WASH were seen to be completely devoid of internal spherical actin structures that appear to be actin-coats surrounding post-lysosomes, previously described by Rauchenberger *et al*., (1997). Although these actin-coats were observable by eye down the microscope, they were often dim and at times masked due to the blurred light from the much brighter signal of nearby cortical actin. Iterative deconvolution was used to improve

the visualisation of these structures. This process reassigns the convolved light back to its source mathematically, requiring multiple images focused at incremental Z positions for each field of view, and a calculated point spread function based on the emission wavelength of the fluorophore and the optics of the microscope. Figure 4.1:A shows deconvolved images of parental and *wshA*^{null} cells showing actin coated vesicles (arrows) that are lost upon WASH depletion. These were counted, excluding any spherical structures in contact with cortical actin as being macropinosomes. Parental cells contain on average 3-4 actin-coats per cell (Figure 4.1:B), but from rigorous quantification of 86 cells, and casually observing many more since, *wshA*^{null} cells were never observed to contain a single actin-coated vesicle.

Exogenously expressing GFP-WASH in *wshA*^{null} cells was previously shown to rescue the defect in defecation, demonstrating that WASH was not hindered by the presence of an N terminal GFP tag. Therefore we fixed cells expressing GFP-WASH and GFP-WASHΔVCA to observe their cellular localisation. GFP-WASH rescued the loss of actin-coats in *wshA*^{null} cells and localised to the same vesicular compartments implying a direct role in its formation (Figure 4.2:A). This was also shown by the expression of GFP-WASHΔVCA. This construct did not rescue the loss of actin coats but its localisation was similar to GFP-WASH, showing that the vesicles that possess actin-coats in parental cells are still present, but their lack of actin-coats is due to the loss of WASH-dependent arp2/3 activation.

This data shows that WASH is a nucleation promoting factor responsible for driving the formation of actin-coats around post-lysosomes in *Dictyostelium*. It has been the consensus that the domains within the N terminus of WASP family proteins control their localisation and

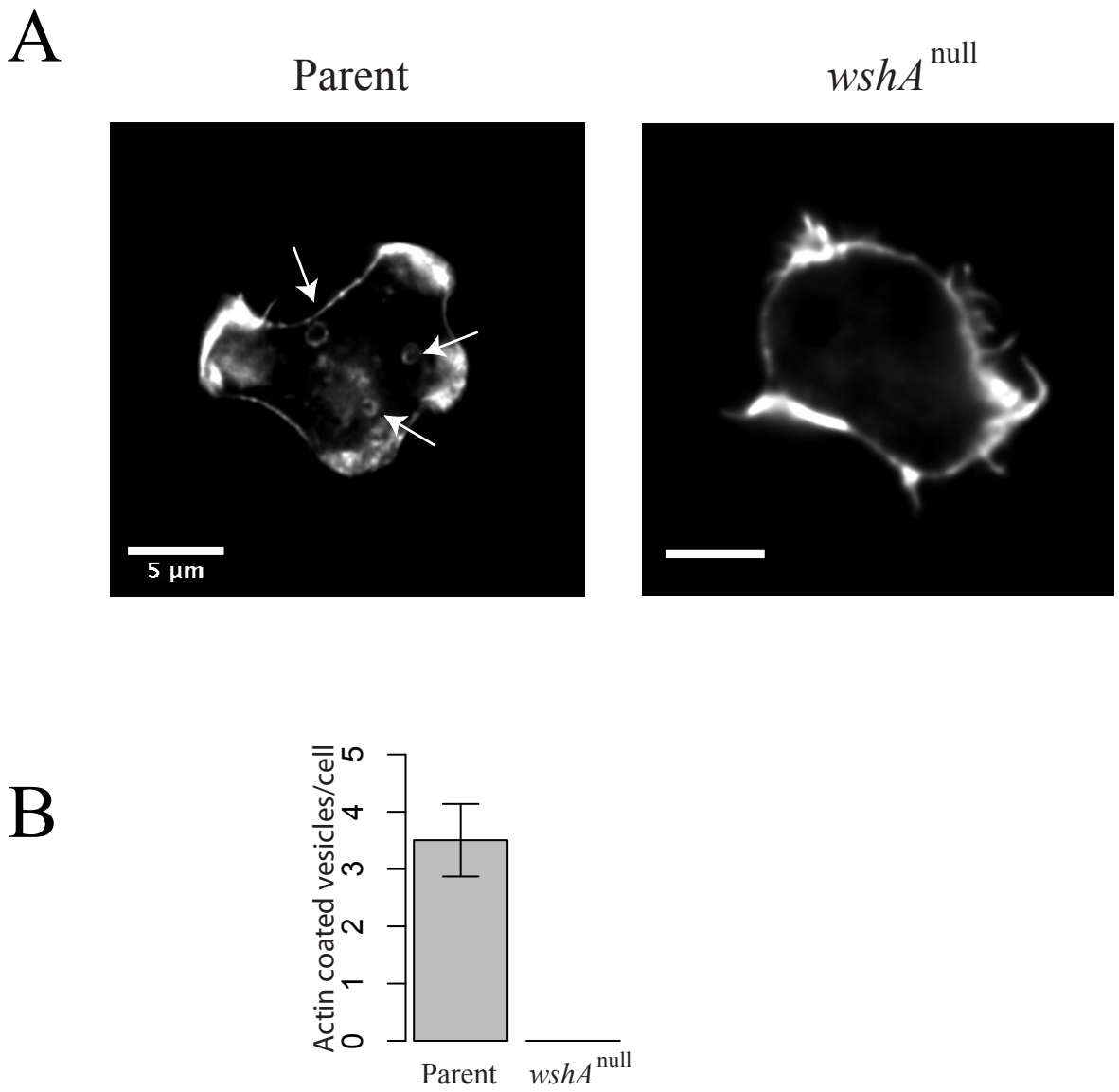

Figure 4.1: Visualising F-actin structures in parental and *wshA*^{null} cells after fixation

(A) Deconvolved images of fixed cells labelled with TexasRed-Phalloidin to visualise F-actin. Actin-coats around intracellular vesicles (arrows) are absent from *wshA*^{null} cells. Scale bar shows 5µm. (B) Mean number of actin-coated vesicles observed per cell. Values represent mean number of vesicles per cell. Error bars represent standard error from 3 independently performed experiments.

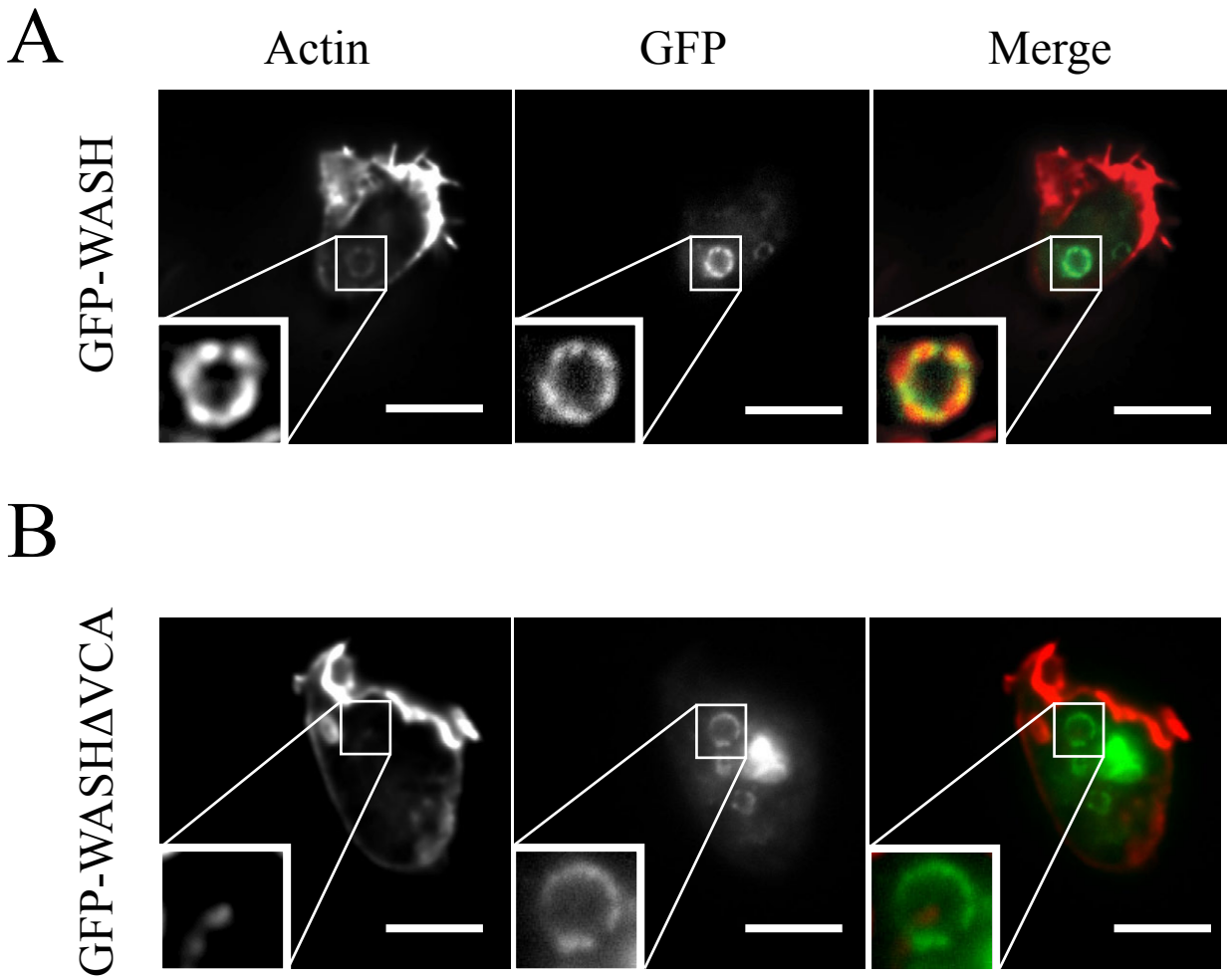

Figure 4.2: The VCA domain of WASH is required for actin-coat formation around intracellular vesicles.

wshA^{null} cells expressing GFP-WASH or GFP-WASHΔVCA were fixed with formaldehyde and stained with TexasRed-phalloidin to visualise F-actin. Magnified areas are also contrast enhanced. (A) GFP-WASH rescues the loss of actin-coats and localises to the same compartment. (B) GFP-WASHΔVCA failed to rescue the loss of actin coats whilst maintaining a vesicular localisation, plus an increased nuclear accumulation in ~30% of cells. This shows the VCA domain of WASH is essential for its role in regulating actin-coat formation, as well as regulating its nuclear accumulation. Scale bar shows 5 μm.

regulation whilst the C terminal is the active region. Although this does primarily appear to be the case with WASH, shown by a C terminal truncation resulting in loss of function yet retention of vesicular localisation, it was noted that a sub-population of these cells showed a strong nuclear localisation (see Figure 4.2:B) suggesting the C terminus also has roles in the spatial distribution of WASH.

4.2 WASH possesses a nuclear export signal in its C region

The observation that removal of the VCA domain could at times result in the nuclear accumulation of GFP-WASH suggested the presence of a nuclear export signal (NES) within this region. Linardopoulou *et al*., (2007) suggested WASH may have possible roles in the nucleus due to conserved nuclear import and export signals with vertebrate WASH homologous. To confirm if *Dictyostelium* WASH contains a NES within its VCA domain cells expressing GFP-WASH were incubated with an inhibitor of nuclear export to see if its cellular localisation phenocopies that of the VCA truncated construct. Cells were treated with 10ng/ml of Leptomycin B, a specific inhibitor of the nuclear export receptor CRM1 that when disrupted blocks nuclear export of proteins containing nuclear export signals. Figure 4.3 shows the percentage of GFP-WASH or GFP-WASHΔVCA expressing cells showing nuclear accumulation, seen by fluorescence microscopy. It shows that deletion of the VCA domain resulted in 33% of cells showing nuclear accumulation in comparison to 0% with full length WASH. Leptomycin B treatment of cells expressing GFP-WASH phenocopied that of the VCA truncated construct, with 32% of cells showing nuclear accumulation. The amino acid sequence of WASH was analysed by NetNES (www.cbs.dtu.dk/services/NetNES/) for

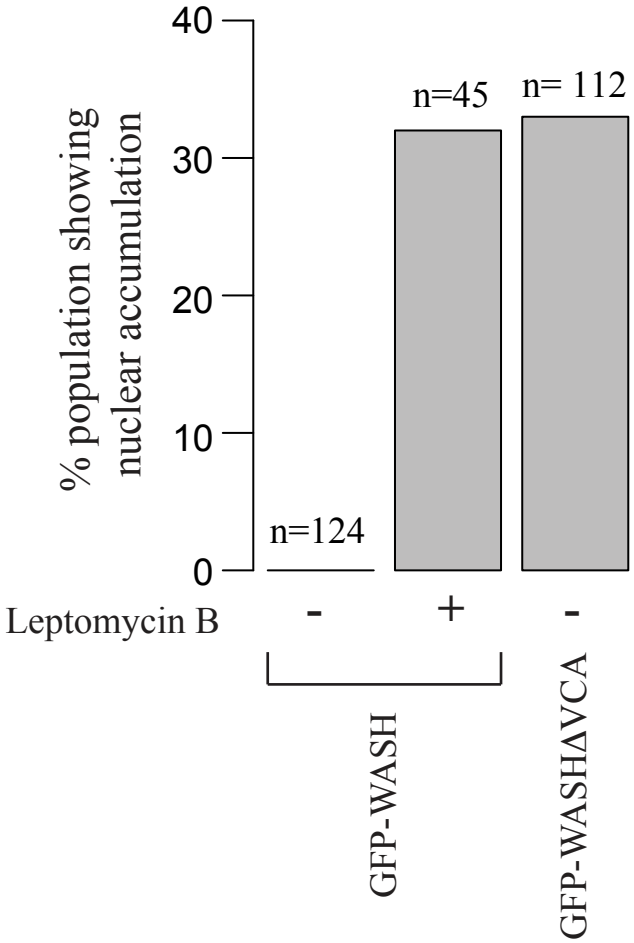

Figure 4.3: Leptomycin B treatment of cells expressing GFP-WASH.

Cells expressing GFP-WASH and GFP-WASHΔVCA were observed for nuclear accumulation by fluorescence microscopy. Values were calculated from multiple still images showing what percentage of the population at any one time has strong nuclear accumulation. 33% of cells expressing GFP-WASHΔVCA had nuclear accumulation in comparison to 0% with GFP-WASH. Treatment of GFP-WASH expressing cells with the nuclear export inhibitor Leptomycin B resulted in 32% of cells showing nuclear accumulation.

putative nuclear export signals. Figure 4.4 shows a graphic representation of the nuclear export signal (NES) score for each amino acid in the WASH sequence. A nuclear export signal is predicted if this score is above a set threshold (green line). A nuclear export signal was predicted within the C motif of the VCA domain of *Dictyostelium* WASH, consistent with experimental data. To see if this was a conserved feature of the C motif other WASH homologues were also assessed for putative nuclear export signals. No nuclear export signals were predicted within the C regions, with the exception of *S. mollendorffii*, however it was common for this region to generate a nuclear export signal score just below the threshold for identification. The high frequency of this pattern would suggest that this could be a common trait of the C motif but the predictive software may be quite cautious in its predictions. Other WASP family members in *Dictyostelium* were also tested for predicted nuclear export signals in their C region showing a confirmed prediction for SCAR but not WASP (Figure 4.5).

4.3 WASH is required for post-lysosome formation

Actin-coats surrounding endocytic compartments have been described previously in *Dictyostelium* (Rauchenberger *et al*., 1997). They had been shown to form around late endocytic vesicles, called post-lysosomes that are characterised by a neutral pH (Padh *et al*., 1993). Having identified WASH as the NPF responsible for actin-coat formation we set out to determine the consequences of its disruption on post-lysosomes.

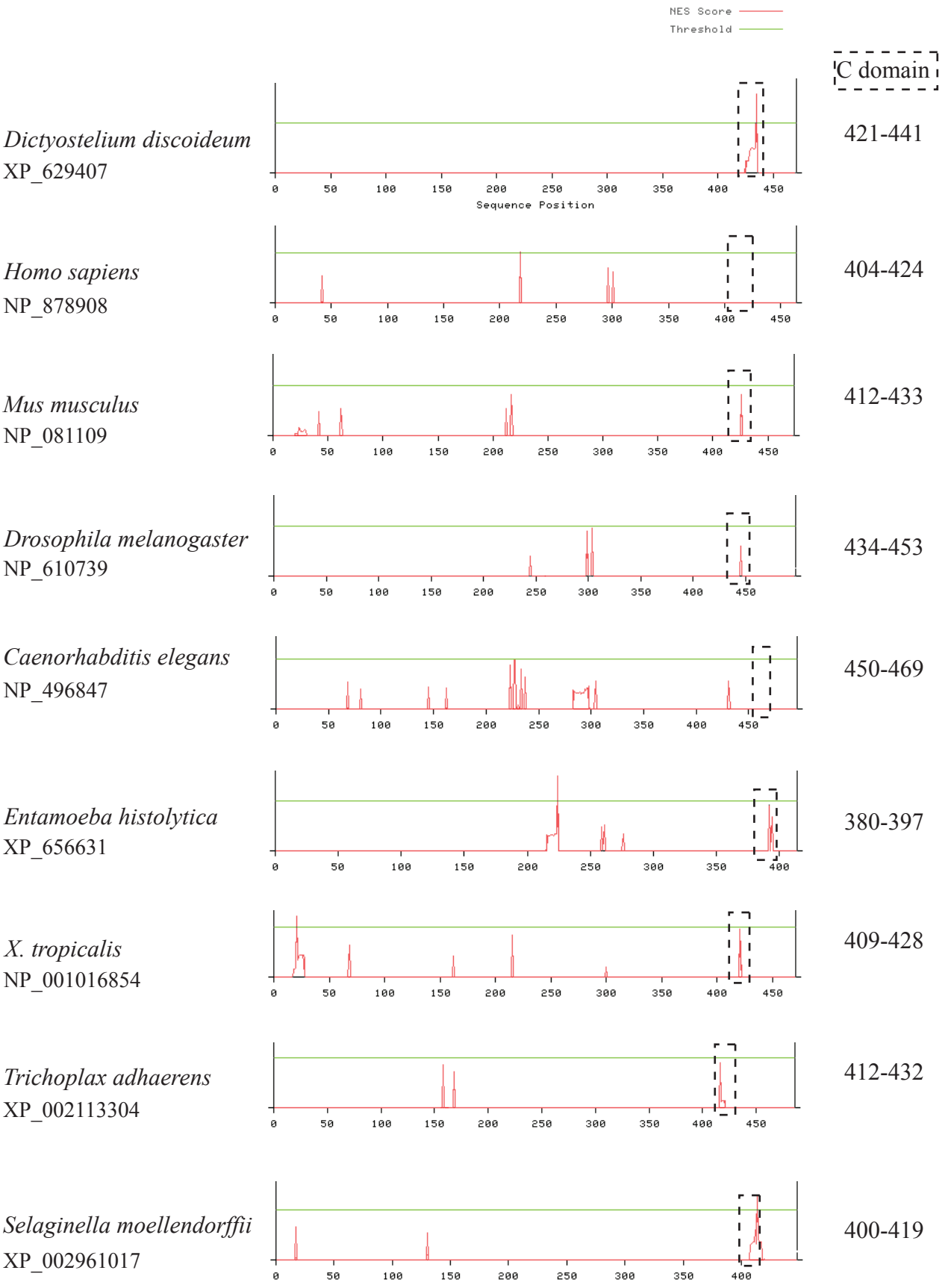
NES Score
Threshold
C domain
Dictyostelium discoideum
XP_629407
421-441
Sequence Position
Homo sapiens
NP_878908
404-424
Mus musculus
NP_081109
412-433
Drosophila melanogaster
NP_610739
434-453
Caenorhabditis elegans
NP_496847
450-469
Entamoeba histolytica
XP_656631
380-397
X. tropicalis
NP_001016854
409-428
Trichoplax adhaerens
XP_002113304
412-432
Selaginella moellendorffii
XP_002961017
400-419

Figure 4.4: Predicted nuclear export signal in WASH homologues

Graphs showing predicted nuclear export signals (NES) from multiple WASH homologues using NetNes. Red line shows NES score for each amin acid and green line shows threshold for predicted NES. Dashed box shows position of C region in each homologue.

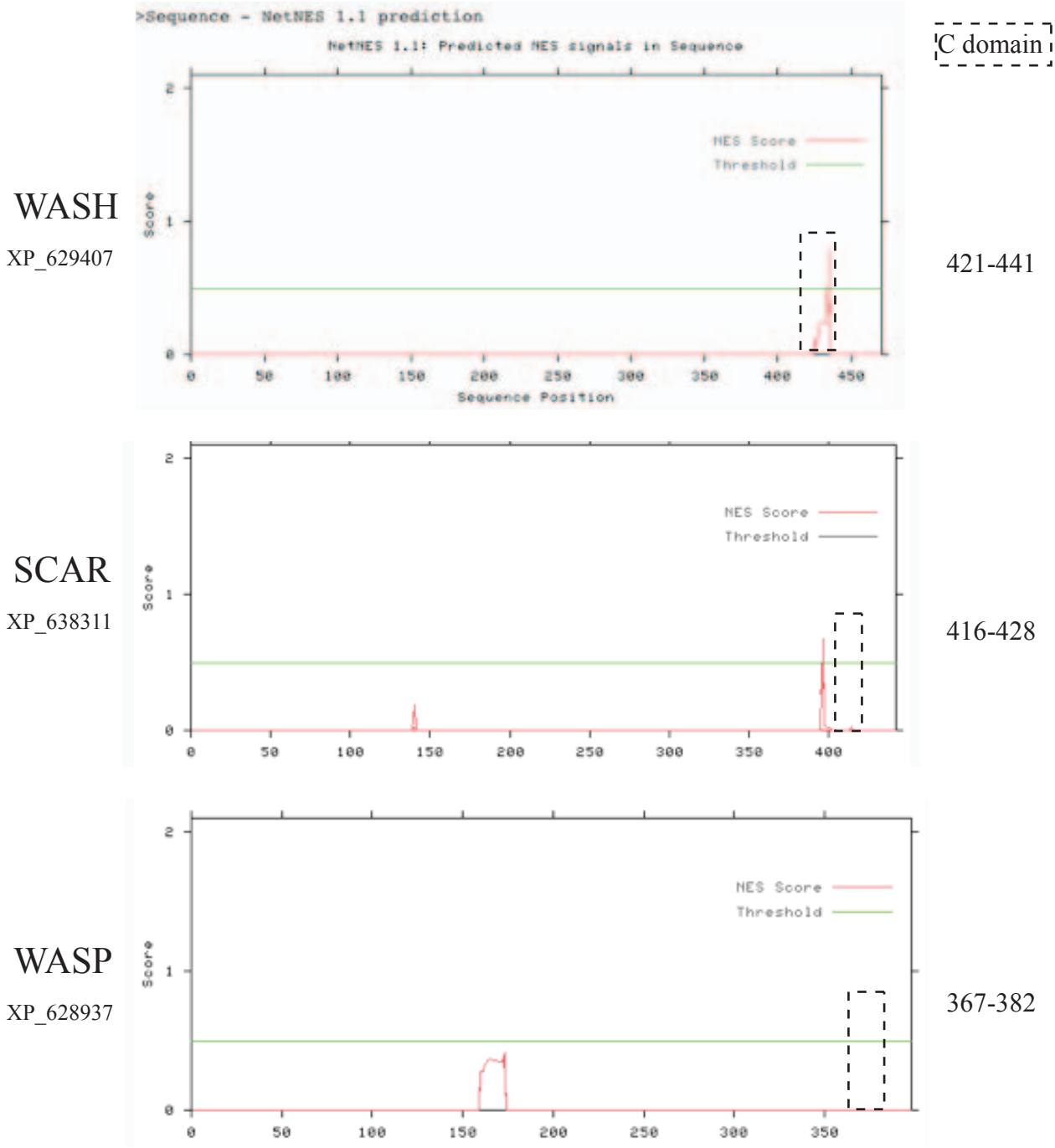

Figure 4.5: Nuclear Export Signal prediction of *Dictyostelium* WASP family proteins

Graphs showing predicted nuclear export signals from the three WASP family proteins in *Dictyostelium*. Red line shows predicted nuclear export signal score, and the green lines represents the threshold for prediction. Dashed box shows position of C motif in each protein. The nucear export properties of the WASH C motif are unique to WASH.

Compartments of the endocytic pathway in *Dictyostelium* can be visually distinguished based on their size, morphology, pH and luminal concentration of indigestible material when incubated in the presence of pH sensitive and insensitive dextrans. TRITC-dextran is pH insensitive and acts as a marker for fluorescently visualising the entire endocytic pathway, revealing the size and shape of endocytic compartments. The intensity of its fluorescent signal is dependent upon concentration. FITC-dextran is pH sensitive with its fluorescent signal decreasing with decreasing pH. Changes in the ratio between FITC and TRITC signal therefore indicate a relative pH change (Rivero & Maniak, 2006).

Early macropinosomes are large and have varying morphology with similar pH and dextran concentration as the surrounding medium. As they mature the luminal pH drops and membrane retrieval results the compartment decreasing in size locally concentrating the dextran. These later fuse with other endocytic vesicles eventually resulting in large, highly concentrated spherical compartments. The last and most noticeable change is upon the formation of post-lysosomes, where the large highly concentrated compartments have a sudden increase in luminal pH (neutralisation).

Figure 4.6 shows representative images of cells incubated in FITC and TRITC conjugated dextran for 1 hour and imaged by confocal microscopy. The red and green channels show TRITC and FITC emissions respectively. An overlay results in acidic vesicles appearing red whilst neutralised post-lysosomes look yellow or green. Disruption of WASH shows a complete loss of post-lysosomes that are clearly visible in parental cells (arrows). Cells lacking WASH still contained large concentrated acidic vesicles indicative of lysosomes. Like previously observed defects of defecation and loss of actin-coats, expression of GFP-WASH rescued the loss of post-lysosomes and this was dependent upon its VCA domain (Figure 4.6).

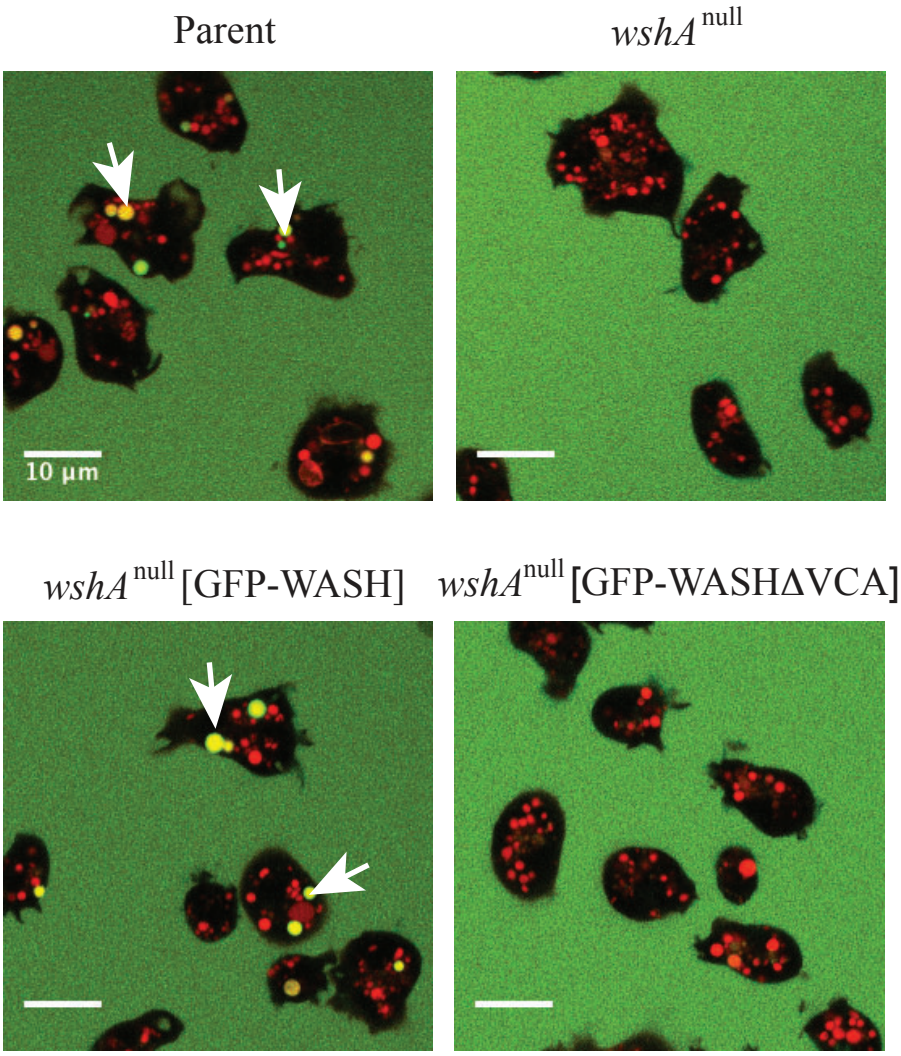

Figure 4.6: Visualisation of post-lysosomes in parental and *wshA*^{null} cells

Cells were loaded with FITC (pH sensitive) and TRITC (pH insensitive) conjugated dextran to differentiate between acidic and neutral vesicles. Acidic vesicles appear red due to the decreased FITC signal, whilst neutral vesicles are yellow or green (arrows). wshA^{null} cells lack post-lysosomes that can be seen in parental cells, and this can be rescued by expression of GFP-WASH but not GFP-WASHΔVCA. Scale bars show 10µm.

In addition, two other GFP constructs were created to attempt to disrupt WASH function whilst retaining its NES within the C motif. Expression of GFP-WASHΔA where the acidic region was removed failed to rescue the appearance of post-lysosomes showing this region is essential for WASH function (Figure 4.7). Within the acidic region of WASP family proteins there is a conserved tryptophan. Experiments showed that mutation of this residue to alanine reduces the efficiency of arp2/3 binding activation in vitro (Marchand *et al*., 2001). The lack of function of the *Drosophila* WHAMM has also been attributed to its loss of its C terminal tryptophan (Liu *et al*., 2009). Expression of GFP-WASHW471A in wshA^{null} cells resulted in formation of neutral post-lysosomes. This data shows that WASH and the actin-coats it nucleates are responsible for the formation or maintenance of neutral post-lysosomes in *Dictyostelium*. This suggests two possibilities. Firstly, WASH-dependent actin may act as a physical barrier (Drengk *et al*., 2003) preventing re-acidification of post-lysosomes by fusion with acidic compartments, and its disruption prevents the cell from maintaining any neutral vesicles. Secondly, WASH dependent actin may have an earlier function in the endocytic pathway than previously thought, and its disruption blocks the initial formation of post-lysosomes. The first hypothesis was tested using an actin depolymerizing drug, Latrunculin A. This drug binds to actin monomers depleting the pool of G-actin resulting in F-actin disassembly (Spector *et al*., 1982). To see if neutral post-lysosomes re-acidify without an actin-coat Latrunculin A was added to parental dishes 1 hour into the post-lysosome visualisation assay. After 15 minutes of treatment cells had rounded up indicative of disruption of cellular F-actin. In these cells post-lysosomes could still be seen (Figure 4.8). This suggests that actin-coats are not required to maintain a neutral pH. This experiment however does not rule out that re-acidification may also be actin dependent, and would require a method to specifically disrupt WASH function on demand after the formation

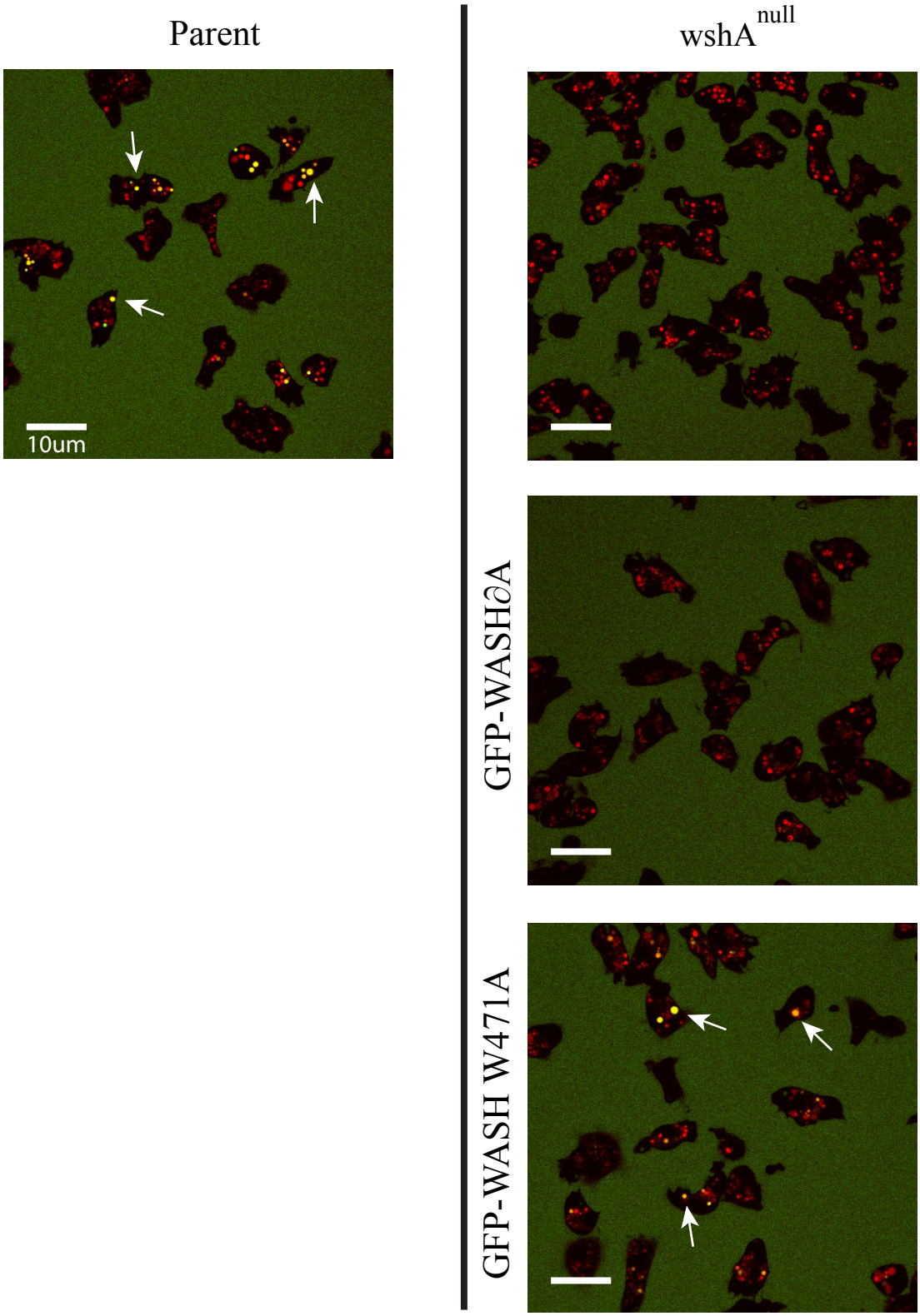

Figure 4.7: Effect of an acidic region deletion or tryptophan point mutation on WASH dependent post-lysosome formation

Vesicle neutralisation assay. Cells were loaded with FITC-dextran (pH sensitive) and

TRITC-dextran (pH insensitive) to distinguish acidic and neutral vesicles. Post-lysosomes appear yellow (arrows) and are absent in wshA^{null} cells. Exogenous expression of WASHΔA failed to rescue the loss of post-lysosomes. Deletion of the conserved tryptophanin the acidic region to alanine (W471A) was capable of rescuing the phenotype showing that the acidic domain is essential for function whereas the conserved tryptophan is not. Scale bar shows 10μm.

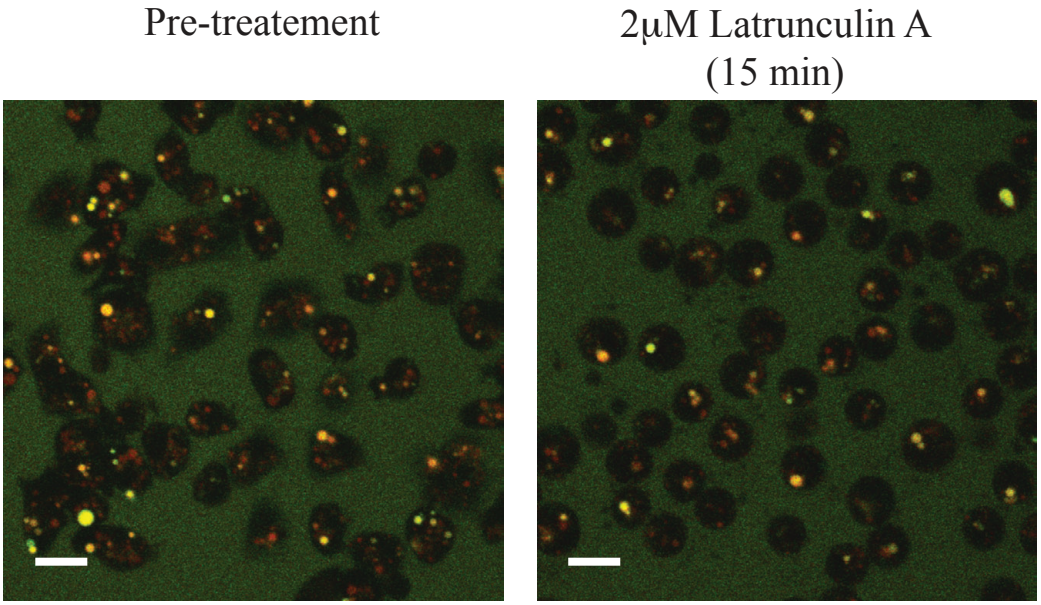

Figure 4.8: Effect of latrunculin A on maintaining neutralised post-lysosomes

Cells were loaded with FITC (pH sensitive) and TRITC (pH insensitive) conjugated dextran to differentiate between acidic and neutral vesicles. Acidic vesicles appear red due to the decreased FITC signal, whilst neutral vesicles are yellow or green. Images show presence of neutral post-lysosomes after 1 hour of incubation in fluorescently labelled dextran and these remain even after treatment of cells with 2μM latrunculin A. Scale bars show 10μm.

of post-lysosomes to conclusively rule this out.

4.4 Actin is required for post-lysosome formation

To test the hypothesis that actin-coats are important for post-lysosome formation, the effect of latrunculin A on lysosome neutralisation was assessed in parental (*wshA*$^{+}$) cells.

Two problems needed to be overcome to test this hypothesis. Firstly, treatment with latrunculin A disrupts all cellular F-actin structures indiscriminately. Some of these have earlier roles than WASH in the endocytic pathway, and disruption of these would prevent dextran markers reaching lysosomes. Therefore a pulse chase experiment was devised allowing cells to internalise dextran and traffic it unhindered prior to latrunculin A treatment. Secondly, this experiment required an accurate prediction of when lysosome neutralisation would occur, otherwise an absence of post-lysosomes following latrunculin A addition could not be credited to drug treatment with any degree of confidence.

Cells were incubated in medium containing FITC-dextran for 20 minutes. Following replacement with non-fluorescent medium cells were monitored by fluorescence time-lapse microscopy for the appearance of FITC in post-lysosomes identified by a sudden increase in fluorescence signal. Cells were monitored at low magnification ensuring at least 30 cells were in the field of view. Figure 4.9 shows the number of FITC-dextran containing post-lysosomes

in the field of view during the course of imaging, with the x axis denoting time from the commencement of the pulse chase. It was observed that within a population there was a surge of post-lysosomes formed containing FITC-dextran around ~40 minutes after the initial addition of FITC-dextran. It should be noted that this time is dependent upon the setup of the microscope and thresholds set during image processing, however from 3 repeats it was seen that this 40 minute onset was reproducible using identical parameters. The consistency of this observation provided a suitable target for the addition of Latrunculin A.

We decided to add latrunculin A 36 minutes after commencement of the experiment giving several minutes for the drug to diffuse and sequester actin monomers prior to the predicted onset of lysosome neutralisation. Figure 4.9 shows that addition of latrunculin A at 36 minutes was sufficient to block the formation of post-lysosomes. This block was also shown to be reversible by removal of latrunculin A, with neutralisation commencing after a short recovery period. Although the addition and removal of latrunculin A appears to have affected the rate of formation and their persistence within the cell, this can be attributed to an inability to completely remove all latrunculin A during washes. The initial onset of vesicle neutralisation is indicated on Figure 4.9 by red lines. It is of importance to note these points are offset by roughly the same time period as latrunculin A treatment.

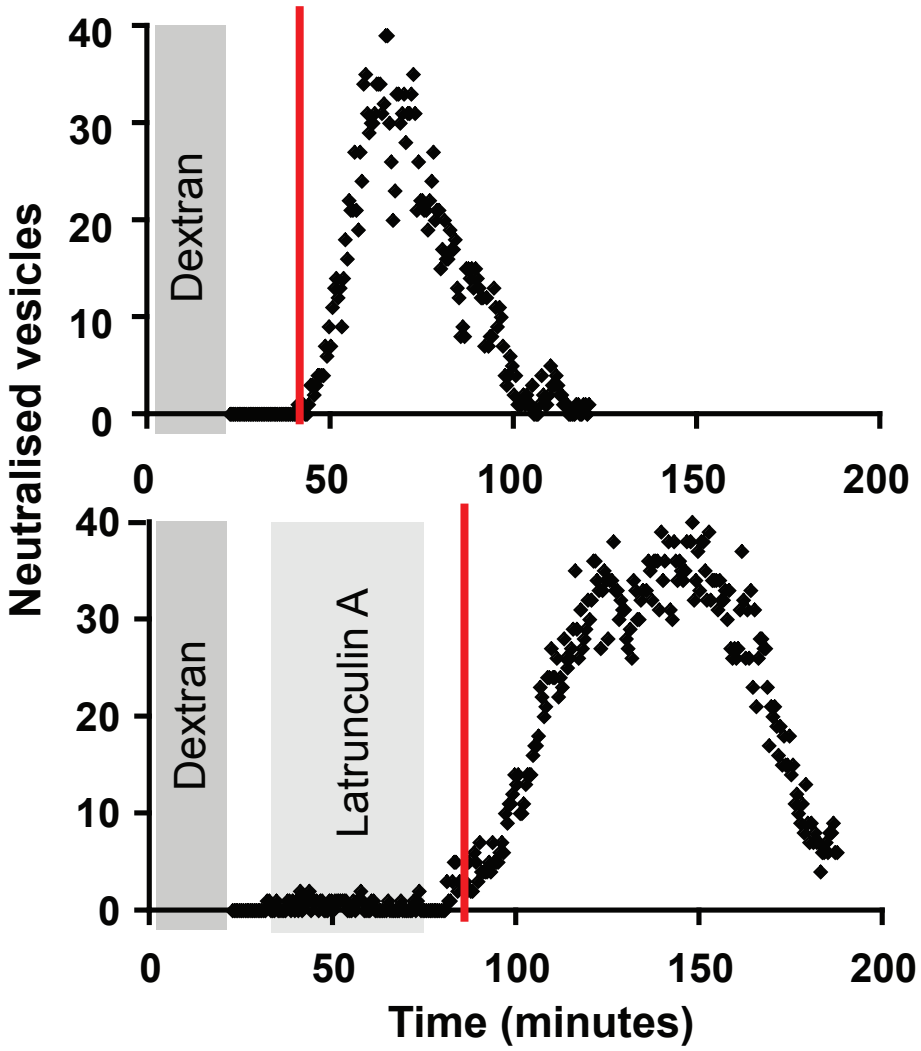

Figure 4.9: Effect of latrunculin A on vesicle neutralisation

Wildtype Ax2 cells were pulse chased with FITC-Dextran and its transit into neutralised post-lysosomes was measured by time lapse microscopy. Graphs show representative graphs from quantifying the number of post-lysosomes in the field of view during imaging, showing the appearance of post-lysosomes ~45 minutes after the commencement of the FITC-dextran pulse. Addition of 2μM Latrunculin A reversibly blocks the appearance of post-lysosomes. Red lines indicate the commencement of vesicle neutralisation

4.5 Conclusions

This work shows that WASH is the NPF responsible for the formation of actin-coats around late endocytic vesicles in *Dictyostelium*. Previously the role of these actin-coats were largely unknown but were proposed to function as physical barriers to prevent vesicle tethering and fusion. This was due to studies in mammalian cells showing that cortical actin functions as a physical barrier and must first be locally disrupted for exocytosis (Muallem *et al*., 1995). Additionally, by increasing the rate of actin-coat depolymerisation in *Dictyostelium* Drengk *et al*., (2003) observed a clustering of post-lysosomes. Here we show that actin-coats function further upstream than previously thought with roles in post-lysosome formation. Actin-coats persist during the transit of post-lysosomes through the endocytic pathway, roughly 30 minutes (Rauchenberger *et al*., 1997). As this coat remains for roughly 30 minutes after neutralization it could also serve a secondary function in preventing vesicle tethering and fusion as previously proposed (Drengk *et al*., 2003), and this may be required to maintain neutrality.

The loss of actin-coats presumably accounts for the defect in defecation seen in *wshA*^{null} cells due to a block in vesicle maturation. Interestingly, it has been documented that actin associates with secretory granules from chromaffin cells of the adrenal medulla (Meyer & Burger, 1979). As the endocytic and biosynthetic pathways are similar in that both undergo

gradual acidification during trafficking, it could be possible that a late association of actin in both pathways is essential for neutralization prior to exocytosis. It is not yet clear why lysosomes require neutralization.

Further study of these actin-coats would benefit from the generation of temperature sensitive WASH mutants. This would allow post-lysosomes to form followed by immediate WASH disruption, to investigate its role in vesicle fusion and neutralization that is currently hindered by the lack of post-lysosomes.

It is fortunate that disruption of WASH in *Dictyostelium* produced viable cells with no obvious defects in growth, yet yields clear unambiguous phenotypes. This provides an ideal system for further investigating the regulatory mechanisms of WASH and elucidating the mechanistic details of its actions. This work makes a start by showing that in vivo the acidic region is essential for arp2/3 mediated actin nucleation, whereas the widely conserved tryptophan in the acidic domain is not.

Chapter 5

WASH drives the neutralisation of lysosomes by the removal of the Vacuolar H+ ATPase.

The vacuolar H+ ATPase (V-ATPase) is an evolutionarily conserved enzyme that functions to acidify the lumen of intracellular organelles in eukaryotic cells. Several publications have documented relationships between the V-ATPase and the actin cytoskeleton, namely observations that subunits B and C bind filamentous actin (Vitavska *et al*., 2003; Chen *et al*., 2004), and perturbing proteins that modulate the actin cytoskeleton have been noted to affect V-ATPase localisation (Beaulieu *et al*., 2005). Here we investigate the role of WASH in lysosome neutralisation as a potential regulator of V-ATPase trafficking.

5.1 Lysosome neutralisation is caused by V-ATPase removal

Because vesicular compartments are proton 'leaky' and the cytosol of cells is pH neutral, vesicle neutralisation can be a passive process requiring only the inhibition of acidification. This is demonstrated by the common use of V-ATPase inhibitors to force neutralisation of endocytic compartments. Therefore to further understand the process of lysosome neutralisation in *Dictyostelium* we monitored the sub-cellular localisation of V-ATPase during this event.

The V-ATPase is composed of two sub-complexes, V_1 and V_0, each containing multiple subunits. We tagged the B subunit of V_1 (*vatB*) at its C terminus with mRFP as a probe to

monitor V-ATPase localisation by fluorescence microscopy. The fusion protein localised to a wide range of vesicular compartments, including the contractile vacuole, consistent with the previous reports of V-ATPase distribution (Clarke *et al*., 2002). To aid the practicalities of tracking a single vesicle during its transit through the endocytic pathway cells were incubated with agarose microsize beads. Once engulfed the bead ensures the vesicle maintains a constant size and shape making it easily identifiable between time-lapse images, and in the case of large beads helping to keep it in the plane of focus. We discovered that by allowing molten agarose to set in a hydrophobic liquid whilst being continually agitated, microscopic agarose beads could be created within the lab. Being able to custom make beads allowed insertion of any desirable substance into the molten agarose before it set, such as Oregon Green conjugated dextran. Similar to FITC, Oregon green is a pH sensitive fluorophore that becomes less fluorescent with decreasing pH. As the bead prevents the cellular compartment from reducing in size the local concentration of fluorescent dextran remains fixed, therefore any change in fluorescent signal can be attributed to a change in luminal pH.

Cells expressing *vatB*-mRFP were incubated with Oregon Green agarose beads to observe the localisation of V-ATPase during lysosome neutralisation. Figure 5.1 shows selected images from a time-lapse movie (supp. Movie 5) of cells having engulfed Oregon Green beads, and a graph showing the fluorescent intensity of a bead (arrow) during the course of the movie. It was repeatedly observed that removal of vatB from the membrane of phagosomes resulted in a constant elevated pH. This shows that late in the endocytic pathway lysosome neutralisation is caused by the removal of the V-ATPase proton pump. Interestingly, some phagocytosed beads showed oscillating pH changes that were not observed previously during fluid phase trafficking of FITC-dextran. It is possible that phagosomes and macropinosomes have

A

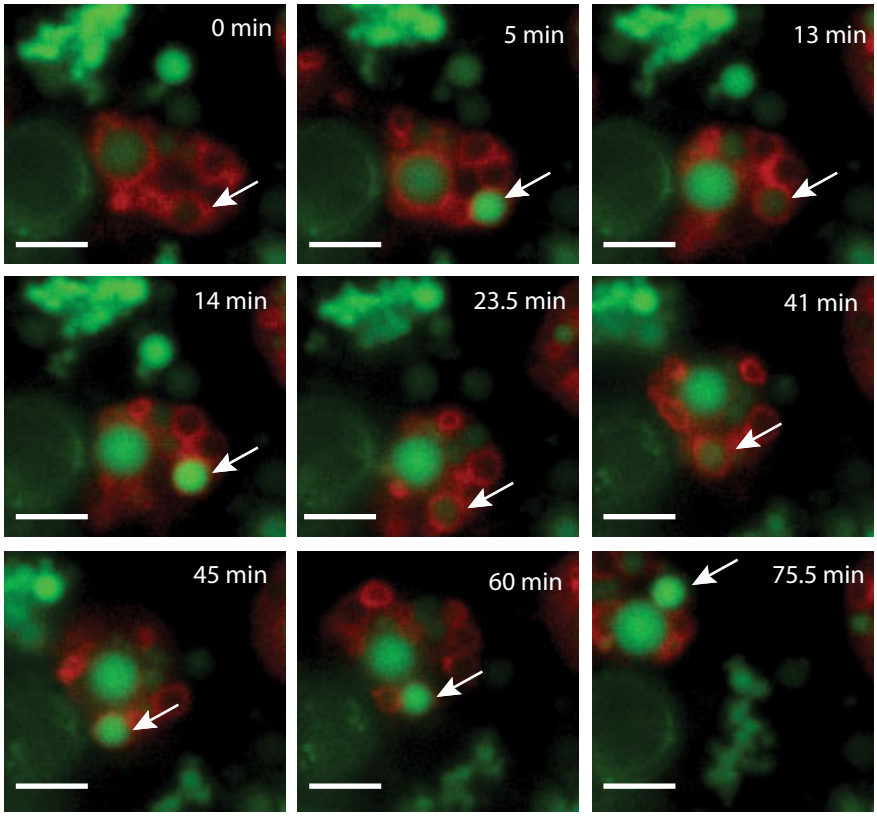
0 min
5 min
13 min
14 min
23.5 min
41 min
45 min
60 min
75.5 min

B

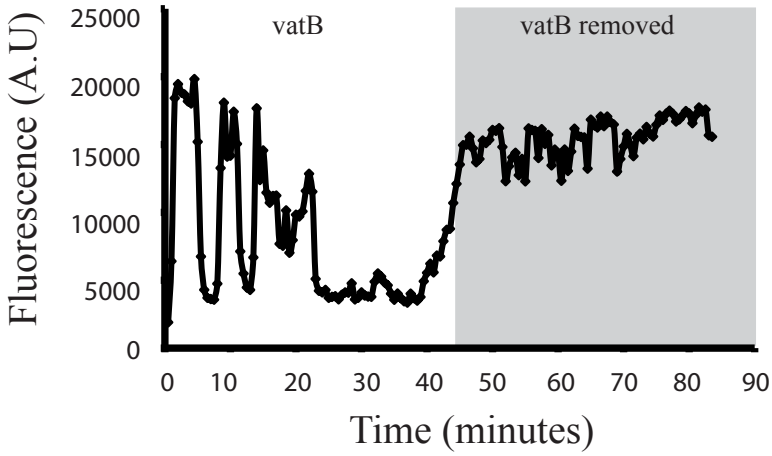
Fluorescence (A.U)
25000
20000
15000
10000
5000
0
vatB
vatB removed
0
10
20
30
40
50
60
70
80
90
Time (minutes)

Figure 5.1: Visualisation of *vatB* localisation and changes in luminal pH.

Ax2 cells expressing *vatB*-mRFP were fed agarose beads containing OregonGreen-dextran. The fluorescence of the bead decreases with decreasing pH. (A) Stills from time-lapse movie showing removal of *vatB* from a tracked vesicle (arrowed) between 40-45 minutes. Scale bars show 5μm. (B) Graph showing fluorescence of engulfed bead representing vesicular pH, showing oscillating changes with a *vatB* coat, but upon its removal is consistently bright indicating a neutral pH.

different pH dynamics due to size differences. However, with *vatB* present on the compartment, transient neutralisation is followed by acidification, suggesting sustained post-lysosomal neutralisation requires V-ATPase removal.

5.2 WASH recruitment coincides with V-ATPase removal

WASH was previously shown to be required for lysosome neutralisation. Having shown that this process requires the removal of V-ATPase, the correlation between WASH recruitment and V-ATPase removal was assessed quantitatively.

GFP-WASH and *vatB*-mRFP were co-expressed in *wshA*^{null} cells fed non-labelled agarose beads. It was noticed from observing numerous cells down the microscope that GFP-WASH and *vatB*-mRFP were mutually exclusive on internal organelles. Vesicles contained either a coat of GFP-WASH or *vatB*-mRFP, but never both. Vesicles progressed from a coat of *vatB* replaced by a WASH coat, consistent with acidification of early and WASH dependent neutralisation of late endocytic compartments. Confocal microscopy was used to quantify the levels of GFP-WASH and *vatB*-mRFP on phagosomes during their transit through the endocytic pathway. Figure 5.2:A shows selected images from a representative neutralisation event captured by time-lapse microscopy (supp. Movie 6). Doughnut shaped regions of interest were drawn around the periphery of the tracked phagosome in every frame and the average intensity was measured in each channel. Figure 5.2:B shows a graph of the normalised values obtained after background subtraction. It was found that GFP-WASH

recruitment coincides with the removal of *vatB*-mRFP. This data taken with previous findings that V-ATPase removal drives neutralisation, and neutralisation is dependent upon WASH, suggests that WASH recruitment has an active role in V-ATPase removal.

Studies in yeast have shown the V-ATPase is inactivated by the dissociation of its V_1 and V_0 sub-complexes (Kane, 1995). As *vatB* is a component of the cytosolic V_1 sub-complex another subunit was cloned from the trans-membrane V_0 complex (*vatM*) to observe if WASH recruitment causes neutralisation by dissociation of V_1 and V_0. A co-expression experiment showed that mRFP-*vatM* was removed from the vesicle upon recruitment of GFP-WASH in a similar manner as previously observed with *vatB* (Figure 5.3) (supp. movie 7). This suggests the V-ATPase is trafficked as a complete unit.

As lysosome neutralisation is not a result of V-ATPase dissociation, and the V_0 subcomplex is trans-membrane, we imaged WASH-dependent V-ATPase removal for signs of budding. mRFP-*vatB* and GFP-WASH were imaged using widefield microscopy for improved time resolution. Using the highest attainable magnification and resolution at our disposal (100x objective + 1.6x optivar, NA1.49) images of WASH-dependent V-ATPase removal were captured. Figure 5.4 shows stills taken from a successfully captured neutralisation event (sup. Movie 8). It shows that prior to WASH recruitment the V-ATPase coat is smooth and static. After WASH begins to accumulate on the compartment the V-ATPase coat becomes more dynamic, and what appears to be budding vesicles can be seen forming and detaching from the phagosome (arrows). Most areas of activity also possess WASH puncta. However, it is not

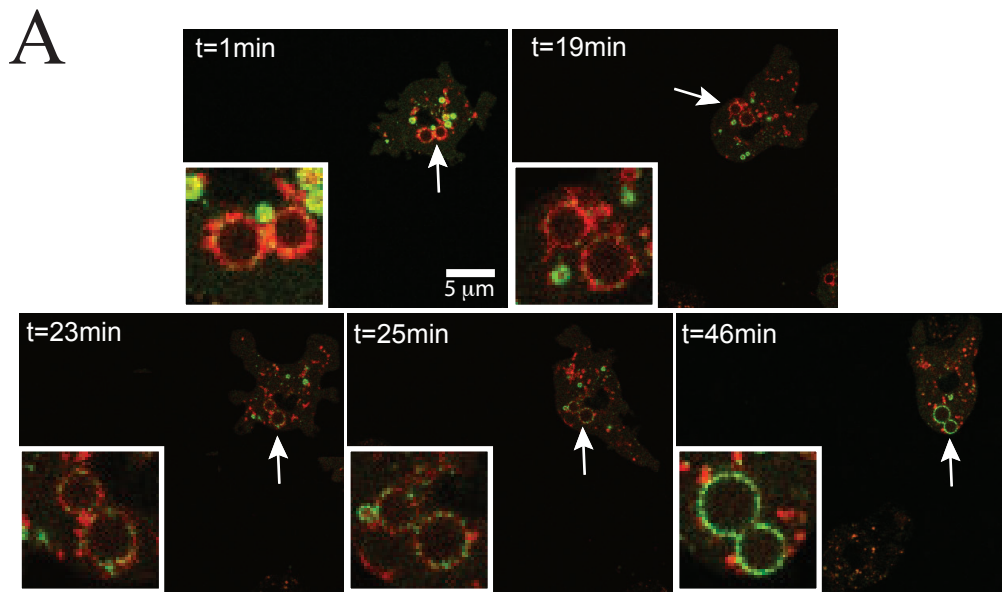

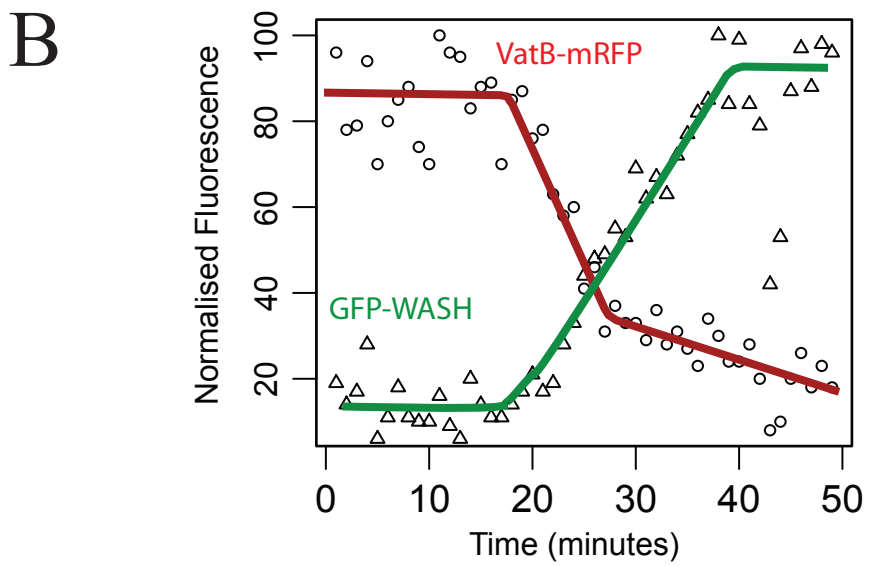

Figure 5.2: Vesicular localisation of GFP-WASH and vatB-mRFP

Cells expressing GFP-WASH and *vatB*-mRFP were fed agarose beads and imaged under a layer of agarose using confocal microscopy. (A) Selected images from time-lapse movie of a neutralisation event. Inset image shows magnification of bead used for quantification (arrow). (B) Quantification of GFP-WASH and *vatB*-mRFP . Donut shaped regions of interest were used to quantify average fluorescence intensity. Background fluorescence was subtracted from each value and then normalised.

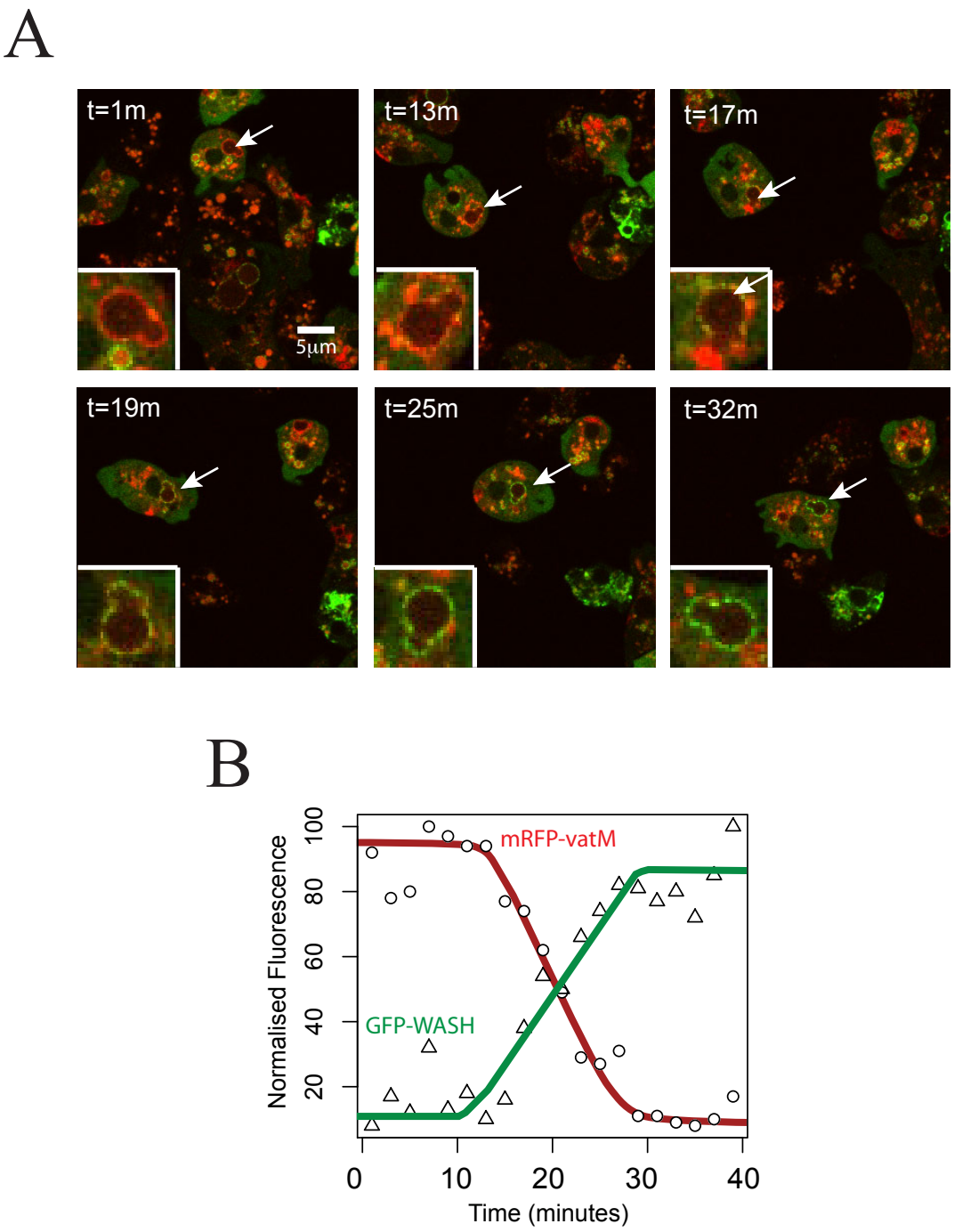

Figure 5.3: Vesicular localisation of GFP-WASH and mRFP-*vatM*

Cells expressing GFP-WASH and mRFP-*vatM* fed agarose beads and imaged under a layer of agarose using confocal microscopy. (A) Selected images from time-lapse movie of a neutralisation event. Inset image shows magnification of bead used for quantification (arrow). (B) Quantification of GFP-WASH and mRFP-*vatM* . Donut shaped regions of interest were used to quantify average fluorescence intensity. Background fluorescence was subtracted from each value and then normalised.

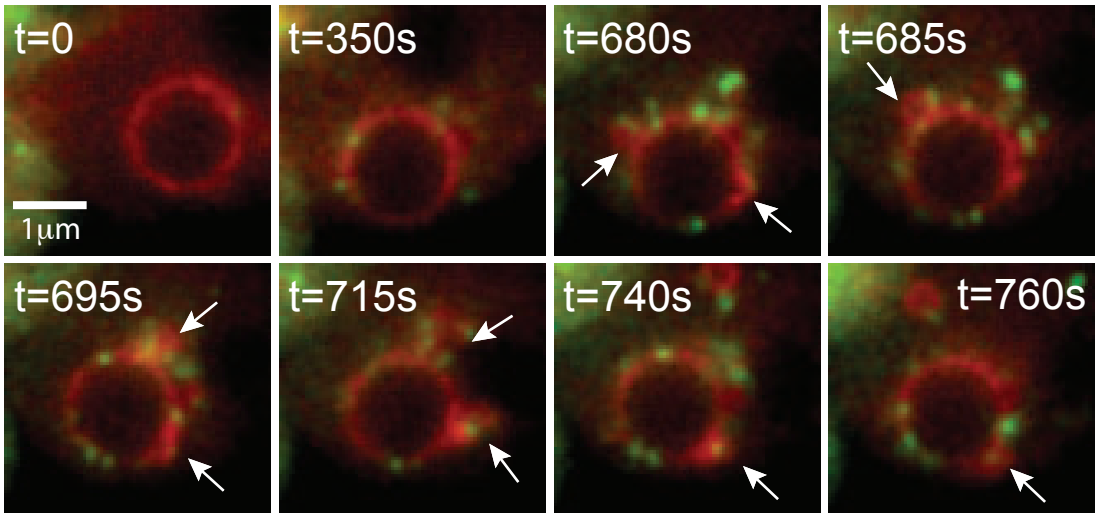

Figure 5.4: High resolution widefield microscopy of GFP-WASH and vatB-mRFP Dynamics.

Still images of a phagosome in a *wshA*^{null} cell expressing GFP-WASH and vatB-mRFP captured by widefield microscopy. Arrows show regions of membrane activity.

possible to completely rule out that these are smaller V-ATPase coated vesicles entering the field of view from either above or below this compartment.

5.4 Enoxacin treatment does not prevent vesicle neutralisation.

Previous reports show that the V-ATPase interacts directly with actin filaments. To date, both subunit B (Holliday *et al*., 2000) and C (Vitavska *et al*., 2005) of V_1 have been shown to directly bind with filamentous actin. As the B subunit is present in three copies per V-ATPase complex, whereas the C subunit is found only once, this subunit accounts for the majority of the known actin binding sites. This actin binding site has been mapped to a stretch of 11 amino acids near its N terminus (Chen *et al*., 2004) and a study in yeast has shown that this site can be altered and still yield a functional V-ATPase (Zuo *et al*., 2008). Figure 5.5 shows a sequence alignment of B subunit homologues from various species, highlighting the actin binding site. Recently a structural *in silico* screen identified enoxacin as a compound that disrupts the interaction between F-actin and subunit B (Ostrov *et al*., 2009). To test if the interaction between actin and subunit B is involved in the WASH-dependent removal of V-ATPase from lysosomes, wild type Ax2 cells were incubated with enoxacin for 24 hour before and during assays for post-lysosome visualisation. Various concentrations were tested but even at the maximum attainable concentration of 100µM cells were still able to form post-lysosomes (Figure 5.6). This suggests that the interaction between subunit B and actin does

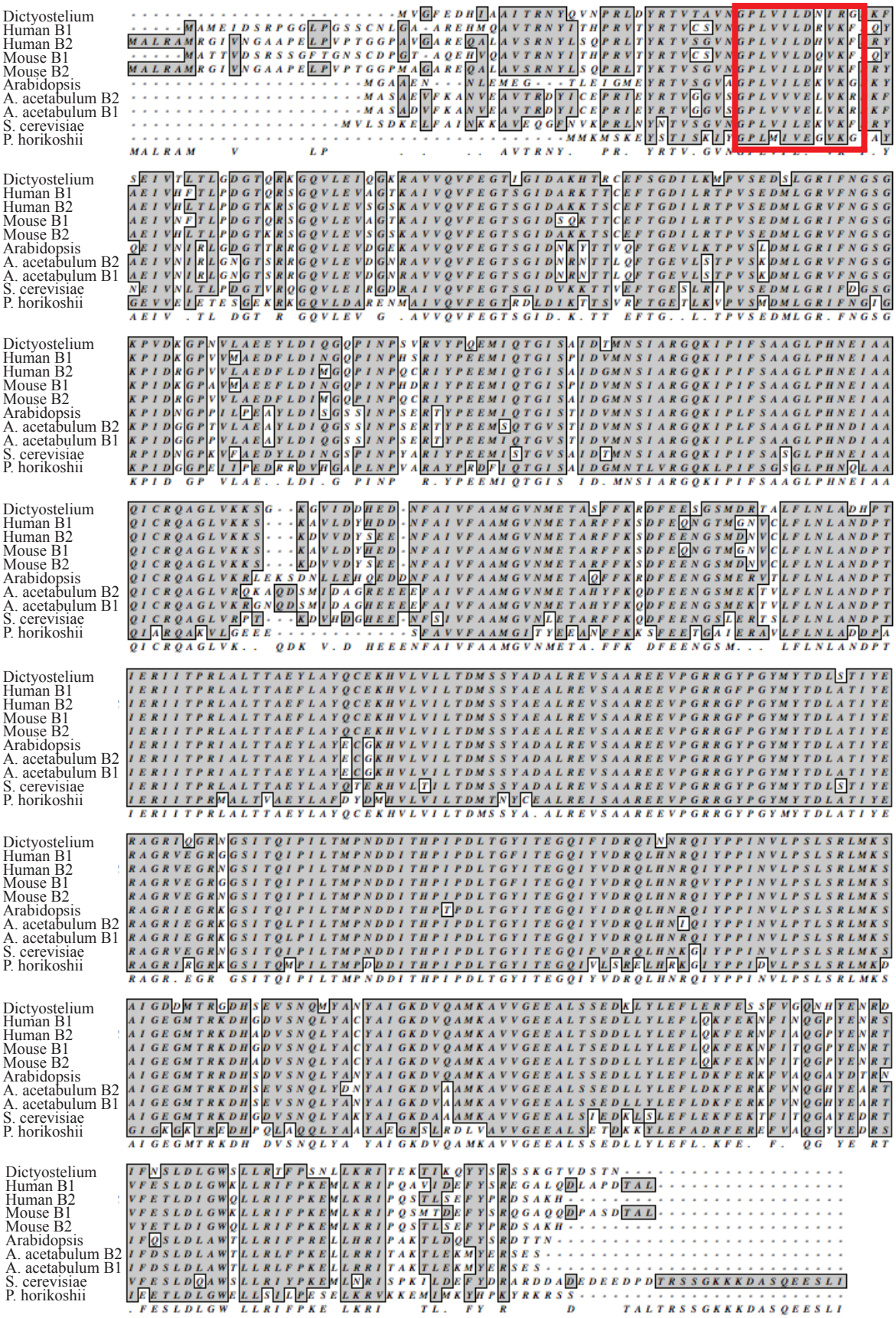

Figure 5.5: Alignment of V ATPase B subunit homologues

Multiple sequence alignment of B subunit homologues of the V ATPase. Red box shows identified actin binding domain by Chen et al. (2004).

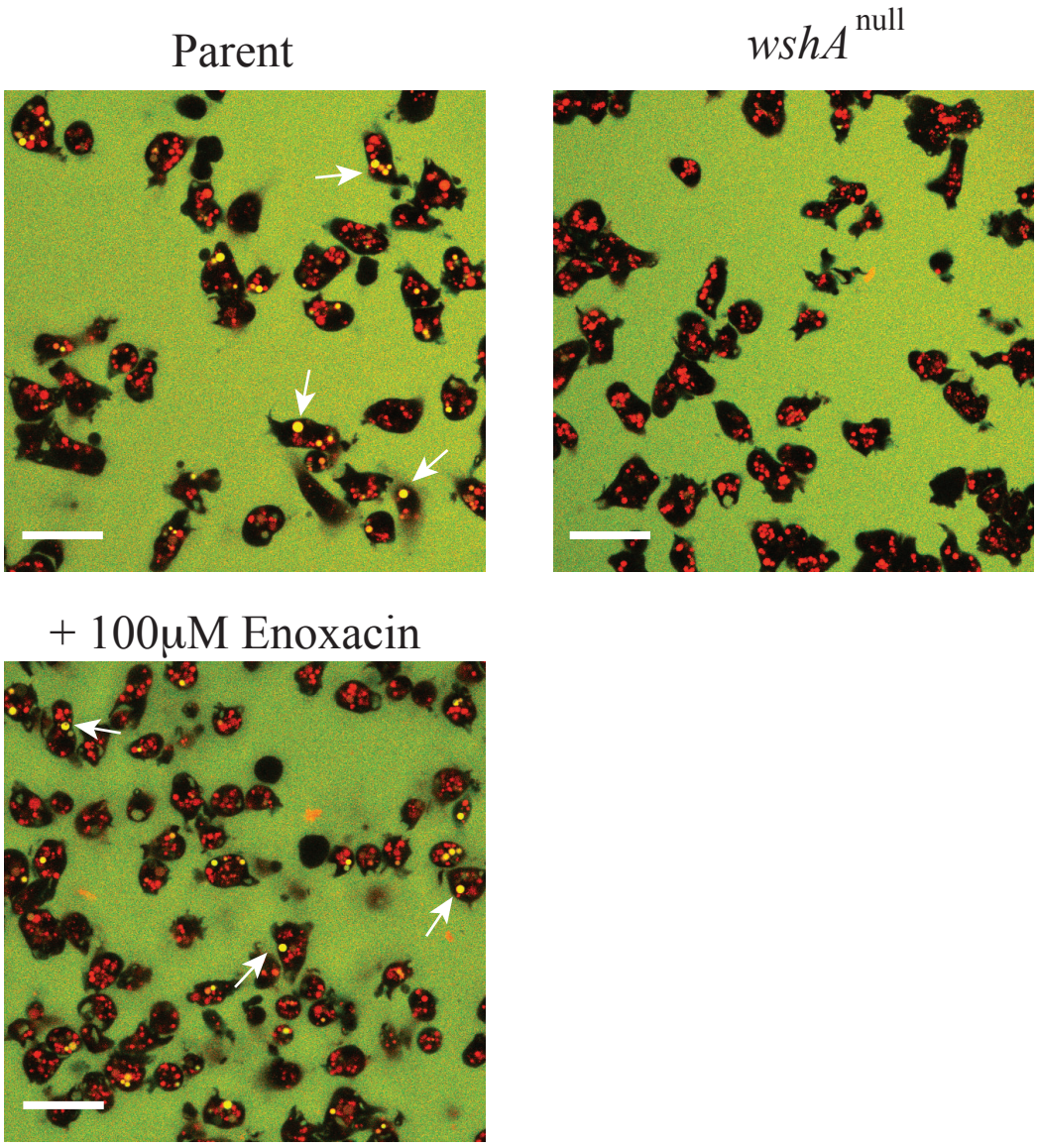

Figure 5.6: Effect of enoxacin on post-lysosome formation.

Vesicle neutralisation assay. Cells were loaded with FITC-dextran (pH sensitive) and TRITC-dextran (pH insensitive) to distinguish acidic and neutral vesicles. Post-lysosomes appear yellow (arrows) and are absent in wshA^{null} cells. Parental cells were incubated with 100µM enoxacin for 24 hours prior to and during the course of this assay. Enoxacin did not inhibit the formation of post-lysosomes. Scale bars show 10µm.

not play an essential role in vesicle neutralisation, however there were no obvious controls to show that this interaction was truly being disrupted in Dictyostelium, and to what extent.

5.5 Generation of *vatB* recombinants

To conclusively determine the role of the actin binding site in subunit B a genetic approach was undertaken. As the B subunit is present in 3 copies per V-ATPase molecule simply expressing an altered exogenous copy would be inadequate, as endogenous subunits may incorporate into the same molecule retaining some actin binding domains. Therefore we took an approach to alter the endogenous coding sequence. Two different cell lines were created. One based on Chen *et al*. (2004) replacing the endogenous VILDNIRGPKF with GSVEGGKG (MC7). The other based on Zuo *et al*. (2008) replacing the endogenous LDNIR with VAGGA (MC9).

Figure 5.7:A depicts how the endogenous sequence was augmented. DNA constructs were made to introduce a Blasticidin resistance cassette immediately after a gene upstream of vatB (DDB0304668) by homologous recombination. The downstream recombination arm included the sequence for vatB and its endogenous promotor. Recombination constructs pMJC87 and pMJC88 each contained different alterations to this actin binding site based on Chen *et al* (2004) and Zuo *et al* (2008) respectively. During insertion of the Blasticidin resistance cassette upstream of vatB providing homologous recombination happens downstream of this altered site it will be introduced into the genome. Wild type Ax2 cells were electroporated with either pMJC87 or pMJC88. After 24 hours transfected cells were plated into 5 x 96 well

plates in HL-5 medium containing Blasticidin. Transformants were screened for integration of the Blasticidin resistance cassette into the desired locus by PCR. Successful transformants could be identified by using a PCR primer to a site not present in the recombination construct to PCR the desired locus. An increase in the PCR product indicates the successful insertion of the BSR cassette upstream of vatB. Cell lines MC7 and MC9 were identified (Figure 5.7:B+C) from transformants electroporated with pMJC87 and pMJC88 respectively. The vatB gene was then amplified by PCR using a C terminal primer not present in the recombination construct and this product was sequenced to confirm alteration of endogenous vatB.

5.6 Actin binding site on subunit B is not essential for lysosomes neutralisation.

Cell lines where the actin binding site on subunit B of the V-ATPase had been disrupted were assessed for their ability to form neutralised post-lysosomes. Figure 5.8 shows cells incubated in FITC and TRITC dextran for 1 hour and visualised by confocal microscopy. It shows that the actin binding site of subunit B is not essential for lysosome neutralisation as post lysosomes are clearly visible (arrows).

However, the remaining actin binding site on subunit C may be enough to still yield a significant interaction. Given time the ability of the V-ATPase in these cells to bind to F-actin should be assessed in vitro. In addition, whilst trying to identify the site responsible for actin binding Chen *et al*., (2004) made two assertions that appear to be incorrect. Firstly the

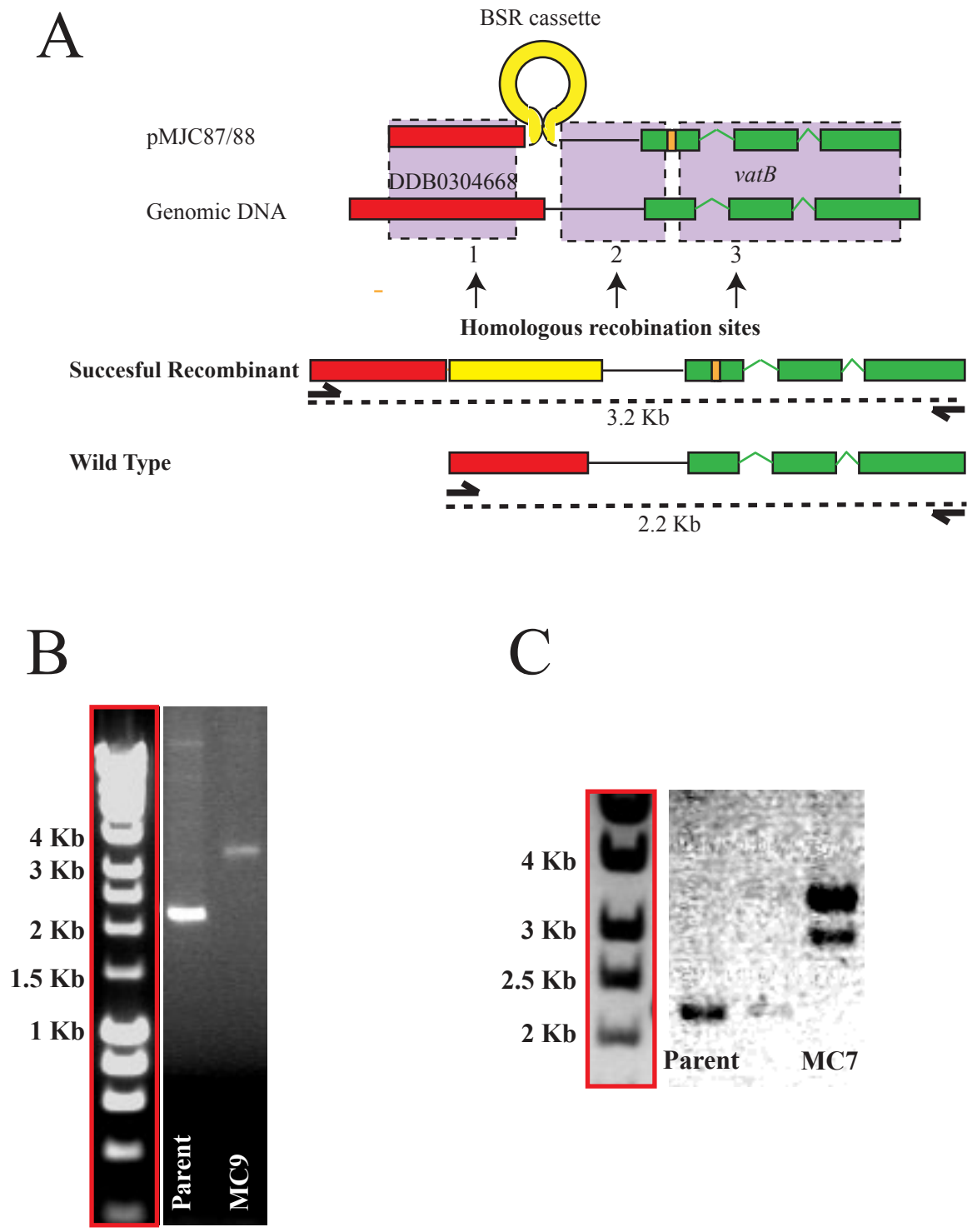

Figure 5.7: Generation of non-actin binding vatB cell lines

(A) Schematic representation of method to disrupt endogenous *vatB* actin binding sites. Constructs pMJC87 and pMJC88 inserted a Blasticidin resistence cassette between

DDB0304668 and *vatB* by homologous recombination. Each construct had a specific alteration to the actin binding domain of *vatB (*orange box). Providing recombination occured downstrean of this site (site 3) the endogenous sequence will be altered during insertion of the Blasticidin resistance cassette. (B) and (C) DNA gels from PCR products using primers in DDB0304668 and *vatB* using genomic DNA from Blasticidin resistant transformants. (B) shows identification of MC9 obtained using pMJC88 and (C) shows identification of MC7 obtained using pMJC87 by an increase in product size. Both cell lines were later sequenced confirming alterations to actin binding sites.

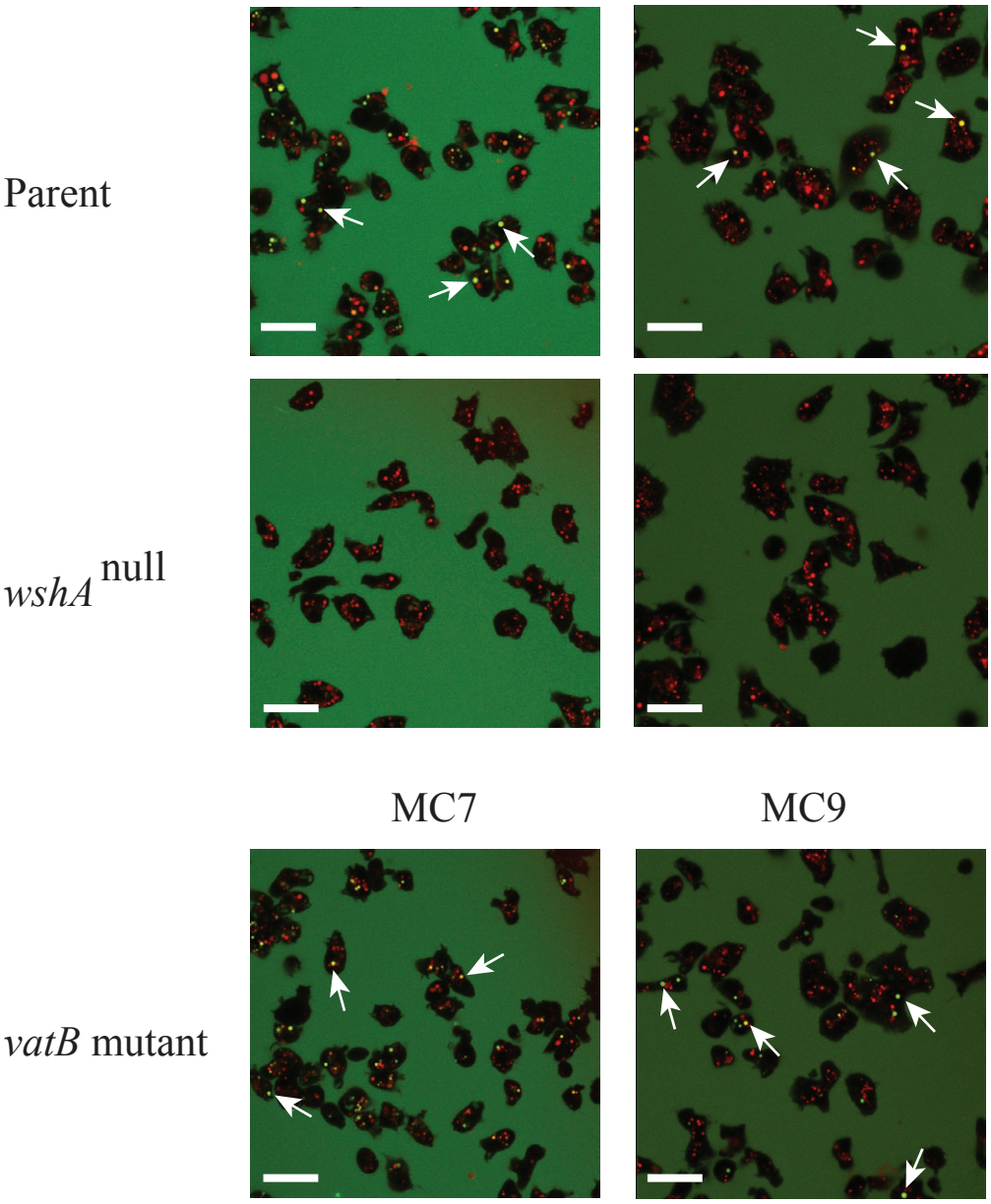

Figure 5.8: Visualisation of post-lysosomes in non-actin binding vatB cell lines.

Post-lysosome visualisation assay where cells are loaded with FITC and TRITC dextran for 1 hour and imaged by confocal micrsocopy. Post lysosomes appear as bright yellow or green compartments (arrows) due to their neutral lumen. MC7 and MC9 cell lines both contained large neutralised post-lysosomes. Error bars show 10μm.

proposed actin binding site was identified due to homology with profilin. Figure 5.9 shows the crystal structure of human profilin I (blue) bound to Dictyostelium actin (green). The residues suggested to be homologous between profilin and subunit B of the V-ATPase has been coloured red. None of these residues are involved with direct binding to actin. Chen *et al* (2004) also argued that replacement of this proposed actin binding site on the human B subunit with the equivalent sequence from of *P. horikoshii*, an archea that lacks an actin cytoskeleton and therefore should not possess the actin binding site, was sufficient to abolish actin binding. Figure 5.5 shows a sequence alignment of B subunits in which we have included *P. horikoshii*. We find that with the exception of a single methionine the sequence of *P. horikoshii* is functionally similar to B subunits from a range of eukaryotes. Also, when constructing peptides for binding experiments, they replaced the methionine with glycine for cloning purposes, making their *P. horikoshii* more functionally similar to the valine present in eukaryotes. Had these replacements worked in *Dictyostelium* this would have been strong evidence for an interaction for actin and the V-ATPase, however with the apparent discrepancies this data only provides weak negative data due to concerns over the validity of this being a true actin binding site.

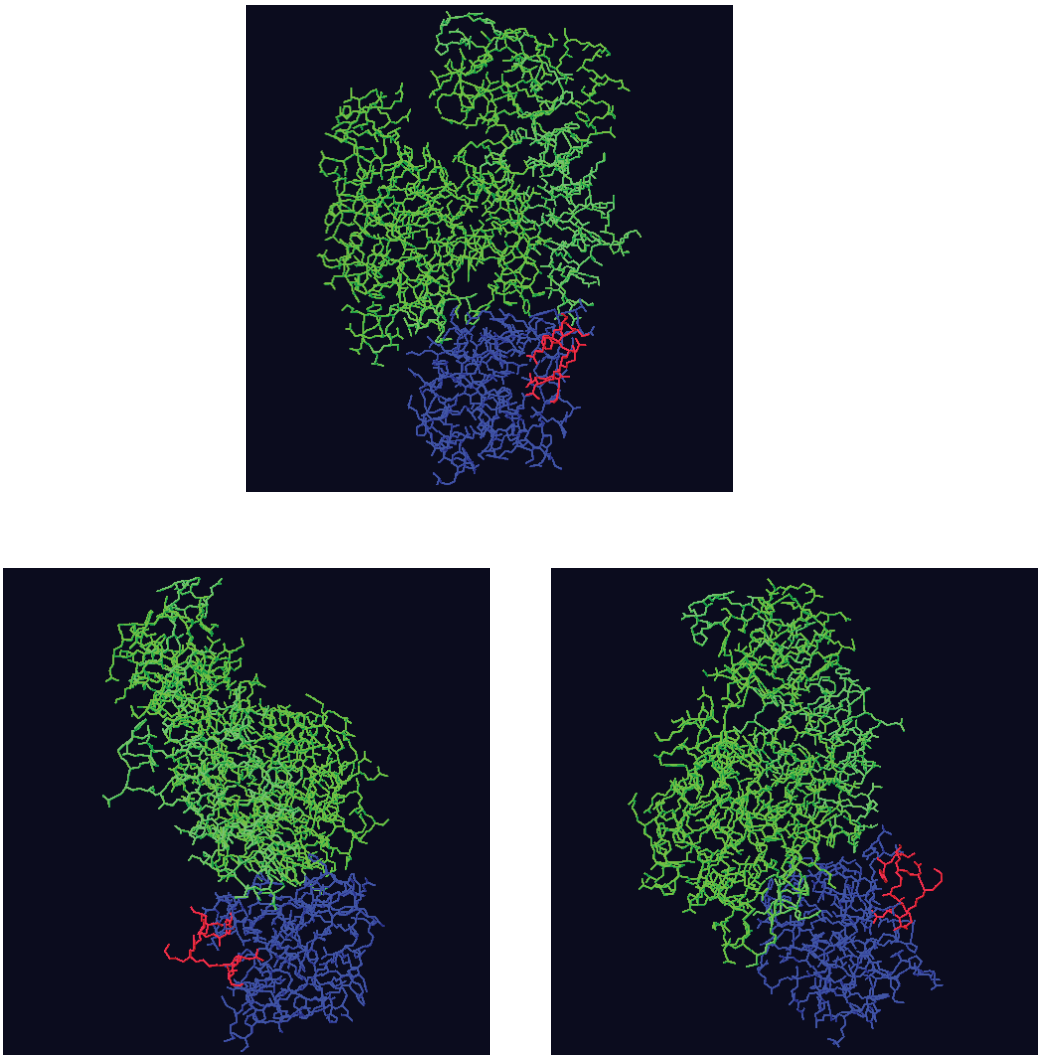

Figure 5.9: Binding of human profilin I to Dictyostelium actin.

Crystal structure of profilin I bound to actin, published by Baek et al., (2008). The structure was downloaded from the RCSB protein database (www.pdb.org) and viewed using Swiss-pdbviewer v4. Actin was coloured green and profilin I blue, with the region proposed to resemble homology with subunit B of the V ATPase highlight in red. This shows that the region does not contain any residues directly involved in the binding of profilin I with actin.

5.7 Conclusions

This work shows that lysosome neutralisation in *Dictyostelium* is caused by the removal of V-ATPase from the lysosomal membrane, likely through selective budding. As of yet nothing is known as to why mature lysosomes require neutralising prior to exocytosis, although it may be to maintain a vesicular localisation of the V-ATPase preventing it from entering the plasma membrane during vesicle fusion. Clarke *et al*., (2010) has also noted what appears to be removal of vatM through budding whilst studying the process of premature exocytosis in *Dictyostelium*.

Given that actin is implicated in clathrin-mediated endocytosis it is natural to presume that WASH is facilitating a similar role on internal organelles. However, if the actin cytoskeleton is an essential requirement for vesicle budding then it would be expected to be ubiquitously distributed on almost all intracellular vesicles. As this is not the case it would appear that the role of WASH-dependent actin has a more specialised function. The high avidity of the V-ATPase for actin filaments suggests a possible explanation. When two molecules have a high affinity it would generally be expected that they show a reasonable level of colocalisation. Interestingly, actin and V-ATPase are almost entirely mutually exclusive throughout the endocytic pathway. V-ATPase starts to accumulate on macropinosomes just after the residual actin coat has been disassembled (Rauchenberger *et al.,* 1997; Clarke *et al*., 2002), and its removal is dependent on, and occurs simultaneously with the generation of WASH-dependent actin. Taken together this suggests that it may be the interaction between V-ATPase and actin

that aids its removal. To test this hypothesis it is necessary to disrupt these interactions and observe the effect on V-ATPase trafficking. A start has been made by genetically disrupting a region in the B subunit previously published to be a site of F-actin binding. This disruption did not prevent neutralisation, however, this study is still incomplete. It remains necessary to further disrupt the actin binding site within the C subunit and assess if this V-ATPase complex is still functional, and incapable of binding actin.

Chapter 6

Final conclusions and future perspectives

6.1 The role of WASH in *Dictyostelium discoideum*

The actin cytoskeleton is a collection of filamentous structures involved in generating protrusive and contractive forces, rigid scaffolds and manipulation of cellular membranes. It has long been known to be essential for a variety of processes requiring changes in cell morphology, such as cell motility, cytokinesis and endocytosis. Recently it has become clear that the actin cytoskeleton serves broader functions within the cell. These include vesicle propulsion and aiding fission of budding vesicles. This work identifies a new role for actin in the endocytic pathway in controlling vesicle identity and maturation.

Genetically disrupting WASH in *Dictyostelium* has allowed us to identify it as the NPF responsible for the formation of actin-coats around late endocytic compartments. These actin-coats were shown to be essential for the formation of neutralised post-lysosomes, and that disruption of this process resulted in an inability to exocytose material from the endocytic pathway. This presumably is a disruption in a vesicle maturation pathway were by V-ATPase must be removed prior to exocytosis preventing the proton pump from entering the plasma membrane. During live cell imaging of fluorescent fusion proteins it was noticed that WASH first appeared in punctate patches, and a large proportion of the V-ATPase was removed before it had attained a full coat of WASH. Observing that the transmembrane domain of the V-ATPase was removed simultaneously with WASH recruitment suggested that this process was driven by budding, and this was also observed during high speed acquisition with widefield microscopy.

Due to the essential role of actin in clathrin-mediated endocytosis in yeast (Ayscough *et al* 1997) it is natural to presume that WASH-dependent actin is performing a similar role in scission of budding vesicles on endosomal compartments; as proposed by Derivery *et al*., (2009). However, here we propose an alternative mechanism.

The role of actin in clathrin-mediated endocytosis has recently been shown to facilitate the invagination of the plasma-membrane against turgor pressure in yeast (Aghamohammadzadeh & Ayscough, 2009). By decreasing turgor pressure clathrin-mediated endocytosis became less dependent upon actin, showing that actin is not essential for budding or scission but merely serves to provide force for difficult to deform membranes. Budding of intracellular vesicles is more favourable due to the lack of turgor pressure and an already positive membrane curvature. It is also a common event on almost all compartments of the endocytic and biosynthetic pathways, and given actin is not equally ubiquitous on all these it suggests it too is not essential for budding on internal compartments. We suggest that the defects observed in *Dictyostelium* and mammalian cells are not due to the inability to bud vesicles and that WASH-dependent actin has a specific and antagonistic role in regulating the localisation of V-ATPase, providing a facilitative role in targeting it to sites of budding. This is based on the observation that although V-ATPase has a high avidity for filamentous actin (Chen *et al*., 2004; Vitavska *et al*., 2005; Zuo *et al*., 2008), its location is mutually exclusive with actin throughout the endocytic pathway in *Dictyostelium*. V-ATPase is only incorporated into newly formed macropinosomes after disassembly of a residual actin coat (Rauchenberger *et al*., 1997; Clarke *et al*., 2002) and is then removed at a later stage in a WASH and actin dependent manner. There have also been several reports that disruption of the actin

cytoskeleton can result in altered localisation of the V-ATPase (Beauileu *et al*., 2005; Shum *et al*., 2010)

Figure 6.1 depicts our proposed model. WASH arrives in punctate patches on acidic vesicles generating localised patches of actin assembly. V-ATPase molecules that are freely diffusible within the membrane are sequestered in these patches due to their avidity for actin. These regions may then be targeted as sites of budding that may or may not be facilitated by force generated by actin polymerisation, allowing selective and efficient removal of V-ATPase from the membrane. The actin-coat may then persist as a barrier for exocytosis as previously proposed (Drengk *et al*., 2003) or serve to prevent re-acidification. This vesicle can then be exocytosed without causing V-ATPase incorporation into the plasma-membrane.

6.2 WASH in Dictyostelium and Mammalian cells

Here we report a different localisation of WASH in *Dictyostelium* to that previously published in mammalian cells. By colocalisation with a range of endocytic markers Derivery *et al*., (2009) showed WASH to be present on a range of endocytic compartments. It was shown to be more abundant on early sorting and recycling endosomes and less so on late endosomes and lysosomes. This is in contrast to the recruitment of WASH to late endocytic compartments in *Dictyostelium*.

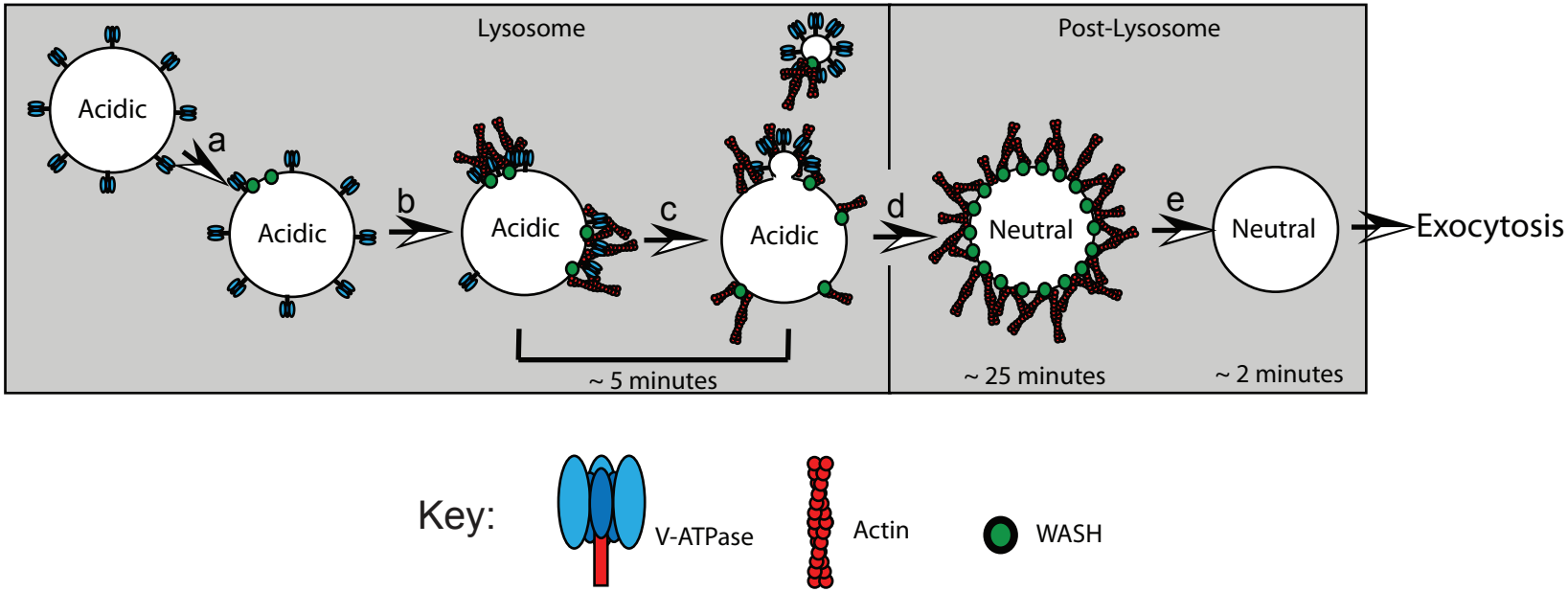

Figure 6.1: Model of WASH-mediated lysosome neutralization

(a) WASH appears on acidic vesicles in discrete puncta.. (b) WASH patches generate actin patches that sequester freely diffusible V-ATPase. (C) These V-ATPase dense regions may then be targeted as sites of budding by currently unknown mechanisms to efficiently remove V-ATPase from the vesicle causing it to neutralise. (d) Actin coat remains potentially to prevent fussion with other compartments of the plasma membrane. (e) WASH is removed prior to exocytosis and the compartment fuses with the plasma membrane.

Depletion of WASH by RNAi revealed defects in trafficking of the transferrin receptor, the retromer-dependent transport of CI-MPR back to the golgi, and EGF transport to late endosomes (Derivery *et al*., 2009; Gomez & Billadeau, 2009; Duleh & Welch, 2010). An increase in tubulation of these compartments was also observed (Duleh & Welch, 2010) as was a punctate localisation of WASH (Derivery *et al*., 2009; Gomez & Billadeau, 2009). It was proposed that WASH is required for nucleating actin on these compartments driving scission of vesicles, and its disruption therefore results in tubulated structures and trafficking defects due the inability to generate transport vesicles.

It is interesting that WASH becomes less abundant on compartments along the endocytic pathway in mammalian cells, which is also accompanied by increasing acidity. Figure 6.2 depicts the localisation of WASH on the endocytic pathway in mammalian cells showing the luminal pH of each compartment. Given the data obtained from this work we suggest an alternative interpretation of the mammalian data set. WASH could be regulating the density of V-ATPase on endocytic compartments by driving V-ATPase removal. The punctate nature of WASH on these compartments would allow V-ATPase to be inserted in actin clear regions and selectively removed at WASH patches. As WASH becomes less prominent on late endocytic vesicles a higher V-ATPase density can be achieved by a reduction in its removal, and result in a lower luminal pH. In this case depleting WASH would be expected to disrupt the gradual pH drops between compartments necessary for receptor trafficking consistent with the trafficking defects observed. Regarding vesicle morphology it has been shown that treatment of cells with the V-ATPase inhibitor Bafilomycin resulted in tubulation of endocytic vesicles (D'Arrigo *et al*., 1997). Although this drug causes neutralisation of

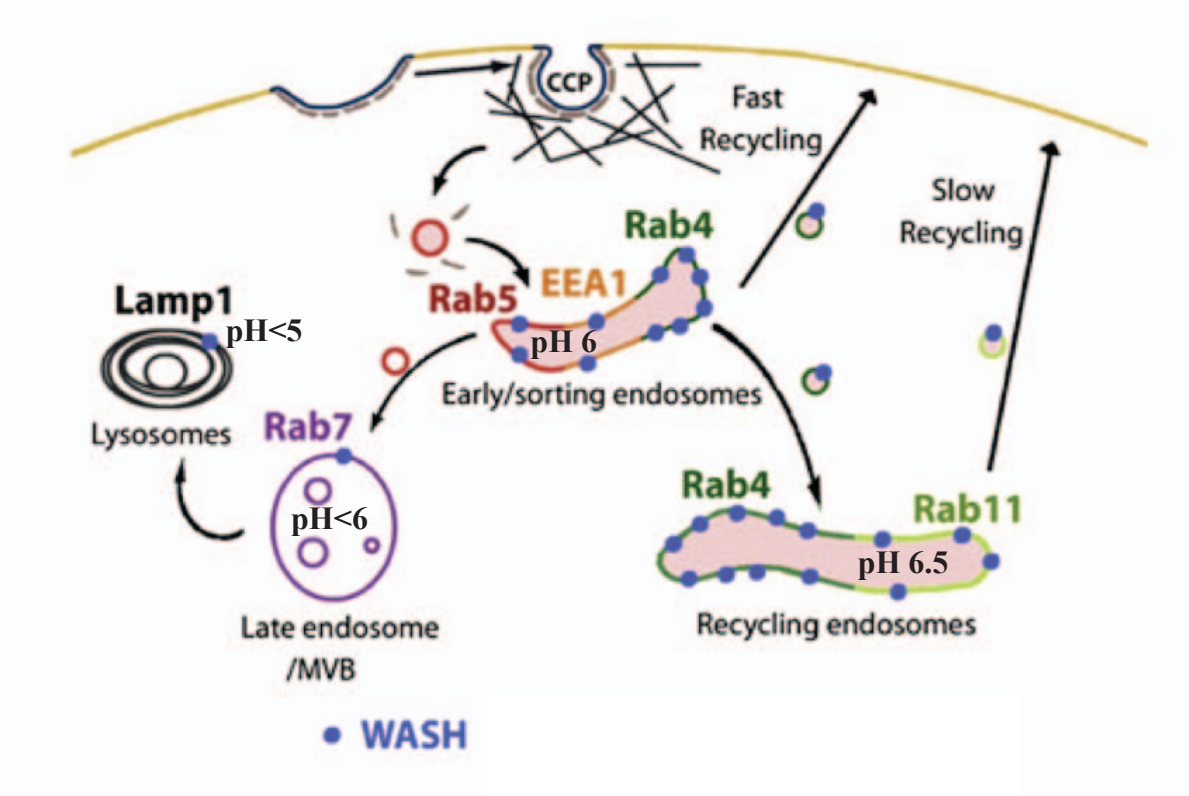

Figure 6.2: Distribution of WASH on the endocytic pathway in mammalian cells

Illustration taken from Derivery et al., (2009) showing the distribution of WASH on compartments based on colocalisation with the illustrated markers. Image was modified to show luminal pH to illustrate that correlation between decreasing WASH and increasing acidity.

compartments, rather than the increased acidity we are proposing, it demonstrates that maintaining the correct luminal pH is important for endosome morphology. This hypothesis is further supported by work on transferrin receptor recycling. After internalisation the transferrin receptor passes briefly through an acidic compartment before entering a more neutral structure. Purification of this compartment revealed the lack of V-ATPase (Gagescu *et al*., 2000), showing that luminal pH can be regulated by adjusting the amount of V-ATPase within the membrane.

6.3 Future perspectives

As WASH was only recently discovered little is known regarding its regulation or function. What is known about its regulation is inferred from similarities with another member of the WASP protein family, SCAR (Jia *et al*., 2010), and regarding its function little is known beyond it having a role in the endocytic pathway. This work presents an advance in the understanding of WASH function, and opens up future possibilities for understanding its regulation.

Dictyostelium may prove to be an ideal model organism for the further study of WASH. In addition to its generic advantages of being genetically tractable and easily handled, the

differences between the endocytic pathway in *Dictyostelium* and mammals may prove advantageous. Interpretation of disruption studies in mammalian cells could be complicated by secondary effects from disrupting early trafficking events, such as growth, receptor recycling and signalling pathways. The role of WASH late in the endocytic pathway in *Dictyostelium* has allowed its disruption with little effect on cell viability in laboratory culture medium.

It is fortunate that disruption of WASH yielded viable cells and at the same times such clear and currently unique phenotypes. All subunits of the WASH complex identified by Derivery *et al* (2009) have been identified in *Dictyostelium* (Veltman *et al*., 2010), suggesting conservation of its regulation. By screening REMI generated mutant libraries for cells with normal growth yet defects in exocytosis, further key players in WASH regulation can be identified.

This work could impact on several other previously unconnected areas of research. A great deal of work on the interaction of V-ATPase with the actin cytoskeleton has been focused in specialised cells that accumulate V-ATPase at the plasma membrane, such as osteoclasts and epididymal clear cells (Zuo *et al*., 2006; Shum *et al*., 2010). As this work suggests the interaction may be essential in preventing its accumulation at the plasma membrane rather than targeting it there, this work provides a fresh perspective.

Additionally, the biosynthetic secretory pathway is also accompanied by gradual drops in luminal pH between compartments. This results in secretory vesicles being acidic and densely covered in V-ATPase. It has previously been documented that secretory granules from chromaffin cells of the adrenal medulla are surrounded by a dense web of actin filaments (Meyer & Burger, 1979). In light of new data this suggests that a similar actin-dependent mechanism for V-ATPase removal may be functioning in the secretory pathway, and by a similar mechanism observed in *Dictyostelium* these coats may be required for exocytosis rather than acting as an inhibitor.

In summary, WASH in *Dictyostelium* is required for successful transit of material through the endocytic pathway by facilitating the removal of V-ATPase from lysosomes. This provides new insights into the role of WASH in mammalian cells and may provide a newly identified mechanism by which the pH of the endosomal lumen may be regulated.

References

Aguado-Velasco, C. and Bretscher, M. S. 1999. Circulation of the plasma membrane in Dictyostelium. Mol Biol Cell. 10, 12, 4419-4427.

Ahuja, R., Pinyol, R., Reichenbach, N., Custer, L., Klingensmith, J., Kessels, M. M., and Qualmann, B. 2007. Cordon-bleu is an actin nucleation factor and controls neuronal morphology. Cell. 131, 2, 337-350.

Ammann, A.T., and Hong, R (1989) Disorders of the T-Cell ystem in immunologic disorders in infants and children, ed E. R Stiehm, Philadelpia; W. B. aunders, 257-315

Aschenbrenner, L., Lee, T., and Hasson, T. 2003. Myo6 facilitates the translocation of endocytic vesicles from cell peripheries. Mol Biol Cell. 14, 7, 2728-2743.

Aubry, L., Klein, G., Martiel, J. L., and Satre, M. 1993. Kinetics of endosomal pH evolution in Dictyostelium discoideum amoebae. Study by fluorescence spectroscopy. J Cell Sci. 105, Pt 3, 861-866.

Bear, J. E., Rawls, J. F., and Saxe, C. L. r. 1998. SCAR, a WASP-related protein, isolated as a suppressor of receptor defects in late Dictyostelium development. J Cell Biol. 142, 5, 1325-1335.

Beaulieu, V., Da Silva, N., Pastor-Soler, N., Brown, C. R., Smith, P. J., Brown, D., and Breton, S. 2005. Modulation of the actin cytoskeleton via gelsolin regulates vacuolar H+-ATPase recycling. J Biol Chem. 280, 9, 8452-8463.

Benesch, S., Polo, S., Lai, F. P., Anderson, K. I., Stradal, T. E., Wehland, J., and Rottner, K. 2005. N-WASP deficiency impairs EGF internalization and actin assembly at clathrin-coated pits. J Cell Sci. 118, Pt 14, 3103-3115.

Bensenor, L. B., Kan, H. M., Wang, N., Wallrabe, H., Davidson, L. A., Cai, Y., Schafer, D. A., and Bloom, G. S. 2007. IQGAP1 regulates cell motility by linking growth factor signaling to actin assembly. J Cell Sci. 120, Pt 4, 658-669.

Ben-Yaacov, S., Le Borgne, R., Abramson, I., Schweisguth, F., and Schejter, E. D. 2001. Wasp, the Drosophila Wiskott-Aldrich syndrome gene homologue, is required for cell fate decisions mediated by Notch signaling. J Cell Biol. 152, 1, 1-13.

Blagg, S. L., Stewart, M., Sambles, C., and Insall, R. H. 2003. PIR121 regulates pseudopod dynamics and SCAR activity in Dictyostelium. Curr Biol. 13, 17, 1480-1487.

Blair, H. C., Teitelbaum, S. L., Ghiselli, R., and Gluck, S. 1989. Osteoclastic bone resorption by a polarized vacuolar proton pump. Science. 245, 4920, 855-857.

Boczkowska, M., Rebowski, G., Petoukhov, M. V., Hayes, D. B., Svergun, D. I., and Dominguez, R. 2008. X-ray scattering study of activated Arp2/3 complex with bound actin-WCA. Structure. 16, 5, 695-704.

Brisseau, G. F., Grinstein, S., Hackam, D. J., Nordstrom, T., Manolson, M. F., Khine, A. A., and Rotstein, O. D. 1996. Interleukin-1 increases vacuolar-type H+-ATPase activity in murine peritoneal macrophages. J Biol Chem. 271, 4, 2005-2011.

Cameron, L. A., Svitkina, T. M., Vignjevic, D., Theriot, J. A., and Borisy, G. G. 2001. Dendritic organization of actin comet tails. Curr Biol. 11, 2, 130-135.

Campellone, K. G., Webb, N. J., Znameroski, E. A., and Welch, M. D. 2008. WHAMM is an Arp2/3 complex activator that binds microtubules and functions in ER to Golgi transport. Cell. 134, 1, 148-161.

Cardelli, J. 2001. Phagocytosis and macropinocytosis in Dictyostelium: phosphoinositide-based processes, biochemically distinct. Traffic. 2, 5, 311-320.

Carter, S. B. 1967. Effects of cytochalasins on mammalian cells. Nature. 213, 5073, 261-264.

Chang, F., Drubin, D., and Nurse, P. 1997. cdc12p, a protein required for cytokinesis in fission yeast, is a component of the cell division ring and interacts with profilin. J Cell Biol. 137, 1, 169-182.

Chen, S. H., Bubb, M. R., Yarmola, E. G., Zuo, J., Jiang, J., Lee, B. S., Lu, M., Gluck, S. L., Hurst, I. R., and Holliday, L. S. 2004. Vacuolar H+-ATPase binding to microfilaments: regulation in response to phosphatidylinositol 3-kinase activity and detailed characterization of the actin-binding site in subunit B. J Biol Chem. 279, 9, 7988-7998.

Chen, W. T. 1989. Proteolytic activity of specialized surface protrusions formed at rosette contact sites of transformed cells. J Exp Zool. 251, 2, 167-185.

Chereau, D., Boczkowska, M., Skwarek-Maruszewska, A., Fujiwara, I., Hayes, D. B., Rebowski, G., Lappalainen, P., Pollard, T. D., and Dominguez, R. 2008. Leiomodin is an actin filament nucleator in muscle cells. Science. 320, 5873, 239-243.

Chubb, J. R., Wilkins, A., Thomas, G. M., and Insall, R. H. 2000. The Dictyostelium RasS protein is required for macropinocytosis, phagocytosis and the control of cell movement. J Cell Sci. 113, Pt 4, 709-719.

Clarke, M., Kohler, J., Heuser, J., and Gerisch, G. 2002. Endosome fusion and microtubule-based dynamics in the early endocytic pathway of dictyostelium. Traffic. 3, 11, 791-800.

Clarke, M., Maddera, L., Engel, U., and Gerisch, G. 2010. Retrieval of the vacuolar H-ATPase from phagosomes revealed by live cell imaging. PLoS One. 5, 1, e8585.

Cross, R. L. and Muller, V. 2004. The evolution of A-, F-, and V-type ATP synthases and ATPases: reversals in function and changes in the H+/ATP coupling ratio. FEBS Lett. 576, 1-2, 1-4.

D'Arrigo, A., Bucci, C., Toh, B. H., and Stenmark, H. 1997. Microtubules are involved in bafilomycin A1-induced tubulation and Rab5-dependent vacuolation of early endosomes. Eur J Cell Biol. 72, 2, 95-103.

Dahl, J. P., Wang-Dunlop, J., Gonzales, C., Goad, M. E., Mark, R. J., and Kwak, S. P. 2003. Characterization of the WAVE1 knock-out mouse: implications for CNS development. J Neurosci. 23, 8, 3343-3352.

Dayel, M. J., Holleran, E. A., and Mullins, R. D. 2001. Arp2/3 complex requires hydrolyzable ATP for nucleation of new actin filaments. Proc Natl Acad Sci U S A. 98, 26, 14871-14876.

Demaurex, N. 2002. pH Homeostasis of cellular organelles. News Physiol Sci. 17, 1-5.

Demaurex, N., Furuya, W., D'Souza, S., Bonifacino, J. S., and Grinstein, S. 1998. Mechanism of acidification of the trans-Golgi network (TGN). In situ measurements of pH using retrieval of TGN38 and furin from the cell surface. J Biol Chem. 273, 4, 2044-2051.

Derivery, E. and Gautreau, A. 2010. Evolutionary conservation of the WASH complex, an actin polymerization machine involved in endosomal fission. Commun Integr Biol. 3, 3, 227-230.

Derivery, E., Sousa, C., Gautier, J. J., Lombard, B., Loew, D., and Gautreau, A. 2009. The Arp2/3 activator WASH controls the fission of endosomes through a large multiprotein complex. Dev Cell. 17, 5, 712-723.

Derry, J. M., Ochs, H. D., and Francke, U. 1994. Isolation of a novel gene mutated in Wiskott-Aldrich syndrome. Cell. 78, 4, 635-644.

Diakov, T. T. and Kane, P. M. 2010. Regulation of vacuolar proton-translocating ATPase activity and assembly by extracellular pH. J Biol Chem. 285, 31, 23771-23778.

Dimond, R. L., Burns, R. A., and Jordan, K. B. 1981. Secretion of Lysosomal enzymes in the cellular slime mold, Dictyostelium discoideum. J Biol Chem. 256, 13, 6565-6572.

Duleh, S. N. and Welch, M. D. 2010. WASH and the Arp2/3 complex regulate endosome shape and trafficking. Cytoskeleton (Hoboken). 67, 3, 193-206.

Dunn, K. W., McGraw, T. E., and Maxfield, F. R. 1989. Iterative fractionation of recycling receptors from lysosomally destined ligands in an early sorting endosome. J Cell Biol. 109, 6 Pt 2, 3303-3314.

Eden, S., Rohatgi, R., Podtelejnikov, A. V., Mann, M., and Kirschner, M. W. 2002. Mechanism of regulation of WAVE1-induced actin nucleation by Rac1 and Nck. Nature. 418, 6899, 790-793.

Egile, C., Rouiller, I., Xu, X. P., Volkmann, N., Li, R., and Hanein, D. 2005. Mechanism of filament nucleation and branch stability revealed by the structure of the Arp2/3 complex at actin branch junctions. PLoS Biol. 3, 11, e383.

Eichinger, L., Pachebat, J. A., Glockner, G., Rajandream, M. A., Sucgang, R., Berriman, M., Song, J., Olsen, R., Szafranski, K., Xu, Q., Tunggal, B., Kummerfeld, S., Madera, M., Konfortov, B. A., Rivero, F., Bankier, A. T., Lehmann, R., Hamlin, N., Davies, R., Gaudet, P., Fey, P., Pilcher, K., Chen, G., Saunders, D., Sodergren, E., Davis, P., Kerhornou, A., Nie, X., Hall, N., Anjard, C., Hemphill, L., Bason, N., Farbrother, P., Desany, B., Just, E., Morio, T., Rost, R., Churcher, C., Cooper, J., Haydock, S., van Driessche, N., Cronin, A., Goodhead,

I., Muzny, D., Mourier, T., Pain, A., Lu, M., Harper, D., Lindsay, R., Hauser, H., James, K., Quiles, M., Madan Babu, M., Saito, T., Buchrieser, C., Wardroper, A., Felder, M., Thangavelu, M., Johnson, D., Knights, A., Loulseged, H., Mungall, K., Oliver, K., Price, C., Quail, M. A., Urushihara, H., Hernandez, J., Rabbinowitsch, E., Steffen, D., Sanders, M., Ma, J., Kohara, Y., Sharp, S., Simmonds, M., Spiegler, S., Tivey, A., Sugano, S., White, B., Walker, D., Woodward, J., Winckler, T., Tanaka, Y., Shaulsky, G., Schleicher, M., Weinstock, G., Rosenthal, A., Cox, E. C., Chisholm, R. L., Gibbs, R., Loomis, W. F., Platzer, M., Kay, R. R., Williams, J., Dear, P. H., Noegel, A. A., Barrell, B., and Kuspa, A. 2005. The genome of the social amoeba Dictyostelium discoideum. Nature. 435, 7038, 43-57.

Faix, J., Kreppel, L., Shaulsky, G., Schleicher, M., and Kimmel, A. R. 2004. A rapid and efficient method to generate multiple gene disruptions in Dictyostelium discoideum using a single selectable marker and the Cre-loxP system. Nucleic Acids Res. 32, 19, e143.

Fuchs, R., Schmid, S., and Mellman, I. 1989. A possible role for Na+,K+-ATPase in regulating ATP-dependent endosome acidification. Proc Natl Acad Sci U S A. 86, 2, 539-543.

Gagescu, R., Demaurex, N., Parton, R. G., Hunziker, W., Huber, L. A., and Gruenberg, J. 2000. The recycling endosome of Madin-Darby canine kidney cells is a mildly acidic compartment rich in raft components. Mol Biol Cell. 11, 8, 2775-2791.

Goley, E. D., Rodenbusch, S. E., Martin, A. C., and Welch, M. D. 2004. Critical conformational changes in the Arp2/3 complex are induced by nucleotide and nucleation promoting factor. Mol Cell. 16, 2, 269-279.

Gomez, T. S. and Billadeau, D. D. 2009. A FAM21-containing WASH complex regulates retromer-dependent sorting. Dev Cell. 17, 5, 699-711. DOI=10.1016/j.devcel.2009.09.009.

Gu, F. and Gruenberg, J. 2000. ARF1 regulates pH-dependent COP functions in the early endocytic pathway. J Biol Chem. 275, 11, 8154-8160.

Hacker, U., Albrecht, R., and Maniak, M. 1997. Fluid-phase uptake by macropinocytosis in Dictyostelium. J Cell Sci. 110, Pt 2, 105-112.

Hanisch, J., Ehinger, J., Ladwein, M., Rohde, M., Derivery, E., Bosse, T., Steffen, A., Bumann, D., Misselwitz, B., Hardt, W. D., Gautreau, A., Stradal, T. E., and Rottner, K. 2010. Molecular dissection of Salmonella-induced membrane ruffling versus invasion. Cell Microbiol. 12, 1, 84-98.

Higgs, H. N. and Pollard, T. D. 1999. Regulation of actin polymerization by Arp2/3 complex and WASp/Scar proteins. J Biol Chem. 274, 46, 32531-32534.

Hirata, R., Graham, L. A., Takatsuki, A., Stevens, T. H., and Anraku, Y. 1997. VMA11 and VMA16 encode second and third proteolipid subunits of the Saccharomyces cerevisiae vacuolar membrane H+-ATPase. J Biol Chem. 272, 8, 4795-4803.

Holliday, L. S., Lu, M., Lee, B. S., Nelson, R. D., Solivan, S., Zhang, L., and Gluck, S. L. 2000. The amino-terminal domain of the B subunit of vacuolar H+-ATPase contains a filamentous actin binding site. J Biol Chem. 275, 41, 32331-32337.

Howard, P. K., Ahern, K. G., and Firtel, R. A. 1988. Establishment of a transient expression system for Dictyostelium discoideum. Nucleic Acids Res. 16, 6, 2613-2623.

Huang, C. Y., Lu, T. Y., Bair, C. H., Chang, Y. S., Jwo, J. K., and Chang, W. 2008. A novel cellular protein, VPEF, facilitates vaccinia virus penetration into HeLa cells through fluid phase endocytosis. J Virol. 82, 16, 7988-7999.

Ibarra, N., Blagg, S. L., Vazquez, F., and Insall, R. H. 2006. Nap1 regulates Dictyostelium cell motility and adhesion through SCAR-dependent and -independent pathways. Curr Biol. 16, 7, 717-722.

Imamura, H., Nakano, M., Noji, H., Muneyuki, E., Ohkuma, S., Yoshida, M., and Yokoyama, K. 2003. Evidence for rotation of V1-ATPase. Proc Natl Acad Sci U S A. 100, 5, 2312-2315.

Innocenti, M., Gerboth, S., Rottner, K., Lai, F. P., Hertzog, M., Stradal, T. E., Frittoli, E., Didry, D., Polo, S., Disanza, A., Benesch, S., Di Fiore, P. P., Carlier, M. F., and Scita, G. 2005. Abi1 regulates the activity of N-WASP and WAVE in distinct actin-based processes. Nat Cell Biol. 7, 10, 969-976.

Insall, R., Muller-Taubenberger, A., Machesky, L., Kohler, J., Simmeth, E., Atkinson, S. J., Weber, I., and Gerisch, G. 2001. Dynamics of the Dictyostelium Arp2/3 complex in endocytosis, cytokinesis, and chemotaxis. Cell Motil Cytoskeleton. 50, 3, 115-128.

Insall, R., Muller-Taubenberger, A., Machesky, L., Kohler, J., Simmeth, E., Atkinson, S. J., Weber, I., and Gerisch, G. 2001. Dynamics of the Dictyostelium Arp2/3 complex in endocytosis, cytokinesis, and chemotaxis. Cell Motil Cytoskeleton. 50, 3, 115-128.

Iwadate, Y. and Yumura, S. 2008. Actin-based propulsive forces and myosin-II-based contractile forces in migrating Dictyostelium cells. J Cell Sci. 121, Pt 8, 1314-1324.

Jia, D., Gomez, T. S., Metlagel, Z., Umetani, J., Otwinowski, Z., Rosen, M. K., and Billadeau, D. D. 2010. WASH and WAVE actin regulators of the Wiskott-Aldrich syndrome protein (WASP) family are controlled by analogous structurally related complexes. Proc Natl Acad Sci U S A. 107, 23, 10442-10447.

Johnston, S. A., Bramble, J. P., Yeung, C. L., Mendes, P. M., and Machesky, L. M. 2008. Arp2/3 complex activity in filopodia of spreading cells. BMC Cell Biol. 9, 65.

Kane, P. M. 1995. Disassembly and reassembly of the yeast vacuolar H(+)-ATPase in vivo. J Biol Chem. 270, 28, 17025-17032.

Kaplan, G. 1977. Differences in the mode of phagocytosis with Fc and C3 receptors in macrophages. Scand J Immunol. 6, 8, 797-807.

Karet, F. E., Finberg, K. E., Nelson, R. D., Nayir, A., Mocan, H., Sanjad, S. A., Rodriguez-Soriano, J., Santos, F., Cremers, C. W., Di Pietro, A., Hoffbrand, B. I., Winiarski, J., Bakkaloglu, A., Ozen, S., Dusunsel, R., Goodyer, P., Hulton, S. A., Wu, D. K., Skvorak, A. B., Morton, C. C., Cunningham, M. J., Jha, V., and Lifton, R. P. 1999. Mutations in the gene encoding B1 subunit of H+-ATPase cause renal tubular acidosis with sensorineural deafness. Nat Genet. 21, 1, 84-90.

Kawamura, K., Takano, K., Suetsugu, S., Kurisu, S., Yamazaki, D., Miki, H., Takenawa, T., and Endo, T. 2004. N-WASP and WAVE2 acting downstream of phosphatidylinositol 3-kinase are required for myogenic cell migration induced by hepatocyte growth factor. J Biol Chem. 279, 52, 54862-54871.

Kawasaki-Nishi, S., Bowers, K., Nishi, T., Forgac, M., and Stevens, T. H. 2001. The amino-terminal domain of the vacuolar proton-translocating ATPase a subunit controls targeting and in vivo dissociation, and the carboxyl-terminal domain affects coupling of proton transport and ATP hydrolysis. J Biol Chem. 276, 50, 47411-47420.

Kelleher, J. F., Atkinson, S. J., and Pollard, T. D. 1995. Sequences, structural models, and cellular localization of the actin-related proteins Arp2 and Arp3 from Acanthamoeba. J Cell Biol. 131, 2, 385-397.

Kim, A. S., Kakalis, L. T., Abdul-Manan, N., Liu, G. A., and Rosen, M. K. 2000. Autoinhibition and activation mechanisms of the Wiskott-Aldrich syndrome protein. Nature. 404, 6774, 151-158.

Kim, J. H., Johannes, L., Goud, B., Antony, C., Lingwood, C. A., Daneman, R., and Grinstein, S. 1998. Noninvasive measurement of the pH of the endoplasmic reticulum at rest and during calcium release. Proc Natl Acad Sci U S A. 95, 6, 2997-3002.

King, J. and Insall, R. 2006. Parasexual genetics using axenic cells. Methods Mol Biol. 346, 125-135. DOI=10.1385/1-59745-144-4:125.

Kobayashi, K., Kuroda, S., Fukata, M., Nakamura, T., Nagase, T., Nomura, N., Matsuura, Y., Yoshida-Kubomura, N., Iwamatsu, A., and Kaibuchi, K. 1998. p140Sra-1 (specifically Rac1-associated protein) is a novel specific target for Rac1 small GTPase. J Biol Chem. 273, 1, 291-295.

Kobielak, A., Pasolli, H. A., and Fuchs, E. 2004. Mammalian formin-1 participates in adherens junctions and polymerization of linear actin cables. Nat Cell Biol. 6, 1, 21-30.

Kocks, C., Gouin, E., Tabouret, M., Berche, P., Ohayon, H., and Cossart, P. 1992. L. monocytogenes-induced actin assembly requires the actA gene product, a surface protein. Cell. 68, 3, 521-531.

Kocks, C., Hellio, R., Gounon, P., Ohayon, H., and Cossart, P. 1993. Polarized distribution of Listeria monocytogenes surface protein ActA at the site of directional actin assembly. J Cell Sci. 105, Pt 3, 699-710.

Kovacs, E. M., Goodwin, M., Ali, R. G., Paterson, A. D., and Yap, A. S. 2002. Cadherin-directed actin assembly: E-cadherin physically associates with the Arp2/3 complex to direct actin assembly in nascent adhesive contacts. Curr Biol. 12, 5, 379-382.

Kovar, D. R., Harris, E. S., Mahaffy, R., Higgs, H. N., and Pollard, T. D. 2006. Control of the assembly of ATP- and ADP-actin by formins and profilin. Cell. 124, 2, 423-435.

Kovar, D. R., Kuhn, J. R., Tichy, A. L., and Pollard, T. D. 2003. The fission yeast cytokinesis formin Cdc12p is a barbed end actin filament capping protein gated by profilin. J Cell Biol. 161, 5, 875-887.

Kunda, P., Craig, G., Dominguez, V., and Baum, B. 2003. Abi, Sra1, and Kette control the stability and localization of SCAR/WAVE to regulate the formation of actin-based protrusions. Curr Biol. 13, 21, 1867-1875.

Kuspa, A. and Loomis, W. F. 1994. REMI-RFLP mapping in the Dictyostelium genome. Genetics. 138, 3, 665-674.

Laevsky, G. and Knecht, D. A. 2001. Under-agarose folate chemotaxis of Dictyostelium discoideum amoebae in permissive and mechanically inhibited conditions. Biotechniques. 31, 5, 1140-2, 1144, 1146-9.

Lafourcade, C., Sobo, K., Kieffer-Jaquinod, S., Garin, J., and van der Goot, F. G. 2008. Regulation of the V-ATPase along the endocytic pathway occurs through reversible subunit association and membrane localization. PLoS One. 3, 7, e2758.

Le Clainche, C., Pantaloni, D., and Carlier, M. F. 2003. ATP hydrolysis on actin-related protein 2/3 complex causes debranching of dendritic actin arrays. Proc Natl Acad Sci U S A. 100, 11, 6337-6342.

Le Clainche, C., Schlaepfer, D., Ferrari, A., Klingauf, M., Grohmanova, K., Veligodskiy, A., Didry, D., Le, D., Egile, C., Carlier, M. F., and Kroschewski, R. 2007. IQGAP1 stimulates actin assembly through the N-WASP-Arp2/3 pathway. J Biol Chem. 282, 1, 426-435.

Lee, B. S., Gluck, S. L., and Holliday, L. S. 1999. Interaction between vacuolar H(+)-ATPase and microfilaments during osteoclast activation. J Biol Chem. 274, 41, 29164-29171.

Linardopoulou, E. V., Parghi, S. S., Friedman, C., Osborn, G. E., Parkhurst, S. M., and Trask, B. J. 2007. Human subtelomeric WASH genes encode a new subclass of the WASP family. PLoS Genet. 3, 12, e237.

Liu, R., Abreu-Blanco, M. T., Barry, K. C., Linardopoulou, E. V., Osborn, G. E., and Parkhurst, S. M. 2009. Wash functions downstream of Rho and links linear and branched actin nucleation factors. Development. 136, 16, 2849-2860.

Lommel, S., Benesch, S., Rottner, K., Franz, T., Wehland, J., and Kuhn, R. 2001. Actin pedestal formation by enteropathogenic Escherichia coli and intracellular motility of Shigella flexneri are abolished in N-WASP-defective cells. EMBO Rep. 2, 9, 850-857.

Lorenz, M., Yamaguchi, H., Wang, Y., Singer, R. H., and Condeelis, J. 2004. Imaging sites of N-wasp activity in lamellipodia and invadopodia of carcinoma cells. Curr Biol. 14, 8, 697-703.

Machesky, L. M. and Insall, R. H. 1998. Scar1 and the related Wiskott-Aldrich syndrome protein, WASP, regulate the actin cytoskeleton through the Arp2/3 complex. Curr Biol. 8, 25, 1347-1356.

Machesky, L. M., Atkinson, S. J., Ampe, C., Vandekerckhove, J., and Pollard, T. D. 1994. Purification of a cortical complex containing two unconventional actins from Acanthamoeba by affinity chromatography on profilin-agarose. J Cell Biol. 127, 1, 107-115.

Machesky, L. M., Mullins, R. D., Higgs, H. N., Kaiser, D. A., Blanchoin, L., May, R. C., Hall, M. E., and Pollard, T. D. 1999. Scar, a WASp-related protein, activates nucleation of actin filaments by the Arp2/3 complex. Proc Natl Acad Sci U S A. 96, 7, 3739-3744.

Maniak, M. 2003. Fusion and fission events in the endocytic pathway of Dictyostelium. Traffic. 4(1), 1, 1-5.

Maniak, M., Rauchenberger, R., Albrecht, R., Murphy, J., and Gerisch, G. 1995. Coronin involved in phagocytosis: dynamics of particle-induced relocalization visualized by a green fluorescent protein Tag. Cell. 83, 6, 915-924.

Marchand, J. B., Kaiser, D. A., Pollard, T. D., and Higgs, H. N. 2001. Interaction of WASP/Scar proteins with actin and vertebrate Arp2/3 complex. Nat Cell Biol. 3, 1, 76-82.

Marchetti, A., Mercanti, V., Cornillon, S., Alibaud, L., Charette, S. J., and Cosson, P. 2004. Formation of multivesicular endosomes in Dictyostelium. J Cell Sci. 117, Pt 25, 6053-6059.

Marshall, S., Podlecki, D. A., and Olefsky, J. M. 1983. Low pH accelerates dissociation of receptor-bound insulin. Endocrinology. 113, 1, 37-42.

Martin, A. C., Welch, M. D., and Drubin, D. G. 2006. Arp2/3 ATP hydrolysis-catalysed branch dissociation is critical for endocytic force generation. Nat Cell Biol. 8, 8, 826-833.

Martinez-Quiles, N., Rohatgi, R., Anton, I. M., Medina, M., Saville, S. P., Miki, H., Yamaguchi, H., Takenawa, T., Hartwig, J. H., Geha, R. S., and Ramesh, N. 2001. WIP regulates N-WASP-mediated actin polymerization and filopodium formation. Nat Cell Biol. 3, 5, 484-491.

Mellman, I., Fuchs, R., and Helenius, A. 1986. Acidification of the endocytic and exocytic pathways. Annu Rev Biochem. 55, 663-700.

Merrifield, C. J., Moss, S. E., Ballestrem, C., Imhof, B. A., Giese, G., Wunderlich, I., and Almers, W. 1999. Endocytic vesicles move at the tips of actin tails in cultured mast cells. Nat Cell Biol. 1, 1, 72-74.

Meyer, D. I. and Burger, M. M. 1979. The chromaffin granule surface: the presence of actin and the nature of its interaction with the membrane. FEBS Lett. 101, 1, 129-133.

Miki, H., Miura, K., and Takenawa, T. 1996. N-WASP, a novel actin-depolymerizing protein, regulates the cortical cytoskeletal rearrangement in a PIP2-dependent manner downstream of tyrosine kinases. EMBO J. 15, 19, 5326-5335.

Miki, H., Suetsugu, S., and Takenawa, T. 1998. WAVE, a novel WASP-family protein involved in actin reorganization induced by Rac. EMBO J. 17, 23, 6932-6941.

Miyata, H., Nishiyama, S., Akashi, K., and Kinosita, K. J. 1999. Protrusive growth from giant liposomes driven by actin polymerization. Proc Natl Acad Sci U S A. 96, 5, 2048-2053.

Mizutani, K., Miki, H., He, H., Maruta, H., and Takenawa, T. 2002. Essential role of neural Wiskott-Aldrich syndrome protein in podosome formation and degradation of extracellular matrix in src-transformed fibroblasts. Cancer Res. 62, 3, 669-674.

Mogilner, A. and Oster, G. 1996. Cell motility driven by actin polymerization. Biophys J. 71, 6, 3030-3045. DOI=10.1016/S0006-3495(96)79496-1.

Moriyama, Y., Maeda, M., and Futai, M. 1992. The role of V-ATPase in neuronal and endocrine systems. J Exp Biol. 172, 171-178.

Moseley, J. B., Sagot, I., Manning, A. L., Xu, Y., Eck, M. J., Pellman, D., and Goode, B. L. 2004. A conserved mechanism for Bni1- and mDia1-induced actin assembly and dual regulation of Bni1 by Bud6 and profilin. Mol Biol Cell. 15, 2, 896-907.

Muallem, S., Kwiatkowska, K., Xu, X., and Yin, H. L. 1995. Actin filament disassembly is a sufficient final trigger for exocytosis in nonexcitable cells. J Cell Biol. 128, 4, 589-598.

Mullins, R. D., Heuser, J. A., and Pollard, T. D. 1998. The interaction of Arp2/3 complex with actin: nucleation, high affinity pointed end capping, and formation of branching networks of filaments. Proc Natl Acad Sci U S A. 95, 11, 6181-6186.

Mullins, R. D., Stafford, W. F., and Pollard, T. D. 1997. Structure, subunit topology, and actin-binding activity of the Arp2/3 complex from Acanthamoeba. J Cell Biol. 136, 2, 331-343.

Myers, S. A., Han, J. W., Lee, Y., Firtel, R. A., and Chung, C. Y. 2005. A Dictyostelium homologue of WASP is required for polarized F-actin assembly during chemotaxis. Mol Biol Cell. 16, 5, 2191-2206.

Nakanishi-Matsui, M., Sekiya, M., Nakamoto, R. K., and Futai, M. 2010. The mechanism of rotating proton pumping ATPases. Biochim Biophys Acta. 10.1016/j.bbabio.2010.02.014.

Naqvi, S. N., Zahn, R., Mitchell, D. A., Stevenson, B. J., and Munn, A. L. 1998. The WASp homologue Las17p functions with the WIP homologue End5p/verprolin and is essential for endocytosis in yeast. Curr Biol. 8, 17, 959-962.

Nellen, W. and Firtel, R. A. 1985. High-copy-number transformants and co-transformation in Dictyostelium. Gene. 39, 2-3, 155-163.

Nelson, H. and Nelson, N. 1990. Disruption of genes encoding subunits of yeast vacuolar H(+)-ATPase causes conditional lethality. Proc Natl Acad Sci U S A. 87, 9, 3503-3507.

Neuhaus, E. M. and Soldati, T. 2000. A myosin I is involved in membrane recycling from early endosomes. J Cell Biol. 150, 5, 1013-1026.

Neuhaus, E. M., Almers, W., and Soldati, T. 2002. Morphology and dynamics of the endocytic pathway in Dictyostelium discoideum. Mol Biol Cell. 13, 4, 1390-1407.

Nobes, C. D. and Hall, A. 1995. Rho, rac, and cdc42 GTPases regulate the assembly of multimolecular focal complexes associated with actin stress fibers, lamellipodia, and filopodia. Cell. 81, 1, 53-62.

Nolta, K. V., Rodriguez-Paris, J. M., and Steck, T. L. 1994. Analysis of successive endocytic compartments isolated from Dictyostelium discoideum by magnetic fractionation. Biochim Biophys Acta. 1224, 2, 237-246.

Onken, H. and Putzenlechner, M. 1995. A V-ATPase drives active, electrogenic and Na+-independent Cl- absorption across the gills of Eriocheir sinensis. J Exp Biol. 198, Pt 3, 767-774.

Owegi, M. A., Pappas, D. L., Finch, M. W. J., Bilbo, S. A., Resendiz, C. A., Jacquemin, L. J., Warrier, A., Trombley, J. D., McCulloch, K. M., Margalef, K. L., Mertz, M. J., Storms, J. M., Damin, C. A., and Parra, K. J. 2006. Identification of a domain in the V0 subunit d that is critical for coupling of the yeast vacuolar proton-translocating ATPase. J Biol Chem. 281, 40, 30001-30014.

Padh, H., Ha, J., Lavasa, M., and Steck, T. L. 1993. A post-lysosomal compartment in Dictyostelium discoideum. J Biol Chem. 268, 9, 6742-6747.

Pan, F., Egile, C., Lipkin, T., and Li, R. 2004. ARPC1/Arc40 mediates the interaction of the actin-related protein 2 and 3 complex with Wiskott-Aldrich syndrome protein family activators. J Biol Chem. 279, 52, 54629-54636.

Pantaloni, D., Boujemaa, R., Didry, D., Gounon, P., and Carlier, M. F. 2000. The Arp2/3 complex branches filament barbed ends: functional antagonism with capping proteins. Nat Cell Biol. 2, 7, 385-391.

Paroutis, P., Touret, N., and Grinstein, S. 2004. The pH of the secretory pathway: measurement, determinants, and regulation. Physiology (Bethesda). 19, 207-215.

Parra, K. J., Keenan, K. L., and Kane, P. M. 2000. The H subunit (Vma13p) of the yeast V-ATPase inhibits the ATPase activity of cytosolic V1 complexes. J Biol Chem. 275, 28, 21761-21767.

Paunola, E., Mattila, P. K., and Lappalainen, P. 2002. WH2 domain: a small, versatile adapter for actin monomers. FEBS Lett. 513, 1, 92-97.

Peng, J., Wallar, B. J., Flanders, A., Swiatek, P. J., and Alberts, A. S. 2003. Disruption of the Diaphanous-related formin Drf1 gene encoding mDia1 reveals a role for Drf3 as an effector for Cdc42. Curr Biol. 13, 7, 534-545.

Pollard, T. D. and Borisy, G. G. 2003. Cellular motility driven by assembly and disassembly of actin filaments. Cell. 112, 4, 453-465.

Pollard, T. D. and Mooseker, M. S. 1981. Direct measurement of actin polymerization rate constants by electron microscopy of actin filaments nucleated by isolated microvillus cores. J Cell Biol. 88, 3, 654-659.

Pollitt, A. Y. and Insall, R. H. 2008. Abi mutants in Dictyostelium reveal specific roles for the SCAR/WAVE complex in cytokinesis. Curr Biol. 18, 3, 203-210.

Pring, M., Evangelista, M., Boone, C., Yang, C., and Zigmond, S. H. 2003. Mechanism of formin-induced nucleation of actin filaments. Biochemistry. 42, 2, 486-496.

Quinlan, M. E., Heuser, J. E., Kerkhoff, E., and Mullins, R. D. 2005. Drosophila Spire is an actin nucleation factor. Nature. 433, 7024, 382-388.

Ravanel, K., de Chassey, B., Cornillon, S., Benghezal, M., Zulianello, L., Gebbie, L., Letourneur, F., and Cosson, P. 2001. Membrane sorting in the endocytic and phagocytic pathway of Dictyostelium discoideum. Eur J Cell Biol. 80, 12, 754-764.

Rivero, F. and Maniak, M. 2006. Quantitative and microscopic methods for studying the endocytic pathway. Methods Mol Biol. 346, 423-438.

Rodal, A. A., Manning, A. L., Goode, B. L., and Drubin, D. G. 2003. Negative regulation of yeast WASp by two SH3 domain-containing proteins. Curr Biol. 13, 12, 1000-1008.

Rodal, A. A., Sokolova, O., Robins, D. B., Daugherty, K. M., Hippenmeyer, S., Riezman, H., Grigorieff, N., and Goode, B. L. 2005. Conformational changes in the Arp2/3 complex leading to actin nucleation. Nat Struct Mol Biol. 12, 1, 26-31.

Rogers, S. L., Wiedemann, U., Stuurman, N., and Vale, R. D. 2003. Molecular requirements for actin-based lamella formation in Drosophila S2 cells. J Cell Biol. 162, 6, 1079-1088.

Rohatgi, R., Nollau, P., Ho, H. Y., Kirschner, M. W., and Mayer, B. J. 2001. Nck and phosphatidylinositol 4,5-bisphosphate synergistically activate actin polymerization through the N-WASP-Arp2/3 pathway. J Biol Chem. 276, 28, 26448-26452.

Rouiller, I., Xu, X. P., Amann, K. J., Egile, C., Nickell, S., Nicastro, D., Li, R., Pollard, T. D., Volkmann, N., and Hanein, D. 2008. The structural basis of actin filament branching by the Arp2/3 complex. J Cell Biol. 180, 5, 887-895.

Rybak, S. L., Lanni, F., and Murphy, R. F. 1997. Theoretical considerations on the role of membrane potential in the regulation of endosomal pH. Biophys J. 73, 2, 674-687.

Sagot, I., Rodal, A. A., Moseley, J., Goode, B. L., and Pellman, D. 2002. An actin nucleation mechanism mediated by Bni1 and profilin. Nat Cell Biol. 4, 8, 626-631.

Sautin, Y. Y., Lu, M., Gaugler, A., Zhang, L., and Gluck, S. L. 2005. Phosphatidylinositol 3-kinase-mediated effects of glucose on vacuolar H+-ATPase assembly, translocation, and acidification of intracellular compartments in renal epithelial cells. Mol Cell Biol. 25, 2, 575-589. DOI=10.1128/MCB.25.2.575-589.2005.

Schapiro, F. B. and Grinstein, S. 2000. Determinants of the pH of the Golgi complex. J Biol Chem. 275, 28, 21025-21032.

Schmauch, C., Claussner, S., Zoltzer, H., and Maniak, M. 2009. Targeting the actin-binding protein VASP to late endosomes induces the formation of giant actin aggregates. Eur J Cell Biol. 88, 7, 385-396.

Shum, W. C., Silva, N. D., Belleannee, C., Ljubojevic, M., Hill, E., Brown, D., Breton, S. 2010. Actin cytoskeleton remodeling by RhoA and RockII regulates vacuolar H+-ATPase (V-ATPase) recycling in epididymal clear cells. FAEB J. 24: 1002.10

Snapper, S. B., Rosen, F. S., Mizoguchi, E., Cohen, P., Khan, W., Liu, C. H., Hagemann, T. L., Kwan, S. P., Ferrini, R., Davidson, L., Bhan, A. K., and Alt, F. W. 1998. Wiskott-Aldrich syndrome protein-deficient mice reveal a role for WASP in T but not B cell activation. Immunity. 9, 1, 81-91.

Snapper, S. B., Takeshima, F., Anton, I., Liu, C. H., Thomas, S. M., Nguyen, D., Dudley, D., Fraser, H., Purich, D., Lopez-Ilasaca, M., Klein, C., Davidson, L., Bronson, R., Mulligan, R. C., Southwick, F., Geha, R., Goldberg, M. B., Rosen, F. S., Hartwig, J. H., and Alt, F. W. 2001. N-WASP deficiency reveals distinct pathways for cell surface projections and microbial actin-based motility. Nat Cell Biol. 3, 10, 897-904.

Soderling, S. H., Langeberg, L. K., Soderling, J. A., Davee, S. M., Simerly, R., Raber, J., and Scott, J. D. 2003. Loss of WAVE-1 causes sensorimotor retardation and reduced learning and memory in mice. Proc Natl Acad Sci U S A. 100, 4, 1723-1728.

Solomon, J. M. and Isberg, R. R. 2000. Growth of Legionella pneumophila in Dictyostelium discoideum: a novel system for genetic analysis of host-pathogen interactions. Trends Microbiol. 8, 10, 478-480.

Souza, G. M., Mehta, D. P., Lammertz, M., Rodriguez-Paris, J., Wu, R., Cardelli, J. A., and Freeze, H. H. 1997. Dictyostelium lysosomal proteins with different sugar modifications sort to functionally distinct compartments. J Cell Sci. 110, Pt 18, 2239-2248.

Spector, I., Shochet, N. R., Kashman, Y., and Groweiss, A. 1983. Latrunculins: novel marine toxins that disrupt microfilament organization in cultured cells. Science. 219, 4584, 493-495.

Sussman, R. and Sussman, M. 1967. Cultivation of Dictyostelium discoideum in axenic medium. Biochem Biophys Res Commun. 29, 1, 53-55.

Suzuki, T., Miki, H., Takenawa, T., and Sasakawa, C. 1998. Neural Wiskott-Aldrich syndrome protein is implicated in the actin-based motility of Shigella flexneri. EMBO J. 17, 10, 2767-2776.

Svitkina, T. M. and Borisy, G. G. 1999. Arp2/3 complex and actin depolymerizing factor/cofilin in dendritic organization and treadmilling of actin filament array in lamellipodia. J Cell Biol. 145, 5, 1009-1026.

Symons, M., Derry, J. M., Karlak, B., Jiang, S., Lemahieu, V., Mccormick, F., Francke, U., and Abo, A. 1996. Wiskott-Aldrich syndrome protein, a novel effector for the GTPase CDC42Hs, is implicated in actin polymerization. Cell. 84, 5, 723-734.

Tal, T., Vaizel-Ohayon, D., and Schejter, E. D. 2002. Conserved interactions with cytoskeletal but not signaling elements are an essential aspect of Drosophila WASp function. Dev Biol. 243, 2, 260-271.

Taunton, J., Rowning, B. A., Coughlin, M. L., Wu, M., Moon, R. T., Mitchison, T. J., and Larabell, C. A. 2000. Actin-dependent propulsion of endosomes and lysosomes by recruitment of N-WASP. J Cell Biol. 148, 3, 519-530.

Valdmanis, P. N., Meijer, I. A., Reynolds, A., Lei, A., MacLeod, P., Schlesinger, D., Zatz, M., Reid, E., Dion, P. A., Drapeau, P., and Rouleau, G. A. 2007. Mutations in the KIAA0196 gene at the SPG8 locus cause hereditary spastic paraplegia. Am J Hum Genet. 80, 1, 152-161.

van den Ent, F., Amos, L. A., and Lowe, J. 2001. Prokaryotic origin of the actin cytoskeleton. Nature. 413, 6851, 39-44.

Van Dyke, R. W. 1993. Acidification of rat liver lysosomes: quantitation and comparison with endosomes. Am J Physiol. 265, 4 Pt 1, C901-17.

Vasioukhin, V., Bauer, C., Yin, M., and Fuchs, E. 2000. Directed actin polymerization is the driving force for epithelial cell-cell adhesion. Cell. 100, 2, 209-219.

Veltman, D. M. and Insall, R. H. 2010. WASP Family Proteins - Their Evolution and Its Physiological Implications. Mol Biol Cell. 10.1091/mbc.E10-04-0372.

Vitavska, O., Merzendorfer, H., and Wieczorek, H. 2005. The V-ATPase subunit C binds to polymeric F-actin as well as to monomeric G-actin and induces cross-linking of actin filaments. J Biol Chem. 280, 2, 1070-1076.

Vitavska, O., Wieczorek, H., and Merzendorfer, H. 2003. A novel role for subunit C in mediating binding of the H+-V-ATPase to the actin cytoskeleton. J Biol Chem. 278, 20, 18499-18505.

Wagner, C. A., Finberg, K. E., Breton, S., Marshansky, V., Brown, D., and Geibel, J. P. 2004. Renal vacuolar H+-ATPase. Physiol Rev. 84, 4, 1263-1314.

Wehland, J., Stockem, W., and Weber, K. 1978. Cytoplasmic streaming in Amoeba proteus is inhibited by the actin-specific drug phalloidin. Exp Cell Res. 115, 2, 451-454.

Welch, M. D., Rosenblatt, J., Skoble, J., Portnoy, D. A., and Mitchison, T. J. 1998. Interaction of human Arp2/3 complex and the Listeria monocytogenes ActA protein in actin filament nucleation. Science. 281, 5373, 105-108.

Westcott, K. R., Searles, R. P., and Rome, L. H. 1987. Evidence for ligand- and pH-dependent conformational changes in liposome-associated mannose 6-phosphate receptor. J Biol Chem. 262, 13, 6101-6107.

Westerberg, L., Larsson, M., Hardy, S. J., Fernandez, C., Thrasher, A. J., and Severinson, E. 2005. Wiskott-Aldrich syndrome protein deficiency leads to reduced B-cell adhesion, migration, and homing, and a delayed humoral immune response. Blood. 105, 3, 1144-1152.

Wieczorek, H., Putzenlechner, M., Zeiske, W., and Klein, U. 1991. A vacuolar-type proton pump energizes K+/H+ antiport in an animal plasma membrane. J Biol Chem. 266, 23, 15340-15347.

Williams, K. L., Kessin, R. H., and Newell, P. C. 1974. Genetics of growth in axenic medium of the cellular slime mould Dictyostelium discoideum. Nature. 247, 437, 142-143.

Wu, M. M., Llopis, J., Adams, S., McCaffery, J. M., Kulomaa, M. S., Machen, T. E., Moore, H. P., and Tsien, R. Y. 2000. Organelle pH studies using targeted avidin and fluorescein-biotin. Chem Biol. 7, 3, 197-209.

Yamaguchi, H., Lorenz, M., Kempiak, S., Sarmiento, C., Coniglio, S., Symons, M., Segall, J., Eddy, R., Miki, H., Takenawa, T., and Condeelis, J. 2005. Molecular mechanisms of invadopodium formation: the role of the N-WASP-Arp2/3 complex pathway and cofilin. J Cell Biol. 168, 3, 441-452.

Yamashiro, D. J. and Maxfield, F. R. 1984. Acidification of endocytic compartments and the intracellular pathways of ligands and receptors. J Cell Biochem. 26, 4, 231-246.

Yamazaki, D., Suetsugu, S., Miki, H., Kataoka, Y., Nishikawa, S., Fujiwara, T., Yoshida, N., and Takenawa, T. 2003. WAVE2 is required for directed cell migration and cardiovascular development. Nature. 424, 6947, 452-456.

Yan, C., Martinez-Quiles, N., Eden, S., Shibata, T., Takeshima, F., Shinkura, R., Fujiwara, Y., Bronson, R., Snapper, S. B., Kirschner, M. W., Geha, R., Rosen, F. S., and Alt, F. W. 2003. WAVE2 deficiency reveals distinct roles in embryogenesis and Rac-mediated actin-based motility. EMBO J. 22, 14, 3602-3612.

Zallen, J. A., Cohen, Y., Hudson, A. M., Cooley, L., Wieschaus, E., and Schejter, E. D. 2002. SCAR is a primary regulator of Arp2/3-dependent morphological events in Drosophila. J Cell Biol. 156, 4, 689-701.

Zigmond, S. H., Evangelista, M., Boone, C., Yang, C., Dar, A. C., Sicheri, F., Forkey, J., and Pring, M. 2003. Formin leaky cap allows elongation in the presence of tight capping proteins. Curr Biol. 13, 20, 1820-1823.

Zuchero, J. B., Coutts, A. S., Quinlan, M. E., Thangue, N. B., and Mullins, R. D. 2009. p53-cofactor JMY is a multifunctional actin nucleation factor. Nat Cell Biol. 11, 4, 451-459.

Zuo, J., Jiang, J., Chen, S. H., Vergara, S., Gong, Y., Xue, J., Huang, H., Kaku, M., and Holliday, L. S. 2006. Actin binding activity of subunit B of vacuolar H+-ATPase is involved in its targeting to ruffled membranes of osteoclasts. J Bone Miner Res. 21, 5, 714-721.

Zuo, J., Vergara, S., Kohno, S., and Holliday, L. S. 2008. Biochemical and functional characterization of the actin-binding activity of the B subunit of yeast vacuolar H+-ATPase. J Exp Biol. 211,